DSPACE

https://dspace.org/

The integration of measured, modelled and remotely sensed air quality data and its' impacts on the Highveld.

Bhugwandin, Kubeshnie Naicker

2014-02-06
http://hdl.handle.net10539/13679

Downloaded from a DSpace repository. https://dspace.org/



School of Geography, Archaeology and Environmental Studies

University of the Witwatersrand, Johannesburg

THE INTERGRATION OF MEASURED, MODELLED AND REMOTELY SENSED AIR QUALTY DATA AND ITS' IMPACTS ON THE HIGHVELD

Kubeshnie Naicker Bhugwandin

A dissertation submitted to the Faculty of Science, University of the Witwatersrand, in fulfilment of the requirements for the degree of Master of Science

August 2013

Declaration

I declare that this Dissertation is my own, unaided work. It is being submitted for the Degree of Master of Science in the University of the Witwatersrand, Johannesburg. It has not been submitted before for any degree or examination in any other University.

Kubeshnie Naicker Bhugwandin	**20 August 2013**
Name	**Date**

Dedication

To my husband Pranesh

ABSTRACT

Although a vast number of air quality investigations have been conducted on the Mpumalanga Highveld previously, there has been limited attempt to integrate available datasets from the different methods of air quality monitoring (satellite, in-situ and ground-based observations) and modelling. This study compares modelled, satellite and measured data to determine the most accurate estimate of ground level sulphur dioxide (SO_2) and nitrogen oxide (NO_x) concentrations.

The main value of the project comes from the 'improvement' of modelled concentration fields using measurements. Measurements only provide information on air quality at isolated places (for example monitoring stations) or at isolated times (aircraft measurements and satellite observations). Dispersion models predict concentrations continually over a wide area. However, models have inherent inaccuracies based on the assumptions made in developing the model and the variability in the input parameters supplied. These can be accounted for or are part of the inherent variability of the model results. This study assists in the refinement of modelled outputs as well as the verification of satellite data using ground-based measured data as a point of reference.

In the wake of increasing governance on air pollution, industry has been compelled to account for their impacts on the environment. This study aids industry by proposing a method to quantify their impacts on the environment and possibly on human health. Three datasets from 2003 (modelled, measured and satellite) were integrated using a geographic information system in order to analyse and interrogate the data and produce an integrated set of data, maps of potentially sensitive ecosystems and maps of potential exposure to poor air quality of sensitive population groupings.

The results of the study have shown that although the concentration value for the NO_2 tropospheric column is greater than the values observed on the ground there is a good correlation between measured observations and SCIAMACHY retrievals. The sample size was too small to indicate a statistically significant bias.

The results from the validation of the CALPUFF model indicate with respect to SO_2 predictions that the model is only reliable for 62% of the time within the United States Environmental Protection Agency's model performance guideline of acceptance i.e. predictions within a factor of 2, and for NO_2 the predictions are reliable for only 50% of the time. There is also no constant value by which the model under or over predicts. The cumulative distribution function graphs illustrate that the CALPUFF model predicts the highest values from the bulk of the distribution rather that the tail of the distribution where the extremes lie. This could possibly account for the large variance between measured and modelled outputs.

The results of identifying areas of potential harm from SO_2 emissions reveal that hotspots for high to very high risk to human health occur around all power stations. Generally the category of high risk around power stations seems to be located in areas with population agglomerations between 0-1 000 per km^2 and 2001- 5000 per km^2.

Several high risk areas for potential harm to ecosystems from SO_2 emissions can be seen on the Highveld with a large spatial extent around Kendal, Matla and Kriel power station. Approximately 871 wetlands fall within the high risk areas. The vegetation risk map indicates a high risk to several grassland and bushveld types. Model results for this study indicate no potential risk to human health from emissions of NO and subsequent conversion to NO_2 in the atmosphere.

Preface

The Mpumalanga Highveld region is the most industralised area in southern Africa with emission densities ranked amongst the highest in the world. Fifteen coal fired power stations are located on the Highveld and are amongst the main contributors to the poor air quality in this region.

The overarching aim of this study is to improve modelled air quality predictions using measured data. The study also aims to integrate measured, modelled and satellite data to evaluate impacts of power station emissions on human health and ecosystems. The ultimate objective is to be able to credibly predict concentrations without reference to a fixed ground based monitoring stations using models and satellite retrievals.

The objectives of this study are to:

(i) Compare the CALPUFF model results to ground based measurements of SO_2 and NO_2 concentrations;

(ii) Evaluate the representativeness of satellite retrievals to surface concentrations of SO_2 and NO_2;

(iii) Integrate available ambient air quality datasets derived from the different methods of air quality monitoring and modelling in the Mpumalanga Highveld region;

(iv) Improve modelled ground level air pollution concentration fields by utilising measured data;

(v) Identify the hot spots for potential harm to human health and ecosystems from power station emissions based on the results of the new modelling outputs.

The report is divided into eight chapters. **Chapter 1** outlines the background, rationale for this study, limitations of ambient monitoring for exposure estimation, advantages and limitations of air dispersion modelling for exposure estimation, the advantages and limitations of using satellite retrievals for assessing ground level trace gas concentrations and the aims and objectives of this study.

Chapter 2 presents an overview of the study area by providing a general description and discussing the meteorology of the Highveld region. **Chapter 3** discusses the literature review highlighting the atmospheric pollution sources, atmospheric chemistry, atmospheric plume dispersion modelling and geographic information systems. The ambient air quality guideline and standard for SO_2 and NO_2 provides a legislative framework which stipulates concentration limits to prevent or reduce negative effects on human health and ecosystems.

Chapter 4 and **Chapter 5** discusses the data and methodology utilised in this study. The results are presented and discussed in **Chapter 6**. In **Chapter 7** the key findings are summarised and conclusions are presented. **Chapter 8** lists the references utilised in this study.

Sections of this report have been presented to the European Space Agency at the Tropospheric Emission Monitoring Inventory System user workshop which was held in 2007 and 2009 in Frascati, Italy.

Dr S.J. Piketh and Dr K.E. Langerman are acknowledged for their supervision and valuable scientific guidance throughout the study period. A special thanks to Dr. V. Micali for his continued support and guidance in the use of statistical theories. Dr R. van der A and Dr J. van Geffen from the Royal Netherlands Meteorological Institute are thanked for making SCIAMACHY data available to conduct this study. My husband is thanked for his inspiration, motivation and also for his continued support. The Eskom Research, Testing and Development business unit is acknowledged for funding this study.

Table of Contents

Declaration i
Dedication ii
Abstract iii
Preface ..... **v**
Table of Contents vii
List of Figures xi
List of Tables xvi
List of Abbreviations xix

Chapter 1 Introduction

Back ground 1
Rationale for this study 3
Limitations of ambient monitoring for exposure estimation 7
The advantages of air dispersion modelling for exposure estimation 8
Limitations in dispersion modelling 8
The advantages and limitations of using satellite retrievals for assessing ground level trace gases 10
Aims and objectives 13
Structure of dissertation 13

Chapter 2 Overview of Study Area

General description of study area 14
Location of industrialised Highveld 14
Topography and land use 15
Climate 17
Population. 18
Meteorology of the study region 19
Macro scale synoptic circulations 19
Transport of trace gases over Highveld 21

Chapter 3 Literature Review

Atmospheric pollution sources 26
Pollution sources on the Highveld 26
Atmospheric chemistry 30
Nitrogen oxides and nitrates 30
Atmospheric Sulphur 33
Atmospheric plume dispersion modelling 38
Types of models 40
Air quality model performance evaluation 46
Geographic information systems 48
Components of a GIS 49
Data Models 51
Spatially interpolated surfaces 52
Specific spatial interpolation methods 53
Spatial interpolation modelling limitations 56
Ambient air quality guidelines and standards 59
National Policy 60
Consequences of atmospheric pollution 62
Effects on human health 62
Effects on vegetation 66

Chapter 4 Data Collection

Introduction 71
Ground-based measurements 71
Network reliability 73
Meteorological observations and air quality at ground monitoring stations 74
Modelled data 95
Source and emission data inputs 96
Spatial data inputs 97

Chapter 5 Methodology

Introduction 100
SCIAMACHY 101
SCIAMACHY sensor and coverage 101
Differential optical absorption Spectroscopy (DOAS) analysis 102
SCIAMACHY limb and nadir measurements 104
SCIAMACHY analysis 105
The CALPUFF modelling suite 107
The CALPUFF component 108
The CALMET component 109
The modelling domain and receptor locations 110
Analysis of modelled outputs 111
Distribution tail analysis 112
Integration of measured and modelled values 112
Hot Spot Analysis 113

Chapter 6 Results and Discussion

Validation of SCIAMACHY NO_2 retrievals 118
Validation of the CALPUFF model 122
SO_2 statistical analysis of measured and modelled concentrations 122
NO_2 statistical analysis of measured and modelled concentrations 123
Distribution tail analysis 124
Potential for health and vegetation impacts 126
Comparison of South African ambient air quality standards to international best practices 126
Analysis of potential risk from SO_2 concentrations 128
Analysis of potential risk from NO_2 concentrations 148

Chapter 7 Conclusion and Summary

Summary of results 150
Recommendations for future research 152

Chapter 8 References 154

List of Figures

Figure 1: Processes involved in the atmospheric pollution budget (Fourie, 2006) 4

Figure 2: The mean tropospheric column density for 2006 derived from the SCIAMACHY instrument (Collet *et al.*, 2010) 6

Figure 3: The industralised Highveld region 14

Figure 4: Topography of the industrialised Highveld region 16

Figure 5: Land use characteristics of industrialised Highveld 17

Figure 6: Major synoptic ciculation types affecting Southern Africa and their monthly frequency of occurences over a five year period (Preston-Whyte and Tyson, 1988) 20

Figure 7: Transport pathways advecting air to the Mpumalanga Highveld region (Frieman and Piketh, 2003) 23

Figure 8: Five transport pathways from the industrialised Highveld region (Piketh and Pragley, 1998) 24

Figure 9: An air quality modelling system (Zannetti, 1990) 39

Figure 10: Eskom ambient air monitoring network in relation to Eskom power stations 71

Figure 11: Daytime and night-time wind roses at Elandsfontein 75

Figure 12: Diurnal variation of wind speed at Elandsfontein 76

Figure 13: Average daily wind speed at Elandsfontein 77

Figure 14: Diurnal ambient temperature at Elandsfontein 77

Figure 15: Daily average ambient temperature at Elandsfontein 78

Figure 16: Daytime and night-time wind roses at Verkykkop 80

Figure 17: Daytime and night-time wind roses at Palmer 83

Figure 18: Daytime and night-time wind roses at Makalu 86

Figure 19: Daytime and night-time wind roses for Leandra 89

Figure 20: Daytime and night-time wind roses for Kendal 91

Figure 21a: Daytime and night-time wind roses for J1 93

Figure 21b: Daytime and night-time wind roses for J3 94

Figure 22: Typical diurnal profile based on the energy output for winter and summer (Scorgie and Venter, 2005) 97

Figure 23: Differential absorption cross-sections of some trace gases absorbing in the UV/visible wave length spectrum (Stutz and Platt, 1997) 103

Figure 24: CALPUFF modelling system (SRC, 2008) 108

Figure 25: Available SCIAMACHY data within study domain 119

Figure 26: Correlation of measured ground concentrations and SCIAMACHY retrievals at 10:00 120

Figure 27: Correlation of measured ground concentrations and SCIAMACHY retrievals at 09h00 121

Figure 28: Cumulative distribution function graph of NO_2 concentrations at Kendal monitoring station 125

Figure 29: Cumulative distribution function graph of SO_2 concentrations at Verkykkop monitoring station 125

Figure 30: SO_2 diurnal variation at Elandsfontein 129

Figure 31: SO_2 daytime and night-time sector exceednce roses 130

Figure 32: Daytime and night-time SO_2 sector exceedance roses 131

Figure 33: SO_2 daytime and night-time sector exceedance roses 132

Figure 34: SO_2 daytime and night-time sector exceedance roses 132

Figure 35: SO_2 daytime and night-time sector exceedance roses 133

Figure 36: SO_2 daytime and night-time sector exceedance roses 134

Figure 37a: SO_2 daytime and night-time sector exceedance roses at J3 135

Figure 37b: SO_2 daytime and night-time sector exceedance roses at J1 135

Figure 38: Highest SO_2 hourly average exceedences on populated areas 137

Figure 39: Potential risk to human health from highest hourly SO_2 concentrations 138

Figure 40: Highest SO_2 daily average exceedence on populated areas 139

Figure 41: SO_2 annual average exceedance on populated areas 140

Figure 42: Impact on ecosystems from SO_2 emissions 141

Figure 43: Impact on wetlands from SO_2 emissions 142

Figure 44: Impact on vegetation from SO_2 emissions 143

Figure 45: NO_2 diurnal variation at Elandsfontein 144

Figure 46: NO_2 daytime and night-time sector exceedance roses 145

Figure 47: NO_2 daytime and night-time sector exceedance roses 145

Figure 48: NO_2 daytime and night-time sector exceedance roses 146

Figure 49: NO_2 daytime and night-time sector exceedance roses 147

Figure 50: NO_2 daytime and night-time sector exceedance roses 147

List of Tables

Table 1: Population distribution (StatsSA, 2012) 18

Table 2: The Pasquil stability classes (Beychok, 2005) 42

Table 3: Meteorological conditions that define the Pasquil stability classes (Beychok, 2005) 42

Table 4: National ambient air quality SO_2 standards and compliance dates (Department of Environmental Affairs, 2009b) 61

Table 5: National ambient air quality NO_2 standards and compliance dates (Department of Environmental Affairs, 2009) 61

Table 6: Summary of SO_2 health effects (Raghunanadan *et al*., 2006) 64

Table 7: Percentage data capture 74

Table 8: Highest average hourly, daily and monthly SO_2 concentrations (ppb) 78

Table 9: Highest average hourly, daily and monthly average NO_2 concentrations 79

Table 10: Highest average hourly, daily and monthly SO_2 concentrations (ppb) 81

Table 11: Highest average hourly, daily and monthly average NO_2 concentrations (ppb) 82

Table 12: Highest average hourly, daily and monthly SO_2 concentrations (ppb)....84

Table 13: Highest average hourly, daily and monthly average NO_2 concentrations (ppb)....85

Table 14: Highest average hourly, daily and monthly SO_2 concentrations (ppb) 87

Table 15: Highest average hourly, daily and monthly average NO_2 concentration (ppb) 88

Table 16: Highest average hourly, daily and monthly SO_2 concentrations (ppb)....90

Table 17: Highest average hourly, daily and monthly SO_2 concentrations (ppb)....91

Table 18: Highest average hourly, daily and monthly average NO_2 concentrations (ppb)....92

Table 19: Highest average hourly, daily and monthly SO_2 concentrations (ppb) at J1 and J3 95

Table 20: Thresholds specified for health effects (Scorgie and Gruenewaldt, 2008) 115

Table 21: Thesholds specified for potential harm to vegetation (Scorgie and Grunewaldt, 2008) 116

Table 22: Comparison of measured hourly average concentrations and SCIAMACHY retrievals at 10:00 119

Table 23: Comparison of measured hourly average concentrations and SCIAMACHY retrievals at 09:00 122

Table 24: Comparison of modelled and measured highest hourly SO_2 concentrations (adapted from Scorgie and Venter, 2005) 123

Table 25: Comparison of modelled and measured NO_2 highest hourly concentrations (adapted from Scorgie and Venter, 2005) 124

Table 26: Comparative ambient air quality standards for SO_2 (adapted from Scorgie and Venter, 2005) 127

Table 27: Comparative ambient air quality standards for NO_2 (adapted from Scorgie and Venter, 2005) 128

List of Abbreviations

Atmospheric dispersion modelling system (ADMS)

Cumulative distribution function (CDF)

Department of Environmental Affairs (DEA)

Differential Optical Absorption Spectroscopy (DOAS)

Dinitrogen pentoxide (N_2O_5)

Environmental database-driven web-enabled integrated system (EDWEIS)

Environmental Science Research Institute (ESRI)

Environmental satellite (ENVISAT)

European Community (EC)

European Space Agency (ESA)

Geographic Information Systems (GIS)

Global Ozone Monitoring Equipment (GOME)

Hydrogen Sulphide (H_2S)

International Finance Corporation (IFC)

Inter Tropical Convergence Zone (ITCZ)

Nitrogen dioxide (NO_2)

Nitric Oxide (NO)

Nitrous oxide (N_2O)

Ozone (O3)

Scanning Imaging Absorption Spectrometer for Atmospheric Cartography (SCIAMACHY)

Sulphur dioxide (SO2)

Sulphur trioxide (SO_3)

Sulphuric acid (H_2SO_4)

South African National Accreditation System (SANAS)

South African Weather Services (SAWS)

United States Environmental Protection Agency (US-EPA)

Volatile Organic Carbons (VOCs)

World Health Organisation (WHO)

CHAPTER 1
INTRODUCTION

This chapter presents a brief overview of air quality in the Mpumalanga Highveld. The study is motivated by providing justifications to use air dispersion modelling for exposure estimations. The aims and objectives of this study are discussed. This chapter is concluded by the structure of the dissertation which sets the framework for the research.

1.1 BACK GROUND

South Africa is a major regional contributor of aerosols and trace gases from biomass burning, biogenic processes and anthropogenic activities (Piketh *et al.*, 2002). The Mpumalanga Highveld is the most highly industrialised area in Southern Africa with emission densities ranked amongst the highest in the world (Wenig *et al.*, 2002; Rorich and Galpin, 1998).

Over the years anthropogenic emissions released in the Mpumalanga Highveld region of South Africa from industrial complexes such as power plants, open-cast coal mines, fuel refining processes and domestic coal-fired heating have significantly altered the atmospheric sulphur budget. Over time, released air pollutant gases are transformed into particle aerosols during air mass transport from their various sources. Several studies of the oxidation of sulphur species from surface and stack emissions in open-cast coal mines and coal-fired power plants during plume transport have been made at varying atmospheric conditions (Fugas and Gentilizza, 1978; Rodhe, 1978) which result in the formation of aitken particles and particulate sulphate.

Globally human population growth, industrialisation and other economic activities have led to an accelerated increase in SO_2 and NO_2 emissions, leading to air pollution impacts such as acidification of the water bodies through removal of sulphur gases via wet scavenging and dry deposition (Pham *et al.*, 1995), nitric oxide deposition and increased radiative forcing effects due to absorption of downward

propagating visible light (Richter *et al*, 2005). The increase in SO_2 and NO_2 emissions has led to global as well as localised deterioration in air quality which is influenced by local meteorology and topographical factors (Nunnari *et al.*, 2004; Turner, 1994).

The World Health Organisation (WHO) states that more than 2.7 million deaths have occurred annually due to air pollution (WHO, 2003). Norman *et al.* (2007) estimated that in year 2000 outdoor air pollution in South African urban areas was responsible for 4 637 human deaths. The inhabitants of a typical urban centre may be exposed to about 40 individual chemicals and/or groups of chemicals, totalling more than 100 individual chemical species (WHO, 2000a). An extensive literature review (WHO 2000a, 2001, 2005; Maynard, 2004; Brunekreef and Holgate, 2002) has demonstrated the associations between exposure to SO_2 and NO_2 pollutants and ill-health impacts such as increased hospital admissions for respiratory, cardio vascular disease, congestive heart failure, increase in asthma, increases in acute bronchitis and decreased lung function. Short-term adverse health responses may occur within minutes for example, asthmatic sufferers exposed to SO_2 may experience effects within minutes (WHO 2000b) or may lag the exposure by several hours, up to a period of several days (Lipfert, 1994). Hence there is a need to accurately assess ambient air quality.

Ambient air quality is regulated in most countries across the globe through compliance with ambient air quality standards, which are set to thresholds that protect human health, vegetation and ecosystems. An Air Quality Management Plan (AQMP) includes a comprehensive emissions inventory, ambient monitoring data, dispersion modelling results, emission reduction interventions, meteorological data and public participation processes (Department of Environmental Affairs and Tourism, 2001). This study focuses on the dispersion modelling aspect of an AQMP. In any atmospheric pollution control programme modelling the accumulation and dispersion of pollutants is of the highest priority. Air dispersion models can be used to identify parts of airsheds likely to experience highest concentrations of pollution and therefore assist in the location of ambient air monitoring sites. They can also be utilised to predict future spatial patterns of ambient air pollution concentrations in response to different air quality management strategies, essentially evaluating scenarios of possible emission reductions. In this way they can also be used to evaluate the

effectiveness of existing and proposed AQM strategies and assess whether deadlines for implementation of environmental standards are likely to be met (Sturman, 2008; Ramandh, 2011). Modelled outputs are used to a great extent in decision making and will influence future industrial generation developments in the Highveld region.

1.2 RATIONALE FOR THIS STUDY

From the 1950s to the early 1970s, air pollution was thought to be mostly a localised urban problem and early measures to address this issue in Europe and the United States focused on small urban "airsheds". Air quality legislation was introduced in the 1960s and 1970s to meet societal demands for cleaner air. Air pollution scientists began to also notice alarming trends in rural locations. It was found that the air in many of the rural areas was becoming polluted. In the 1970s both Europe and the United States recognised the emergence of regional-scale air pollution issues, including acid rain, regional haze and smog. These were the results of increased regional emissions and long range transport of air pollution. In the next two decades scientist around the world produced more evidence for regional scale air pollution and ill-health impacts (Bachmann, 2003; Fourie, 2006).

The atmospheric pollution budget is determined by a number of physical and chemical processes occurring in the atmosphere (Figure 1). This information is necessary for understanding source-receptor relationships between emissions from sources and pollution levels measured at specific receptor points (Watt Committee on Energy, 1984). Understanding the atmospheric pathways of important pollutants and quantifying the flux of material along these pathways is vital to accurately estimating ambient pollution concentrations in the atmosphere (Fourie, 2006).

In order to develop an ambient air quality management strategy for a particular area, the ambient pollution concentrations for this area must be determined. This can be done by both ambient air quality monitoring (ground monitoring stations or satellite observations) and atmospheric dispersion modelling.

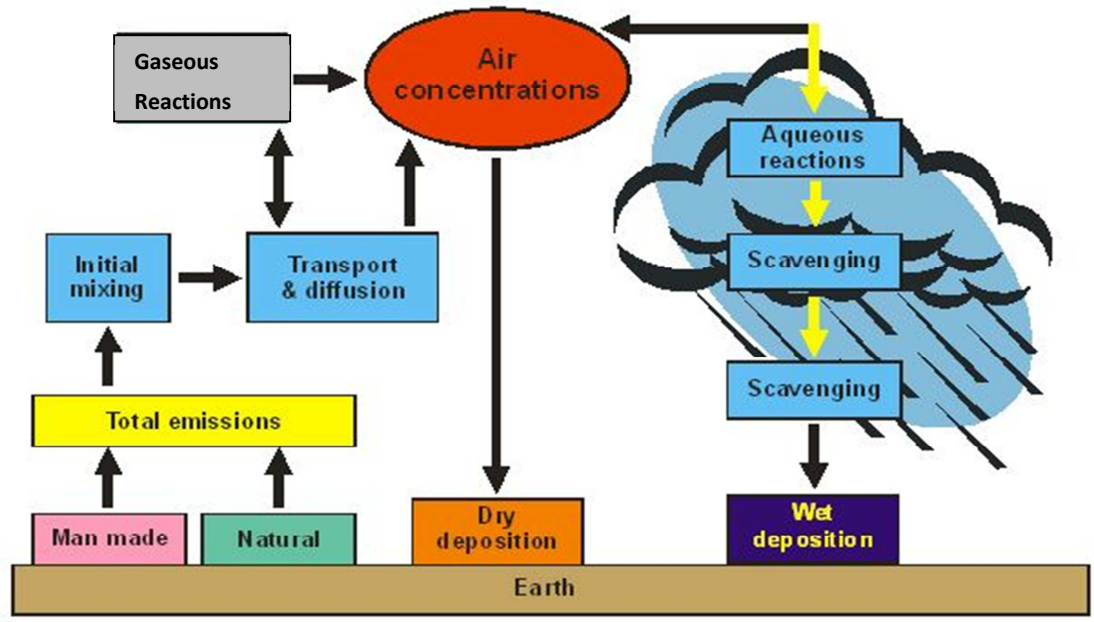


Figure 1: Processes involved in the atmospheric pollution budget (adapted from Fourie, 2006).

Over the years several independent datasets have been created by industry, government and research institutions of ambient air quality on the Highveld. However, the integration of datasets derived from the different methods of air quality monitoring and modelling in this region is limited. Surface measurements are collected at a network of monitoring sites across the region in order to assess compliance with the South African ambient air quality standards and to determine long term trends. A wide range of monitoring methodologies and approaches are utilised with most monitoring located in close proximity to the major urban areas and industrial development nodes (Zunkel *et al*., 2004). Eskom's ground based active monitoring sites date back to the late 1970's (Rorich and Galpin, 1998) and formed part of the data which was utilised for integration and analysis in this study.

In recent years advances in atmospheric dispersion modelling have lead to an increase in the availability of datasets on ground-level pollution concentrations but the outputs from these models have been debatable. A modelling study was conducted by Eskom to assess the impact on air quality of current, future and planned power station operations. This study utilised the US Environmental Protection Agency (US-EPA) approved CALPUFF model which is able to account for spatial variability of meteorological conditions, dry deposition and dispersion over a variety of spatially

differing land surfaces (Scorgie and Venter, 2005). The outputs from this modelling study was utilised as the second dataset for comparison, integration and refinement. Since modelled outputs are utilised for decision making it is imperative that they provide an accurate account of the real world. Improving the accuracy of modelled concentration fields will ultimately assist in better air quality predictions for the Highveld region thereby influencing the air quality management plan of this area.

In addition, remotely sensed data of trace gases such as SO_2, O_3 (ozone) and NO_X (nitrogen oxides) are becoming increasingly available via satellite. SCIAMACHY is an instrument on board the environmental satellite (ENVISAT) which measures trace gases, cloud top heights and aerosol concentrations in the atmosphere. These datasets are currently used around the world to evaluate pollution hotspots and long range transport of emissions (Borell *et al.*, 2003; Burrows *et al.*, 1999). The study area is continuously cited as a hotspot for SO_2 and NO_2 pollution (Figure 2) in remote sensing studies around the globe. This study utilised total column tropospheric SO_2 and NO_X concentrations measured by SCIAMACHY (Scanning Imaging Absorption Spectrometer for Atmospheric Cartography) as the third dataset for validation with ground based measured data and integration.

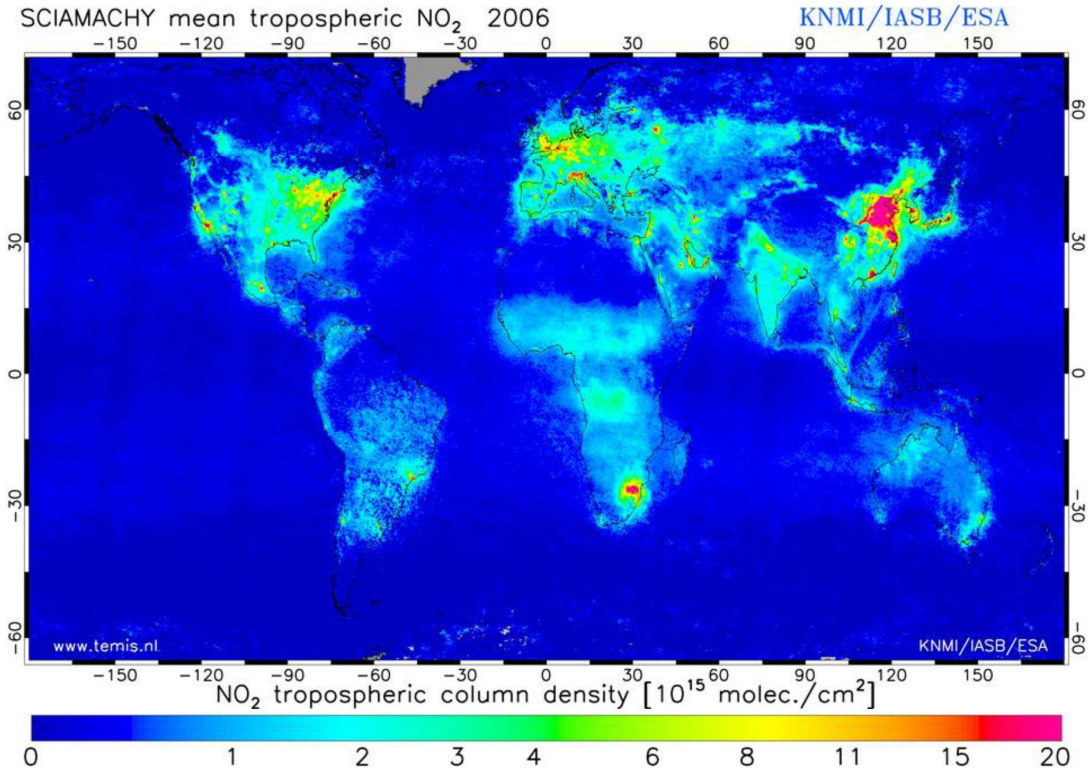


Figure 2: The mean tropospheric column density for 2006 derived from the SCIAMACHY instrument (Collett *et al.*, 2010)

A Geographic Information System (GIS) has the ability to integrate various datasets over different spatial and temporal resolutions to provide answers on impacts and sensitivity studies. The greatest strength of a GIS lies in the ability to visualise spatial features and relationships. Knowledge of the location and description of objects as well as their relationship to other objects or features is important for effective management, planning, operational and investment decisions (Schuurman, 2004).

This technology provides the capability for the refinement of modelled data and enables the development of one dataset from the several independent air quality datasets which exists for the Highveld region. Maps generated by this tool provide an indication of potential risk to human health and ecosystems on the Highveld. This information can be utilised to inform and influence future development in this area.

Currently there is a growing awareness on environmental issues such as global scale air pollution, global climate change and the depletion of natural resources. In

South Africa the concerns about emissions from coal-fired power generation is increasing due to the awareness on human health related problems emanating from the release of gaseous emissions into the atmosphere (Priest *et al.*, 1981). This has resulted in the establishment of stringent environment standards by the government for the regulation of pollutant emissions (Department of Environmental Affairs, 2009). Industries are now forced to formulate and implement effective environmental management policies.

1.2.1 LIMITATIONS OF AMBIENT MONITORING FOR EXPOSURE ESTIMATION

Generally ambient air pollution monitoring has been used to assess exposure for human health studies (Bell, 2006) as it is the only direct method to obtain the ambient concentration of the pollutant of interest. Instruments are placed to answer specific questions which results in accurate temporally resolved information but there can be limitations.

The ability to site locations for ambient air quality ground monitors is limited by the requirement for resources such as electricity and surrounding land use or ownership issues. This implies that ambient ground monitors may not be located in the best spot for assessment of a particular area or source. The accuracy of results derived from ambient monitoring is dependent on the limitations of the instruments used, as well as any human error that may occur during maintenance and calibration of the analysers (Ramandh, 2011).

Ambient monitors are most likely to over estimate the true impact of air pollution on human health as the devices do not have the capability of accommodating for personal activity patterns (Bell, 2006) for example time spent away from the area being monitored for work or a vacation away.

If there are budget constraints within a project then another limitation can be that monitored data may lack adequate spatial coverage over an area (Zunckel *et al.*, 2006; Ramandh, 2011) and ambient monitors may not provide full temporal coverage for a range of pollutants (Bell, 2006).

1.2.2 THE ADVANTAGES OF AIR DISPERSION MODELLING FOR EXPOSURE ESTIMATION

Air quality dispersion models are developed theoretically, tested against measured environments and then refined to best account for local climatic conditions. It is an attempt to describe the interrelation between emissions, atmospheric concentrations and deposition using a set of mathematical equations that simulate these conditions. Air quality modelling is able to overcome some of the limitations discussed in 1.2.1.

Model data typically provides information on air quality at a high spatial and user specific temporal resolution. The cost of predicting air pollution concentrations with an air quality model is generally lower than the costs to operate a network of ambient monitoring stations. Models are excellent at evaluating source and receptor relationships (Turner, 1994; Ramandh, 2011) and allow users to evaluate the results of multiple scenarios on several locations in a manner where variables can be controlled (Holloway, 2005).

Real-time models enable a rapid assessment of the impacts that may result from an air pollution incident as models can be utilised for improved siting of both mobile and fixed ambient air quality monitors and they permit analysis of historic, current or future scenario assessments (Scorgie and Venter, 2005; Zunkel *et al*., 2006).

Improving the accuracy of modelled concentration fields will ultimately assist in better air quality predictions for the Mpumulanga Highveld region.

1.2.3 LIMITATIONS IN DISPERSION MODELLING

Essentially model results are estimates of pollutant concentrations. The accuracy of the model predicted estimates are dependent on three main sources of errors consequential from incorrect input emissions data, inaccurate meteorological data and inadequate scientific formulation of the model (Douglas, 1982; Koosialee, 2006). Since model inputs are only estimates, even the most sophisticated models will

have inherent uncertainties and will have the potential to underestimate or overestimate actual concentrations (U.S.EPA 2005).

There is a possibility that the emissions data that are used as input into the models could be inaccurate due to incorrect source strengths and locations; unaccounted for time variability in emission rates; uncertainties in stack parameters, and incorrect calculations of plume rise after emission (U.S.EPA, 2002; U.S.EPA, 2005).

The inaccuracies associated with the meteorological data could be due to incorrect wind speed and direction; poorly defined dispersion parameters; incorrect determination of the atmospheric thermal structure and non-representativeness of the data from the meteorological surface station with respect to the site of the pollutant source (Douglas, 1982; Michael *et al.*, 1996; Raghunandan *et al*., 2006).

There is a likelihood that the air quality model itself might not be representative of the problems being analysed due to incomplete knowledge of chemical and physical interactions of gases and particles; incorrect formulations of removal processes and poorly specified boundary conditions (Seinfeld and Pandis, 1998). In addition, uncertainty may be associated with the terrain specification for example, the use of a model designed for flat terrain will provide inaccurate estimates of concentrations if it is applied to an area containing complex topography (Carvalho and Degrazi, 2002; U.S.EPA, 2004).

Therefore the extent to which a user has reliable information on emissions data, meteorological data and the correct model physics set-up will influence the accuracy of the model predicted concentrations.

1.2.4 THE ADVANTAGES AND LIMITATIONS OF USING SATELLITE RETRIEVALS FOR ASSESSING GROUND LEVEL TRACE GASES

One of the major challenges is the derivation of good quality quantitative tropospheric NO_2 column amounts for individual ground pixels based on the satellite retrieval. The retrieval of tropospheric trace gas species by satellites are characterised by large uncertainties related to errors caused by measurement noise and spectral fitting, affecting the calculation of the slant column density, errors related to the separation of stratospheric and tropospheric NO_2 affecting the estimate of the stratospheric slant column and errors due to uncertainty in model parameters such as clouds, surface albedo and a *priori* profile shape of the trace gas, affecting the tropospheric air mass factor calculation (Boersma *et al.*, 2004; Jeffery et *al.*, 2005; Sierk *et al.*, 2006; Martin, 2008 ; Josipovic, 2009).

The largest uncertainties are due to clouds, as they will shield near-surface NO_2 from the view of the satellite. The retrieval depends very sensitively on the presence of clouds and even small cloud fractions (between 5 to 20%) have a major impact. High quality observations of the cloud properties (cloud fraction and cloud top height) are necessary for a quantitative retrieval (Boersma *et al.*, 2004; Jeffery *et al.*, 2005).

High quality albedo maps in the relevant spectral range are essential since the surface albedo directly influences the sensitivity of SCIAMACHY for boundary layer NO_2 (Boersma *et al.*, 2004).

Profiles of some trace gases for example NO_2 are characterised by a large range of variability. At emission areas the NO_2 concentration will peak at the surface, while downstream of such areas the pollution plume will peak at higher altitudes. The profile of NO_2 will be determined by aspects like the distribution of emission sources, the stability and height of the boundary layer, wet removal of nitric acid, deep convection and long-range transport by the wind. All these factors are strongly varying in time and space (Sierk *et al.*, 2006; Josipovic, 2009; TEMIS, 2011).

The stratospheric background of trace gases have to be cautiously quantified in order to derive the tropospheric column. A common approach applied to most satellite retrievals is the assumption that stratospheric trace gases for example NO_2 and SO_2 is

zonally uniform, or have only a small longitudinal variation. Such simplification makes the retrieval of small tropospheric NO_2 and SO_2 columns difficult (Bridhikitti, 2011 and Boersma *et al.*, 2005). This is a result of firstly the neglect of the vertical layer that may occur in the atmosphere and secondly the fairly large horizontal footprint does not capture the small or medium scale horizontal variability.

Another source of uncertainty is aerosols. Thick aerosol layers influence the radiation field and the sensitivity of satellites for example Global Ozone Monitoring Equipment (GOME) and SCIAMACHY for near-surface retrievals of trace gases (Boersma *et al.*, 2004; Martin, 2008; Jeffery et *al.*, 2005; Sierk *et al.*, 2006) .

Even though the current satellite measurements of tropospheric trace gases do not achieve the accuracy required for measuring regulated surface air pollutant concentrations, satellite observations are useful for emission characterisation and support assessment of long-range pollutant transport and background concentration using global-scale models (Hidy *et al.*, 2009, Kaynak, 2009, Mijling, 2012. Estimating the strengths of high pollution events is another advantage from satellite retrievals. It is also a practical method of obtaining emission information from remote regions such as Amazonia and Antarctica. Satellite derived products are useful not only in the absence of ground level and airborne in situ data but can be used to refine or corroborate such data (Vijayaraghavan *et al*., 2008).

Satellite remote sensing provides a means to derive trace gas concentration estimates on an on-going basis at global scales. Long time series of satellite retrievals give insight on how human activity contributes to changes of atmospheric composition affecting human health and climate (Mijling, 2012). The wide spectral range of channels together with global coverage and enhanced spatial resolution provides sufficient information for retrieving total column concentrations of various trace gases simultaneously and are widely used for general circulation models and climate studies. (Li *et al.*, 2005). The availability of these observations enables us to extensively evaluate air quality models and to assess model and observation strengths and limitations and to use these observations in order to improve emission inventories (Kaynak, 2009).

1.3 AIMS AND OBJECTIVES

The overarching aim of this dissertation is to improve SO_2 and NO_2 modelled air quality predictions using measured data. The ultimate objective is to be able to credibly predict concentrations without reference to fixed ground based monitoring stations.

The objectives of this study are to:

(i) Compare the CALPUFF model results to ground based measurements of SO_2 and NO_2 concentrations;
(ii) Evaluate the representativeness of satellite retrievals to surface concentrations of SO_2 and NO_2;
(iii) Integrate available ambient air quality datasets derived from the different methods of air quality monitoring and modelling in the Mpumalanga Highveld region;
(iv) Improve modelled ground level air pollution concentration fields by utilising measured data;
(v) Identify the hot spots for potential harm to human health and ecosystems from power station emissions based on the results of the new modelling outputs.

1.4 STRUCTURE OF DISSERTATION

Chapter 2 provides an overview of the study area. It gives a general description of the study area and outlines the dispersion potential of the Highveld. **Chapter 3** discusses the literature review of this study. It describes the atmospheric pollution sources and chemistry of the Highveld. Geographic information systems, dispersion models and ambient air quality standards are also explained. Chapter 3 is concluded with the description of the consequences of atmospheric pollution on human health and vegetation.

Chapter 4 and **Chapter 5** explain all datasets and methodological approaches utilised in this study. The results are presented and discussed in **Chapter 6**. This includes validation of SCHIMACHY satellite retrievals and an evaluation of the CALPUFF modelled outputs. Maps produced from the analysis of potential risk to SO_2 and NO_2 emissions on human health and ecosystems are presented. In **Chapter 7** the key findings are summarised and conclusions outlined.

****

With the above mentioned objectives (section 1.3) in mind the literature examining the atmospheric pollution sources of SO_2 and NO_2, chemistry, meteorology, transport of trace gases and environmental and health impacts are presented in the next chapter. Air dispersion modelling as well as air quality legislation and GISs are also discussed.

CHAPTER 2
OVERVIEW OF STUDY AREA

This chapter presents a general description of the geographic, topographic and climatic characteristics of the study area together with the meteorology and transport of trace gases in the Highveld region.

2.1 GENERAL DESCRIPTION OF STUDY AREA

2.1.1 LOCATION OF INDUSTRIALISED HIGHVELD

Whilst the Highveld region covers an area of approximately 400 000 km^2 this study only focused on the industrialised Highveld region (Figure 3). The industrialised Highveld region covers an area of approximately 30 000 km^2 at an altitude of approximately 1 700 m above sea level (Wells, *et al*., 1996 and Collett *et al.*, 2010). It constitutes most of the Gauteng province and parts of the Mpumulanga, Free State and North West provinces. Due to the abundance of coal and minerals found on the Highveld, the region has developed into a significant industrial hub in South Africa.



Figure 3: The industrialised Highveld region (outlined in blue)

The industrialised Highveld comprises of three metropolitan municipalities (City of Johannesburg, City of Tshwane and Ekurhuleni) and two district municipalities (Sedibeng and West Rand) located in the Gauteng Province, three district municipalities (Gert Sibande, Nkungala and Ehlanzeni) located in the Mpumalanga Province, two district municipalities (Bonjanala and Dr. Kenneth Kunda) in the North West Province and Fezile Dabi District Municipality in the Free State.

Major towns occurring within this region include eMalahleni, Middelburg, Secunda, Balfour, Standerton, Johannesburg, Tshwane, Germiston, Sasolburg, Vereeniging, Randfontein, Rustenburg and Klerksdorp.

2.1.2. TOPOGRAPHY & LAND USE

In terms of the regional scale topography the Highveld plateau slopes gradually downward towards the west and south. To the east lies the Drakensburg escarpment and to the south is the Vaal basin about 1400m above mean sea level, which tends to drain cold air from the surrounding high-lying plateau of the Gauteng Province (Held *et al.*, 1996). The industrialised Highveld is relatively flat with elevations ranging from 1100 m to approximately 1700 m (Figure 4). The slope from East to west is approximately 1,4°. The generally flat terrain is interspered with relatively low hills and rocky outcrops (Department of Environmental Affairs, 2011).

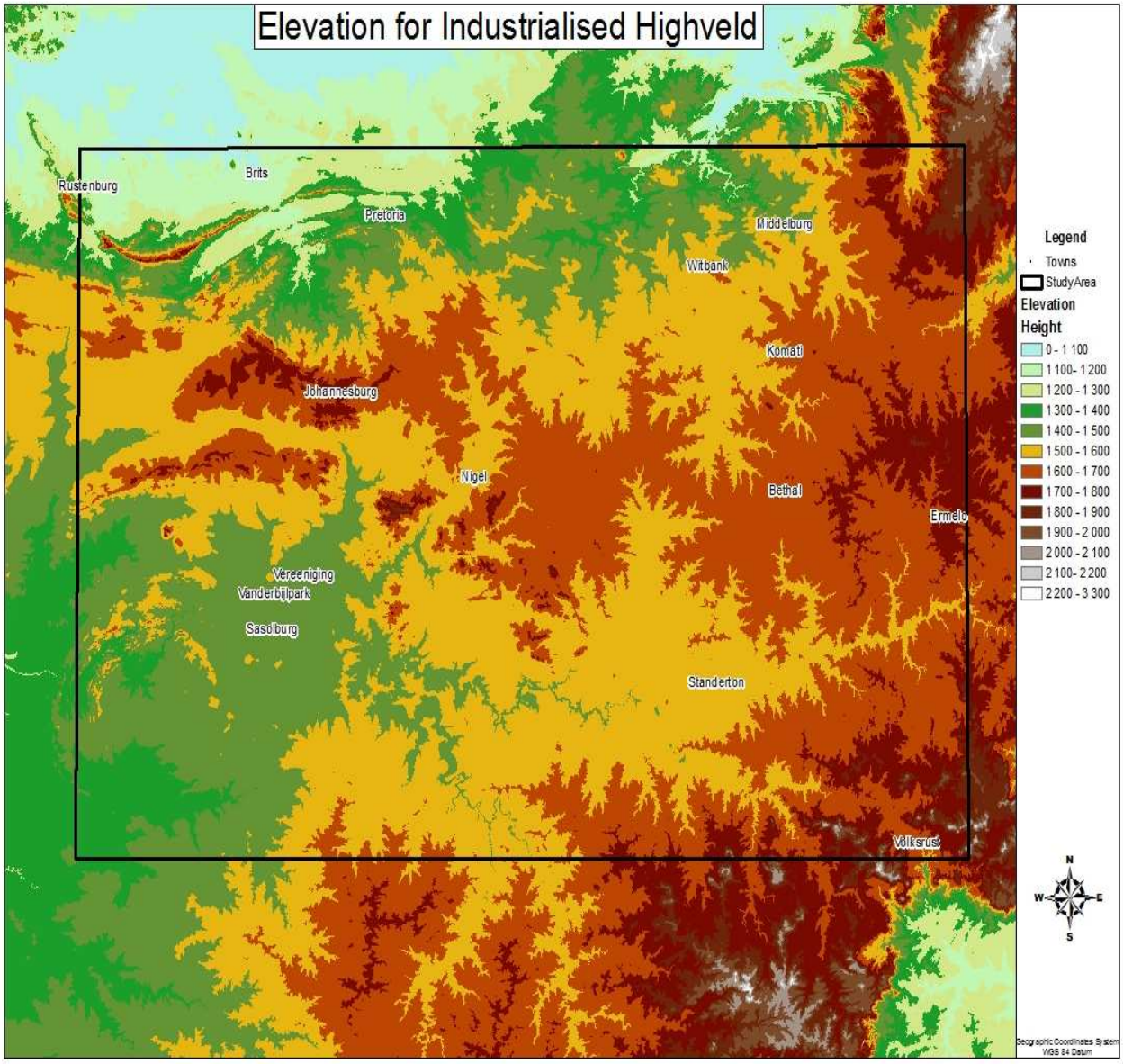


Figure 4: Topography of the industrialised Highveld region

Approximately 70% of the industrial Highveld region is characterised by the grassland biome (Figure 5) and the reminder is utilised for agricultural, urban, mining and industrial activites (Collet *et al.*, 2010, Ramandh, 2011). Urban and built up areas occur throughout the industrial Highveld and make up approximately 8.5% of the total land cover. The most extensive built up areas occur in the metropolitian municipality of the Ekurhuleni, City of Johannesburg and City of Tshwane with other significant areas are found in the larger settlements such as eMalahleni, Middelburg, Ermelo, Standerton, Secunda, Balfour, Delmas, Sasolburg, Vereeniging, Vanderbjil Park, Brits, Volksrust and Klerksdorp. Mining constitutes approximately 2% of the total land cover.

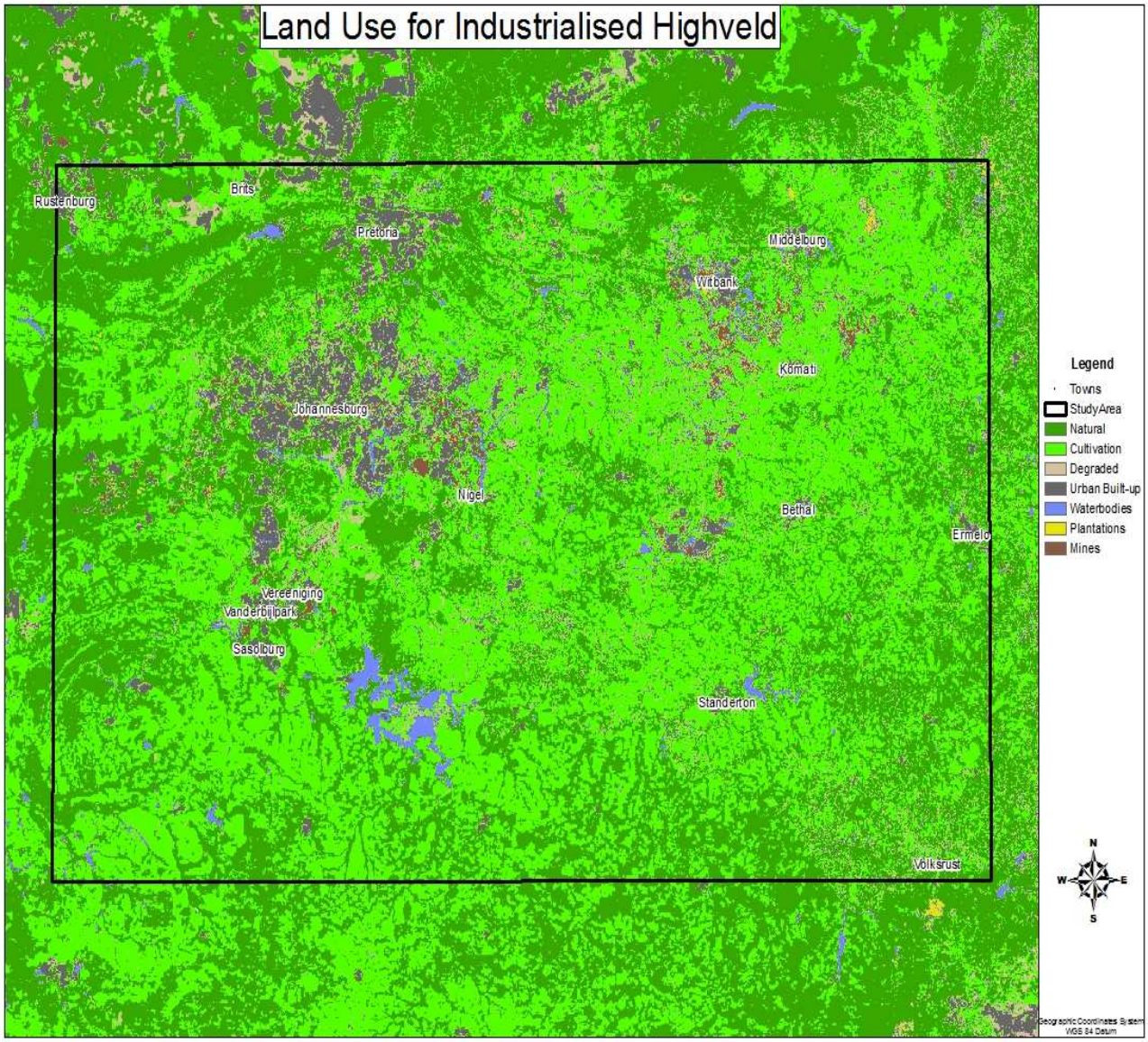


Figure 5: Land use characteristics of industrialised Highveld

2.1.3 CLIMATE

The Highveld region is a summer rainfall region, receiving an annual rainfall of approximately 400-700 mm (Weiner and Harris, 2003). Substantial afternoon thunderstorms occurr mostly in the months of November, December and January with frost in winter.

The average temperatures in the Highveld are mild throughout the year with slightly cooler temperatures in winter. The long term average (1903-1984) maximum

temperature is 27.5°C in summer and 19°C in winter, with extreme maxima of 27.8°C in summer and 21°C in winter (Schulze and Turner, 1996).

2.1.4 POPULATION

According to Census 2011 data (Table 1) the total population of the industrialised Highveld is an estimated 10 534 785 individuals.

Table 1: Population distribution (StatsSA, 2012)

Province	District	Population	Population density (per km^2)
North West	Bonjonala Platinum	1 507 505	82.2
	Dr Kenneth Kaunda	695 933	47.5
Free State	Fezile Dabi	488 036	22.9
Gauteng	Ekurhuleni Metropolitan Municipality	3 178 470	1 652.0
	City of Johannesburg Metropolitan Municipality	4 434 827	2 695.9
	City of Tshwane Metropolitan Municipality	2 921 488	460.4
	Sedibeng	916 484	219.4
	West Rand	820 995	200.9
Mpumalanga	Ehlanzeni	1 688 615	60.5
	Gert Sibande	1 043 194	32.8
	Nkungala	1 308 129	78.1

The Gauteng portion of the industrial Highveld area is home to 71% of the region's population (Ekurhuleni, City of Johannesburg and City of Tshwane). Due to the small land mass contribution made by the Gauteng municipalities, together with the large population figures, the highest population density also occurs there as well. Within the Mpumalanga portion of the industrial Highveld region, the highest

population figures occur in the Mbombela and Bushbuckridge Local Municipalities within the Ehlanzeni District Municipality (StatsSA, 2012).

The 2007 Community Survey conducted by StatsSA, showed significant population increases in the major urban centres of the Highveld region. The large increases in populations within the more developed Mpumalanga regions can be attributed to rural to urban migration. This is confirmed by the decrease in population figures of the less urbanised regions. The reasons for the migration to urban centres are due to the prospects of better employment opportunities becoming available as more industrialisation takes place. As more people move to urban centres, the quality of education and general service delivery improves, making urban centres more attractive destinations (Department of Environmental Affairs, 2011).

2.2 METEOROLOGY OF THE STUDY REGION

The state of the atmosphere determines the rate at which pollution will accumulate and disperse. Once substances have been emitted into the atmosphere the determinant of its dispersion is meteorological and the dilution is a function of wind velocity and atmospheric stability (Tyson *et al*., 1998 and Piketh, 1994).

2.2.1 MACRO SCALE SYNOPTIC CIRCULATIONS

Due to southern Africa's location in the subtropics, it is affected by circulation systems originating in both the tropics to the north and mid-latitudes to the south. Simultaneously it is dominated by semi-permanent, subtropical high-pressure cells of the general circulation of the southern hemisphere. Five synoptic scale circulations affect the circulation over southern Africa at a macroscale which allows for the transport of air and any pollutants contained within over larger distances. These include continental anticyclones, easterly troughs, westerly waves, cut-off lows and ridging anticyclones (Figure 6). The frequency of occurrence of each of these circulation patterns varies seasonally (Tyson and Preston-Whyte, 1988; Tyson *et al*, 1998; Tyson and Preston-Whyte 2000).

The continental anticyclonic circulation occurs up to 70% of the time in winter and 20% in summer making this type of synoptic circulation the most prevalent circulation over southern Africa (Tyson *et al*., 1996a). Easterly waves show an annual cycle, peaking in summer and almost never occurring in winter. Transport associated with ridging highs and westerly waves shows little annual variation; however these westerly waves occur with greater frequency during winter on the Highveld (Garstang *et al*., 1996; Tyson *et al*., 1996a, 1996b).

Anticyclonic circulation and westery disturbances result in the transport of air from Africa to the south east over the Indian Ocean in the Natal plume. This anticyclonic flow results in recirculation, which may remain in the continent or extend over and return from the Indian Ocean. Easterly wave conditions favour transport to the west over the tropical Atlantic Ocean in the Angolan plume. Transient mid-latitude ridging anticyclones result in maxium transport orginating in the mid-latitudes and flowing towards the southern Atlantic Ocean (Piketh and Walton, 2004).

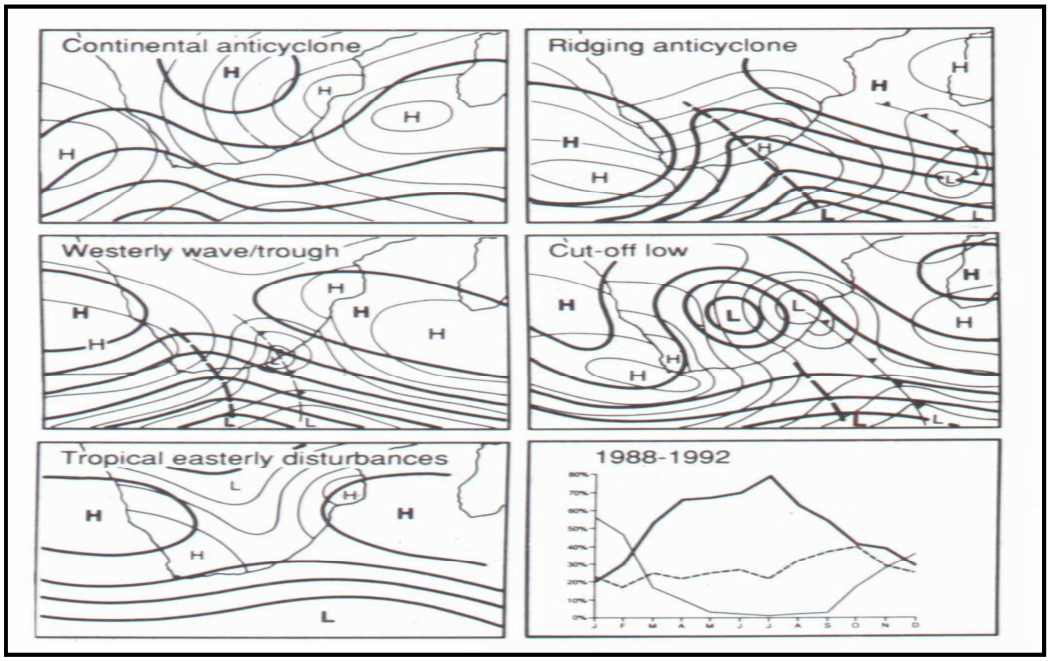


Figure 6: Major synoptic circulation types affecting southern Africa and their monthly frequency of occurrences over a five year period (Preston-Whyte and Tyson, 1988)

2.2.2 TRANSPORT OF TRACE GASES OVER THE HIGHVELD

Substances emitted high into the atmosphere or at near ground level are transported by the same patterns as the air in circulation. Vertical transport is determined by the stability of the atmosphere and horizontal transport by the local topographic winds near the surface or by macroscale synoptic circulation (Garstang *et al*., 1996; Piketh *et al*., 1998; Tyson and Preston-Whyte, 2000).

2.2.2.1 Local, Mesoscale & Macroscale Transport

When boundary layer conditions become stable and inversions begin to develop then cold air will drain into hollows and valleys. The development of local topographically-induced circulation is complex and depends on duration as well as the depth and orientation of the valley. In valleys, the daytime circulations are likely to be up-slope and vice versa for night time circulations. During the day up-valley winds develop and conversely at night down-valley mountain winds blow. During winter and at night such circulations influence the low-level flow field and control the transport of ground emissions of pollution (Tyson *et al.*, 1988).

Shallow mountain-plain and plain-mountain drainage winds occur over the Highveld (Held, 1985; Garstang *et al*., 1985). When pollution from the Highveld is advected over the Escarpment at night, it is advected in a highly stable layer of air draining eastward towards the Lowveld. During the day, the opposite occurs and advection is towards and over the Escarpment in a deeper and more unstable system. To the east of the Highveld, stable mountain-plain winds transport pollution in visible plumes for distances greater than 150 km (Tyson *et al.*, 1988).

Nocturnal mesoscale transport also occurs over the Highveld during surface-inversion conditions over flat terrain in the absence of local winds as air flow decouples at the top of an inversion layer. Low-level jets form as the roughness of the ground surface is replaced by the relative smoothness of the inversion top and rises as the inversion deepens. Any pollutants trapped near the top of the inversion layer are transported away from the source area to distances of 300-500 km per night (Tyson and Preston-Whyte, 2000).

The extent to which synoptic systems and weather disturbances impact on the dispersion potential of the atmosphere is dependent on the height and persistence of elevated inversions. Elevated inversions reduce the height at which pollutants are able to mix and have a strong potential to trap particulate aerosols and trace gases thereby inhibiting the vertical movement of pollutants. These inversions influence both the recirculation of pollutants and influence long-range transport (Department of Environmental Affairs, 2011).

The most common type of elevated inversion that occurs over South Africa is the subsidence inversion. This inversion usually occurs in winter and is associated with the reduction in the atmospheric dispersion potential which results in the accumulation of pollutants over the Highveld (Zunckel *et al.*, 2007).

Cosjin and Tyson (1996) indentified three major and frequently occurring elevated inversions that control the vertical transport of pollutants in the subtropical troposphere at the end of the dry season (August-September). These inversions occur at approximately 3 km, 5 km and 8 km above sea level with mainly the 5 km inversion layer acting as the dominant barrier preventing the vertical movement of pollutants.

Convergence of the upper air impedes the formation of inversions. Cyclonic disturbances are usually associated with the dissipation of inversions, pre-frontal conditions tend to lower the base of elevated inversions thereby reducing the mixing depth. After the passage of a cold front, the mixing depth gradually increases (Scott and Diab, 2000).

SYNOPTIC-SCALE TRANSPORT

The four major transport pathways of air moving to the Highveld region include the flows of the Atlantic Ocean , Indian Ocean, African continent and subcontinent (Figure 7). The Atlantic Ocean flow has the largest frequency of occurency (43 %) followed by the Indian Ocean and African continent, both with 26 % and subcontinental flow of 7% (Frieman and Piketh, 2003). The Atlantic Ocean flow reaching the Highveld region is unlikely to contain industrial pollutants whilst the

African continental transport may bring pollutants from the Zambian copper-belt, biomass burning products in winter and aerolian dust to southern Africa. The Indian Ocean transport carries industrial aerosols and trace gases into the region (Piketh, 1994).

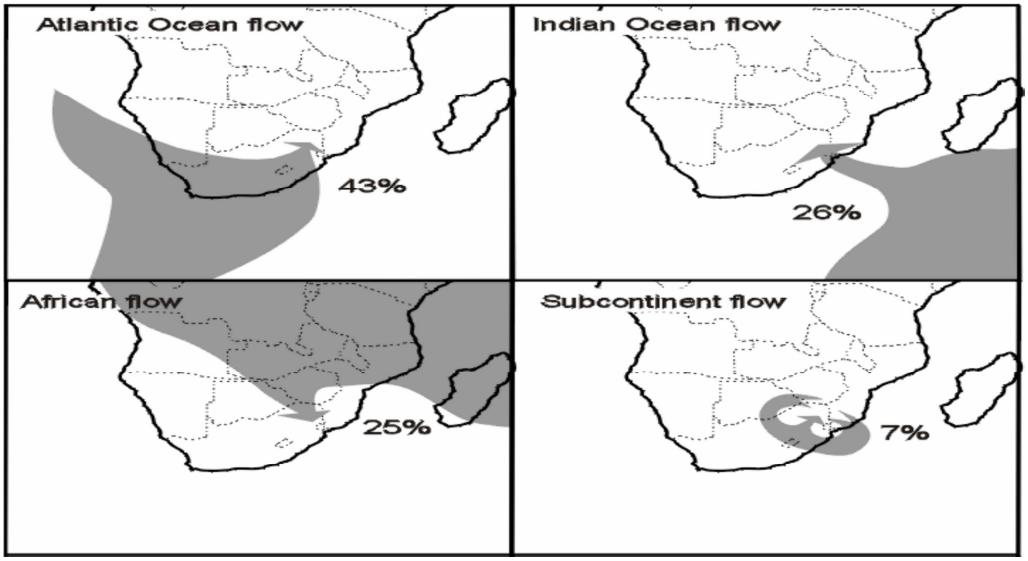


Figure 7: Transport pathways advecting air to the Mpumalanga Highveld region (Frieman and Piketh, 2003). The shaded arrows indicate trajectories between 850 hPa and 500 hPa.

The five major transport pathways of air moving away from the Highveld include Indian Ocean plume, recirculation, southern African plume, Central African plume and Cape plume (Figure 8). The Indian Ocean plume persists for 48 % of the time followed by recirculation 32%, southern African plume 12%, Central African plume 6% and the Cape Plume (1%). The Indian Ocean plume is dominant during winter and autumn but during the summer and spring months its frequency is of the same magnitude as that of the recirculation plume (Piketh and Prangley, 1998).

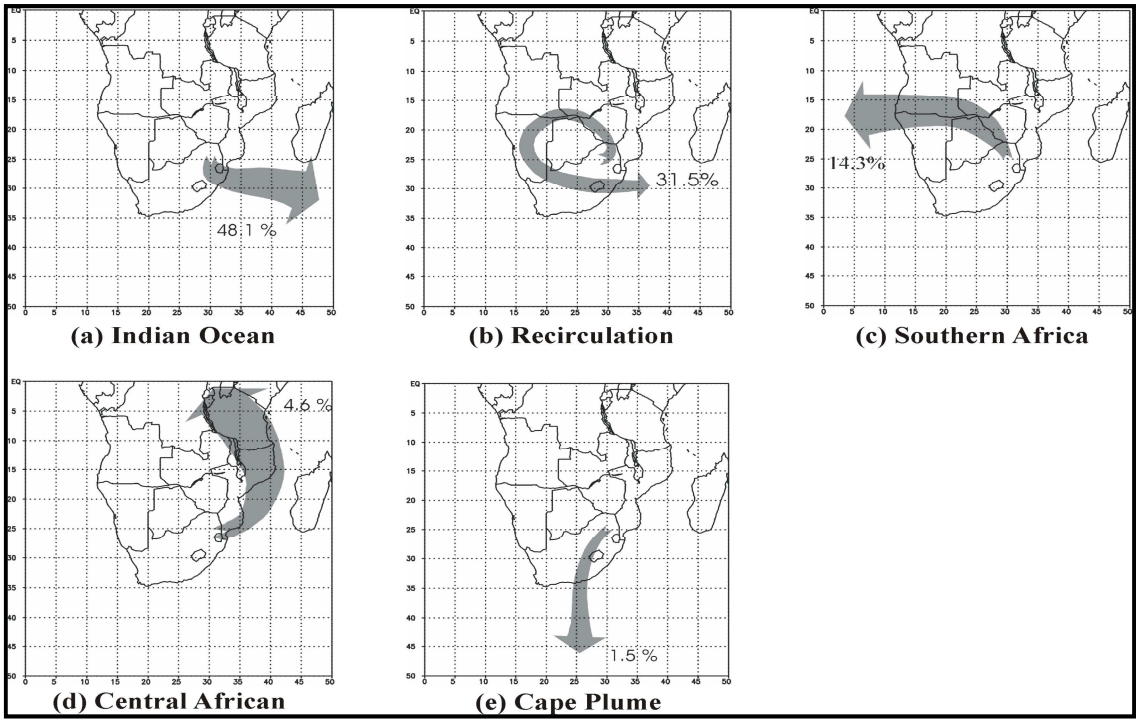


Figure 8: Five transport pathways from the industrialised Highveld region (Piketh and Prangley, 1998). Percentages represent the annual percentage of flow from a five year period.

The dominant transport pathway of air with its constituents is towards the east coast and out over the Indian Ocean in a distinct westerly plume. On average it takes approximately 4 to 5 days to reach 40˚ E over the Indian Ocean. Recirculation back over southern Africa is brought about by anticyclonic circulation, mainly associated with transient ridging highs that follow the passage of westerly waves and cold fronts (Tyson and Preston-Whyte, 2000; Terblanche *et al*., 2000; Piketh, 2002).

Frieman and Piketh (2003) estimate that approximately 41 % of all air transported from the region affects South Africa's neighbouring countries. The polluted air from South Africa also circulates over South Africa or flows northwards over Africa (Figure 8). The dominant eastward flow is evident as a well-defined plume that has been found to eventually pass south of Australia, such that in winter 30% of South African air is found in the Australian vicinity. With weaker westerlies during summer, the occurrence of this plume in the Australian region is less frequent and more air recirculates and exits towards to equator (Tyson and Preston-Whyte, 2000; Freiman and Piketh, 2003).

****

The industrialised Highveld region covers an area of approximately 30 000 km^2 at an altitude of approximately 1 700 m above level (Wells, *et al*., 1996). It constitutes most of the Guateng province and parts of the Mpumulanga, Free State and North West provinces. Due to the abundance of coal and minerals found on the Highveld, the region has developed into a significant industrial hub in South Africa.

In terms of the regional scale topography the Highveld is relatively flat with elevations ranging from 1100 m to aproximately 1700 m. Approximately 70% of the region is characterised by the grassland biome and the remainder is utilised for agricutural, urban, mining and industrial activities (Collet *et al*., 2010, Ramandh, 2011). The Highveld region experiences most of it's rainfall in summer and the average temperatures are mild throughout the year with slightly cooler temperatures in winter. The total population is estimated at 10 534 785 individuals (StatsSA, 2012).

Over southern Africa transport of pollutants occurr both vertically due to convection and horizontally due to synoptic scale circulations or by locally induced topographic winds near the surface.The five major transport pathways of air moving away from the Highveld include Indian Ocean plume, recirculation, southern African plume, Central African plume and Cape plume (Piketh and Prangley, 1998). Pollutants released into the atmosphere at ground-level are transported over long distances by large-scale air fields and dispersed by small-scale turbulence.

This chapter has provided a summary of the topography, land use, population distribution, climatology and meteorology of the Highveld. The next chapter presents the literature review that is applicable to this study.

CHAPTER 3
LITERATURE REVIEW

This chapter presents a description of the atmospheric pollution sources, chemistry over the Highveld region, air dispersion modelling and geographic information systems. The discussion on ambient air quality guidelines and standards for SO_2 and NO_x provides a legislative framework to prevent or reduce harmful effects on human health and ecosystems.

3.1 ATMOSPHERIC POLLUTION SOURCES

Air pollutants are either natural constituents of the atmosphere or result from anthropogenic activities. Pollutants can be potentially harmful to the environment, health of humans and ecosystems. Knowledge of atmospheric pollution sources and levels is essential for the assessment of the air quality in an area and exposure risk for man and the environment.

3.1.1 POLLUTION SOURCES ON THE HIGHVELD

The Highveld is seen to be one of the most polluted regions in southern Africa due to the primary economic activities which include mining, electricity generation, agriculture and forestry. The number of sources registered under the Atmospheric Pollution Prevetion Act (Act 45 of 1965) shows a dominance of industrial processes in Ekurhuleni. Other industrialised municipalities include eMalahleni, Steve Tshwete, Musukaligwa and Govan Mbeki (Department of Environmental Affairs, 2011).

The manufacturing industry is the largest secondary activity contributing to the atmospheric pollution in this region. Within the manufacturing sector, important sub-sectors include wood and wood products, basic iron and steel, chemicals, metallurgical refineries and paper and pulp. The petrochemical sector source inventory is dominated by Sasol's Secunda operations. This is reportedly the largest

industrial chemical complex in the southern hemisphere. The significance of metal containing ores of the Bushveld igneous complex in proximity to the abundant coal reserves in the Highveld region has resulted in numerous metallurgical operations. These consist of primary beneficiation operations as well as secondary operations manufacturing higher value goods. Some of the larger ferro-alloy operations include Highveld Steel, Samancor Chrome, Transalloys, Vanchem, Ferrometals, Rand Carbide, Scaw Metals and Acelor Mittal. Although coal mining dominates the mining sector minerals such as gold, platinum, chrome, asbestos, magnesite, iron ore, vanadium, limestone, dolomite and silica are mined at a large scale (Department of Environmental Affairs and Tourism, 2003; Department of Environmental Affairs, 2011).

The Highveld is the main coal producing region in South Africa and approximately 95% of the country's electricity requirement is generated by coal fired-power stations (Department of Environmental Affairs and Tourism, 2003 and Department of Environmental Affairs, 2011). Fifteen of South Africa's operational coal fired power stations are situated in the Highveld region. Coal is also burnt in industrial plants such as petrochemical works, smelters and manufacturing industries on the Highveld. These plants emit approximately 1.7 - 2 million tons of SO_2 annually and account for 94 % of all South Africa's SO_2 emissions (Piketh *et al*., 2003). By contrast, power generation contributes 73% of the total estimated NO_x emission of 978 781 tons per annum (Department of Environmental Affairs, 2011). The hydrocarbon fuel process plants together with the open-cast coal mines adjacent to the power stations are added sources of several sulphur based pollutant compounds within the area (Igbafe, 2007). These various source types release huge amounts of hydrogen sulphide and SO_2 gases per year especially during winter as the demand for electricity increases this leads to an increase in the amount of coal burnt (Snyman *et al*, 1990).

Besides power station and industrial uses, coal is utilised for domestic heating and cooking in informal and township areas. Although electricity is used where available, it is noteworthy that a range of other factors such as neighbourhood culture, tradition and fuel cost plays a role in the continuing use of "dirty" fuels. Combustion of coal and wood, and in some areas paraffin, remains the most prevalent energy sources in the dense low-income settlements.

Domestic coal burning is a significant source of low-level fine particulate matter ($PM_{2.5}$ and PM_{10}) and contributes significantly to SO_2, carbon monoxide (CO), total organic compunds and benzene emissions. Greenhouse gas emissions are also produced when fuels are combusted in residential appliances, including, but not limited to, carbon dioxide (CO_2), methane (CH_4) and nitrous oxide (N_2O). Pollutants from the combustion of wood (including veldt fires) include respirable particulates, NO_2, CO, polycyclic aromatic hydrocarbons, particulate benzo(a) pyrene and formaldehyde (Department of Environmental Affairs, 2011).

Other near ground sources of air pollution include smouldering coal dumps and motor vehicles. Emissions from motor vehicles arise during the different cycles of driving from start-up, during driving, evaporation from the engine and during re-fuelling. NO_x is formed by the reaction of nitrogen and oxygen under high pressure and temperature conditions in the engine. SO_2 results from the sulphur in the fuel. The amount of emissions released from motor vehicles are dependent on the distance travelled, speed of travel, age of the vehicle, the type of fuel used and the emission abatement technology of the car. Emissions can differ from vehicle to vehicle (Department of Environmental Affairs, 2011).

Emissions are released from airports due to a range of activities including the aircraft operations ground support equipment, vehicular traffic at the airport's roadways, parking lot, electrical generators and fuel storage facilities. The main pollutants include carbon monoxide (CO), NO_x, SO_2, particulate matter and hydrocarbons such as benzene, toluene, ethyl benzene and xylene (Department of Environmental Affairs, 2011). It is important to characterise the emissions from major airports when assessing air quality in a region.

The Oliver R Tambo International Airport located in Ekhuruleni is a major international and domestic airport, covering a significant area and including a number of different source types. Other smaller airports on the Highveld include Grand Central in Midrand, Rand Airport in Germiston and Lanseria near Randburg.

The contribution of these sources and lightning as a major source of NO_x, to the overall air quality of the Highveld should not be overlooked, particularly in the view of the weak atmospheric dispersion potential of the lower atmosphere of the region (Tyson *et al.*, 2000). Lightning is the largest natural source of NO_x on earth and contributes approximately 12% of the total NO_x emissions globally (Lee *et al*., 1997). According to Wenig *et al*. (2003) lightning accounts for approximately 25% of tropospheric NO_x over the Highveld. The estimates of lightning vary substantially because lightning is an uncertain source of NO_x and mainly occurs in the upper tropospheric region. Brunner *et al*. (1998) observed large scale NO_x plumes downwind of thunderstorms, but concluded an uncertainty as to whether this was created by lightning or if it was attributed to NO_x upliftment from the ground.

In winter (from the months of July to September) emissions from biomass burning contribute to the air pollution on the Highveld. Pyrogenic emissions affect the atmosphere in several important ways by influencing greenhouse warming, the oxidising capacity of the troposphere, the acidity of the troposphere, stratospheric ozone depletion and light scattering and absorption (Kirchstetter *et al*., 2003 and Sinha *et al*., 2003).

African fires are responsible for an average of approximately 30 to 50% of the total amount of vegetation burned globally each year, making Africa, the single largest biomass burning emissions source (van der Werf *et al.*, 2003; van der Werf *et al.*, 2006; Roberts *et al.*, 2008). It is typically characterised by a prolonged winter dry season, preceded by summer periods with relatively fast rates of plant growth, leading to fuel accumulation that create conditions conducive to frequent fires. Veld fires commonly occur on the Highveld and are regarded as one of the major sources of NO_x in the study area (Department of Environmental Affairs, 2011).

Emissions from biomass burning include a wide range of gaseous compounds and particles that contribute significantly to the tropospheric budgets on a local, regional and global scale. The emission of CO, CH_4 and volatile organic carbons (VOCs) affect the oxidation capacity of the troposphere by reacting with OH radicles and emissions of nitric oxide and VOCs which lead to the formation of ozone and other photo oxidants. Biomass burning plays an important role in the biogeochemical

cycles of carbon and nitrogen. The emissions are also a source of a number of halogenated compounds such as methyl chloride and methyl bromide that are long lived enough to destroy the ozone in the stratosphere (Koppmann *et al.*, 2005).

3.2 ATMOSPHERIC CHEMISTRY

Several air pollutants have known or suspected harmful effects on human health and the environment. Air pollutants may not only exhibit problems in the immediate vicinity of their sources but can travel long distances, chemically reacting in the atmosphere to produce secondary pollutants such as particulate sulphate and nitrate.

The chemistry of the earth's atmosphere is dynamic and is affected by natural as well as anthropogenic sources and activities. The Highveld region has a significant contingent of anthropogenic activities that impact on atmospheric chemistry. Pollutants released on a significant scale include SO_2 and NO_2.

3.2.1 NITROGEN OXIDES & NITRATES

The oxides of nitrogen present in the atmosphere are nitrous oxide (N_2O), nitric oxide (NO) and nitrogen dioxide (NO_2). Atmospheric N_2O was discovered in 1938 by Adel via infrared absorption features in the solar spectrum. It is not a hazardous pollutant nor does it display any particular chemical activity. There are no gas-phase reactions that remove it from the troposphere. N_2O is an important agent in controlling the stratospheric ozone balance since ozone can be reduced catalytically via chain reactions (Warneck, 1988). It is also one of the greenhouse gases contributing to global warming.

Large quantitites of NO_X are emitted via power plants. The NO_X concentrations in power plant plumes are often high enough that ozone production near the plume source is prevented and there is substaintial loss of ozone through nitrations. As the plume moves further downwind, the concentrations are reduced and the production of ozone in the plume replaces the inital loss of ozone. Overall there is a tendency for

ozone to decrease with increasing NO_X concentrations as a result of ozone chemistry (Department of Environmental Affairs, 2011).

The higher oxides of nitrogen are formed in chemical processes such as nitrations, but the largest contributor is combustion at temperatures greater than 2000 k, whereby NO is formed (equation 1).

$2NO + O_2 \rightarrow 2\ NO_2$ (equation 1)

Most of the non toxic NO in the atmosphere is rapidly oxidised in the presence of O_3 molecules at equilibruim conditions to form NO_2 which is a toxic gas (equation 2) (Atkinson, 2000; Fenger, 2002).

$NO + O_3 \rightarrow NO_2 + O_2$ (equation 2)

Close to a source the NO/NO_2 ratios are high, but as oxidation occurs in the atmosphere, NO_2 becomes the dominant NO_X species (Webb and Hunter, 1998). During the day NO_2 absorbs wave lengths greater than 400 nm and undergoes photodissociation, producing NO and O which quickly bond to molecular oygen to form ozone (equation 3 and 4) (Warneck, 1988, Fenger 2002).

$NO_2 + h\nu \rightarrow NO + O$ (equation 3)

$O_2 + O + M \rightarrow O_3 + M$ (equation 4) *M represents an energy-accepting third body

In the above two-step process equal amounts of NO and O_3 would be produced. Simultanously the total amount of ozone is decreased by the reverse reaction with NO. The rate at which NO converts into NO_2 is highly variable as it depends on varying atmospheric factors such as time of day, disperion, stability and regional atmospheric chemistry. In a plume these rates will be lower as the supply of oxidants decrease with the consumption of O_3. Hewitt (2001) found the rate to be 30% per hour, Gertler *et al*. (1984) estimated the rate at 8% per hour while studies conducted by Collet *et al*. (2010) found the rates range between 11 and 59%.

NO_X is a major precursor for the formation of O_3 in the troposhere. Peroxy radicals (HO_2) in the atmosphere react with NO to produce NO_2 (equation 5). When NO_2 is photolysed, atomic oxygen is formed which in turn reacts with an oxygen

molecule to form O_3 (equation 3 and 4). NO_X acts as a catalyst for O_3 formation when hydro carbons and CO are oxidised. This cycle involving hydrogen oxides (HO_x) and nitrogen oxides (NO_x) is terminated by the reaction of OH with NO_2 to form nitric acid or by the reaction of peroxy radicals with each other to form peroxides (Liptrot 1992).

$HO_2 + NO \rightarrow OH^{\cdot} + NO_2$ (equation 5)

NOx plays a role in the troposphere of regulating the concentration of the hydroxyl radicle ($OH^{\cdot}$) (Bradshaw *et al*., 2000; Hewitt, 2001).

In the presence of O_3, NO_2 is readily oxidised to form (nitrate) NO_3^- (equation 6) which mostly occurs at night. Throughout the diurnal cycle NO_2 conversion to NO_3 is much slower (Jenkin and Clemitshaw, 2000; Hewitt, 2001).

$NO_2 + O_3 \rightarrow NO_3^- + O_2$ (equation 6)

At night the principal reaction of NO_3 is often with NO_2 to set up equilibruim with dinitrogen pentoxide (N_2O_5) (equation 7).

$NO_2 + NO_3^- \rightarrow N_2O_5$ (equation 7)

When dinitrogen pentoxide is hydrated it produces nitric acid (HNO_3) (equation 8). HNO_3 is a product of the oxidation of NO_x in the troposphere via the reaction with the $OH^{\cdot}$ radicle during the day (Bradshaw *et al*., 2000; Jenkin and Clemitshaw, 2000; Hewitt, 2001). NO_3 may also form as a result of the dissociation of HNO_3. The phase changes of NO_3/HNO_3 are temperature dependent. Under high temperatures, NO_3 is volatised and gaseous HNO_3 is formed but under low temperatures NO_3 is generated and HNO_3 concentrations decrease (Jenkin and Clemshaw, 2000; Hewtitt, 2001).

$N_2O_5 + H_2O \rightarrow 2HNO_3$ (equation 8)

NOx has a limited tropospheric lifetime of approximately 1 to 2 days. Equation 5 has a half life of approximately 23 days therefore HNO_3 acts as a store of NO_x, keeping it in the troposphere for longer periods (Holland *et al*., 1999; Atkinson, 2000).

The same end results are obtained in fog droplets where hydration and catalytic oxidation lead to complete conversion of NO_2 to nitric acid (equation 9).

$4\ NO_2 + 2H_2O + O_2 \rightarrow 4HNO_3$ (equation 9)

Both nitric and nitrous acid can be photodecomposed to form the lower oxides (equation 10, 11 and 12) (Jenkin and Clemitshaw, 2000; Atkinson, 2000; Hewtitt, 2001).

$HNO_3 + h\nu \rightarrow HO + NO_2$ (equation 10)

$HNO_2 + h\nu \rightarrow HO + NO$ (equation 11)

$HNO_2 + h\nu \rightarrow H + NO_2$ (equation 12)

In general the atmospheric processes tend to transform the oxides of nitrogen to the nitric acid stage. These oxidation processess vary in duration, and during this time the nitrogen oxides undergo numerous reactions in which they are converted back and forth between the various oxidation stages. The end result is mainly nitrates, which are removed from the nitrogen atmospheric cycle by rain and dry deposition. A smaller percentage is found in aerosols as nitro derivatives of large-molecule organic polymers.

Nitrates are mostly formed at night, when the NO_3 radicle reacts with organics and other cations, which include NH_3 and volatile organic compunds as well as with alkenes, terpenes and benzenes. During the day NO_3 rapidly photolyses via two different pathways (equation 13 and 14) and nitrates cannot be produced (Liptrot, 1992; Atkinson, 2000; Hewitt, 2001).

$NO_3 + hv\ (\lambda\ 700\ nm) \rightarrow NO + O_2$ (equation 13)

$NO_3 + hv\ (\lambda\ 580\ nm) \rightarrow NO + O_2$ (equation 14)

3.2.2 ATMOSPHERIC SULPHUR

Sulphur is a relatively abundant natural element on earth found mainly as sulphide and sulphate ores, whilst in the oceans it is present as dissolved sulphate. It is known that sea bubble spray is associated with approximately 2.65 mg of sulphate per gram of water (Kellogg *et al*, 1972). It has been observed that there is a rapid disappearance of sulphur dioxide in the oceans by oxidation and direct absorption by

sea water, thereby making the oceans which was regarded as a source of sulphate also a sink for SO_2 (Igbafe, 2007). In the Highveld region the sulphur species of importance are hydrogen sulphide, sulphur dioxide and sulphate (Held *et al*, 1993; Scheifinger and Held, 1997).

The main anthropogenic sources of atmospheric sulphur are industries. These industrial sources include combustion of coal and petroleum products in furnaces and boilers, refinery processes and the smelting of non-ferrous ores. The most abundant source of atmospheric sulphur is the burning of coal. Sulphur emissions vary with the type of coal burnt. Hard and lignite coal which is mainly used in power plants, metallurgical and cement industries contain a significant amount of sulphur in the ash (Cullis and Hirschler, 1980).

The role of biomass burning emissions as a source cannot be underestimated (Andrea *et al*, 2008; Josipovic, 2009; Lydia, 2010). South Africa and the whole of Africa is susceptible to large – scale veld and bush fires during the dry season. Also, firewood forms the basis of the domestic energy economy for a large percentage of South African rural populations, while a substantial number of urbanised lower income population burn coal fires (Helas and Pienaar, 1996; Josipovic, 2009; McKechnie, 2010; Puxbaum *et al*, 2000).

The non-biogenic natural sources of sulphur compunds include geothermal emissions resulting from underground sulphur springs. The highest amount of sulphur generated in this manner is derived from volcanoes which release mainly sulphur dioxide and at lower temperatures, hydrogen sulphide accompanied by small amounts of sulphur trioxide and more reduced sulphur (Cullis and Hirschler, 1980).

The most important biogenic natural source of atmospheric sulphur is the biological reduction of sulphur compounds. In the presence of organic matter under anerobic conditions, sulphur in the form of hydrogen sulphide, carbon disulphide and dimethyl sulphide is produced for example marine algae in soils with decaying vegetation and sulphate-reducing bacteria (*Sorovibrio desulphuricans*) present in fine-grained muds (Cullis and Hirschler, 1980).

3.2.2.1 Sulphur Oxides

Gaseous sulphur in the atmosphere, exists mostly as sulphides and oxides. The common sulphide and oxide forms include hydrogen sulphide, carbon disulphide, carbonyl sulphide,dimethyl sulphide, sulphur dioxide and trioxide (Warneck, 1988; Hewitt, 2000). The common gaseous sulphur species found in the Highveld region are hydrogen sulphide and sulphur dioxide from industrial sources (Annegarn *et al*., 1996; Held *et al.*, 1993).

When sulphur, present in reduced form in metal sulphides or in complex organic molecules in oil or coal, is burnt, most of it is released as sulphur dioxide. In a hot plume, for example from smelters or fossil-fuel fired power stations, some of the sulphur dioxide is quickly oxidised to sulphur trioxide. This process is catalysed by metallic elements from the suspended ash. Water vapour, which is also present in such plumes, hydrates the sulphur trioxide (SO_3) to form sulphuric acid (H_2SO_4) (Warneck, 1988).

SO_2 gas could be directly photo-oxidised by either equation15, 16 or 17 (Warneck, 1988; Becker, 2004).

$SO_2 + h\nu \rightarrow SO_2^*$ $0.29 < \lambda < 0.40\ \mu m$ (equation 15) (* denotes excited state)

$SO_2^* + 2O_2 \rightarrow SO_3 + O_3$ (equation 16)

$SO_3 + H_2O \rightarrow H_2SO_4$ (equation 17)

SO_2 is a colourless gas with a strong pungent odour. It is 2.3 times heavier than air with a penetrating smell when the concentration exceeds 1.3 mg m^{-3}. It reacts on the surface of a variety of airbone solid particles and is soluble in water as well as can be oxidised within airborne waterdroplets (Becker, 2004).

Another common reaction whereby sulphur dioxide forms sulphuric acid is through the oxidation of ozone. The hydroxy radical is produced by the photodecomposition of ozone and is highly reactive with any substance. This reaction does not require a catalyst. Other insignificant reactions include the by-product of alkene-zone reactions, oxidation by reaction of N_xO_y species, oxidation by reactive oxygen transients and oxidation by peroxy radicals (Warneck, 1988).

In the aqueous phase sulphur exists in the form of three species (equation 18, 19, 20) (Meszaros, 1981).

$S(IV) \rightarrow SO_2(aq) + HSO_3^{2-} + SO_3^{2-}$ (equation 18)

This dissociation occurs in a two part process:

$SO_2(aq) \rightarrow H^+ + HSO_3^-$ (equation 19)

$HSO_3^-(aq) \rightarrow H^+ + SO_3^{2-}$ (equation 20)

SO_2 can also be formed by the interaction of hydrogen sulphide (H_2S) and atomic oxygen or ozone. Oxidation takes place on the surface of aerosol particles as well as in cloud and precipitation water (equation 21) (Meszaros, 1981; Warnek, 1988).

$H_2S + O_3 \rightarrow SO_2 + H_2O$ (equation 21)

The homogenous oxidation of SO_2 occurs rapidly when air contains NO_2 and ozone. NO_2 absorbs solar radiation in the visible spectrum and dissociates to give atomic oygen. Oygen atoms produce ozone or react with SO_2 to form sulphur trioxide (equation 22) (Meszaros, 1981; Warnek, 1988).

$SO_2 + O + M \rightarrow SO_3 + M$ (equation 22) *M represents an energy accepting third body

3.2.2.2 Sulphates

The most widely studied reactions of sulphur dioxide are the oxidation to sulphate and the reactions with air pollutants and ammonia. In all systems, gaseous sulphur dioxide converts to non-volatile sulphate which forms aerosols. The aerosols can have an effect on the opacity of air, cloud formation , react with other pollutants in the atmosphere or behave as catalysts to other reactions in a polluted atmosphere and they are known to aggravate pre-existing health problems in humans. In addition, unreacted sulphate is a strong acid and excessive acid imposes damage to land, vegetation, buildings and contribute towards corrosion (Manahan, 1991).

There is substantial controversy about the nature of the conversion of sulphur dioxide to sulphate. It is generally accepted that sulphate can be formed either from SO_2 when sulphuric acid vapour is an end product of homogenous gas phase reactions

including photochemical and thermal steps,here sulphuric acid droplets are produced during vapour condensation; or when SO_2 is oxidised in fog and cloud droplets after its absorption, here the sulphate particles are formed by the evaporation of droplets; and when SO_2 is oxidised on the surface of aerosol particles (Meszaros, 1981; Manahan, 1991, Held *et al*., 1996). However, Piketh (2000) argues that very few reactons can take place to sufficiently influence the atmospheric sulphate burden. Majority of the atmospheric sulphate aerosol is formed by oxidation of volatile pecursors to gaseous H_2SO_4 followed by nucleation and condensation processes to form particles . Anthropogenic SO_2 emissions are chemically converted to sulphuric acid in the atmosphere in the gaseous phase. H_2SO_4 is produced via rapid oxidation of SO_2 with OH in the atmosphere to form HSO_3 molecules. HSO_3 reacts with oxygen to form SO_3 and HO_2 which is converted to H_2SO_4 (equation 23, 24, 25) (Meszaros 1981).

$SO_2 + OH \rightarrow HSO_3$ (equation 23)

$HSO_3 + O_2^- \rightarrow SO_3 + HO_2$ (equation 24)

$SO_3 + H_2O \rightarrow H_2SO_4$ (equation 25)

According to Piketh (2000) sulphur dioxide oxidation rate by the hydroyxl radical exceeds all other proesses. Its oxidation rate is highly dependent on the concentration of the hydroxyl radical which in turn is formed by photochemistry and therefore occurs abundantly during day time (Chylek *et al*., 1995). Heterogenous reactions occur in different phases of cloud or fog water or as aerosol droplets involving the transfer of SO_2 and oxidant speciies to the droplet phase with subsequent liquid pahse oxidation (Warneck 1988; Piketh, 2000). The homogenous reaction is assumed to be the dominant reaction over southern Africa. This is as a result of the dry conditions that prevail over the subcontinent for most of the year (Piketh, 2000).

3.3 ATMOSPHERIC PLUME DISPERSION MODELLING

Pollutants released into the atmosphere at ground-level are transported over long distances by large-scale air fields and dispersed by small-scale turbulence. This dispersion process is a complex system due to the presence of different-sized eddies in the atmospheric flow.

An atmospheric dispersion model is a mathematical simulation of the physics and chemistry determining the transport, dispersion and transformation of pollutants in the atmosphere (Pasquill and Smith, 1983) to improve the ability to characterise, understand, predict and manage air pollution in the environment (Douglas, 1982). All air quality modelling systems consist of three major components (Figure 9) namely an emissions, meteorological and air quality model (Zanetti, 1990). It allows for the calculation of downwind air pollution concentrations from sources given information relating to the meterological conditions such as wind speed and direction, atmospheric stability class, mixing height, dry bulb temperature, cloud amount and height, emission parameters for example the source location and height, stack diameter and exit velocity, exit temperature and mass flow rate, terrain elevations at the source and at the receptor locations and the location, height and width of any obstacles in the path of the emitted gaseous plume for example building structures (Carruthers *et al*., 1994; Hall and Spanton, 2002; Pompella, 1998; Scire *et al*., 2000a; Ministry for the Environment, 2004; Zunckel *et al*., 2006).

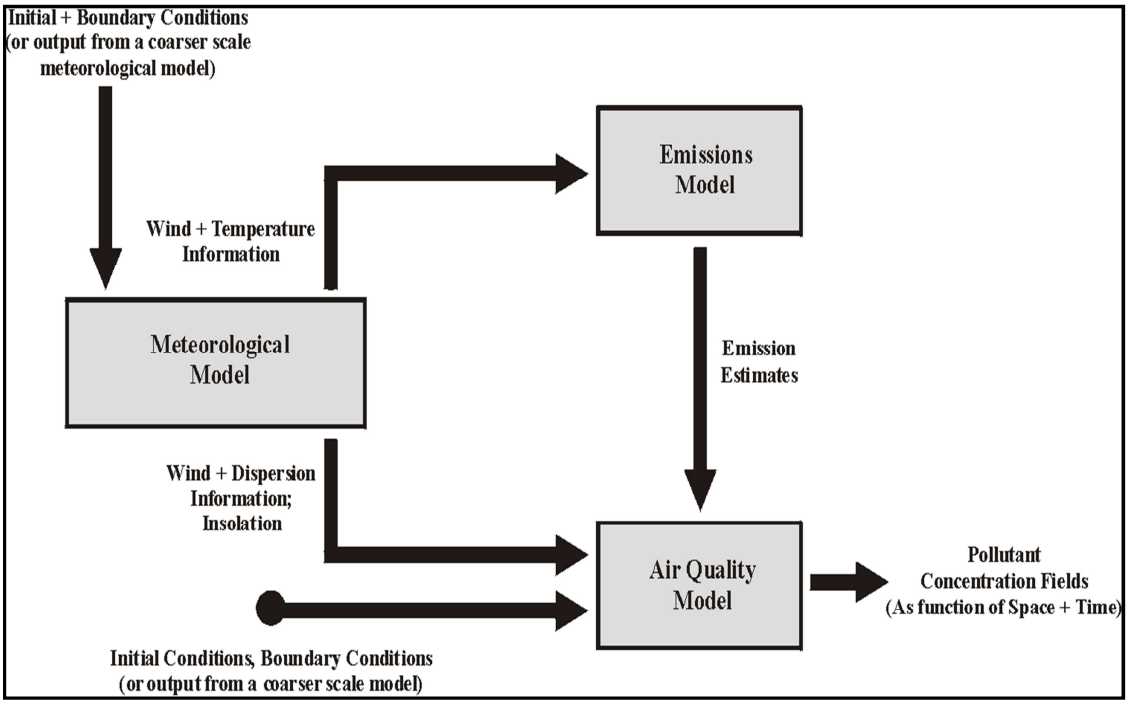


Figure 9: An air quality modelling system (Zannetti, 1990)

Atmospheric dispersion models are also utilised to assist in the design and assessment of various control strategies and abatement technologies for emission reductions through predictive and compliance assessment type studies. Model predictions are useful in a wide variety of air quality decisions, including determining appropriateness of facility location, monitoring network design and stack design. Models also provide information on the areas most influenced by emissions from a source, the contribution of weather to observed trends and the air quality expected under different scenarios, for example future scenarios, short-term episodes and long time trends (Fourie, 2006).

Generally atmospheric dispersion models are employed by government departments to determine whether existing or proposed new industrial facilities are in compliance with ambient air quality standards. This is achieved by superimposing modelled values upon existing or predicted future background air quality concentrations to produce predicted ambient concentrations. Modelled air quality values may be compared for aternative plant locations and alternative pollution abatement measures. Suitable emission standards can then be identified to minimise risk to human health and to ensure compliance to ambient air quality standards/guidelines.

3.3.1 TYPES OF MODELS

Over the years atmospheric dispersion modelling has advanced from one-dimensional simulations to multidimensional simulations involving complex atmospheric chemistry and physics. There are many types of dispersion models which range from simple screening models that simulate air pollution behaviour in the ambient atmosphere in simple terrains, to more complex (also termed refined models) Gaussian plume and puff models which have the functionality to simulate pollutant transformation, removal and transport over different averaging periods for both steady state and spatiotemporal varying meteorology. Different dispersion models have different requirements for user specified inputs and functionality and generally the more complex the case study (complex terrain with many source sector emissions) the more user specified inputs are required (Schulze and Turner, 1996).

The screening models are known to provide conservative estimates of the worst case meteorological scenarios to assess impacts of specific sources (Binkowski and Roselle, 2003; Aghedo *et al*., 2007). In general screening models give a quick initial impression of the highest concentrations that are likely to occur at ground level for point, area, flare and volume sources. These are simple diffusion models that assume the transport and diffusion of pollutants are the main processes that affect the concentration of pollutants with uniform wind speed and state of the atmosphere over the modelling domain (U.S.EPA, 2005).

Examples of simple models include box models and the Atmospheric Turbulence and Diffusion Laboratory (ATDL) model (Ames *et al*., 2002; Zib, 1977) and SCREEN 3. SCREEN 3 is a single source Gaussian plume model. A range of stability classes and wind speeds are examined in order to determine the highest ground level concentrations which result under ‘worst case’ meterological conditions.

Complex models include chemical transformation processes and detailed input data. In addition, complex models assess the control strategies in place for emissions through various emissions scenarios, for example, the AERMOD model (U.S.EPA, 2005). AERMOD can be used for complex modelling scenarios such as the dispersion of vehicle emissions on roads (Venkatram *et al*., 2007).

Models describing the dispersion and transport of emissions can be categorised using different scales for example on the spatial and temporal scales, treatment of transport equations, treatment of various processes and the complexity of the approach.

Zannetti (1990) and Zannetti (1993) distinguished six generic types of atmospheric dispersion models namely Gaussian diffusion, numerical, statistical or semi-empirical, physical, receptor and stochastic models.

3.3.1.1 Gaussian Diffusion Models

GAUSSIAN PLUME MODEL

The Gaussian plume model is the most widely accepted computational approach to calculating the concentration of a pollutant from a single continuous point source (U.S.EPA, 2005; Zanetti, 1993). This model describes the transport and dispersion of pollutants for continuous, buoyant air pollution plumes arising from ground level or elevated sources (Ramadah, 2011). It assumes dispersion in the horizontal and vertical direction will take the form of a normal Gaussian curve with the maximum concentration at the centre of the plume. Depending on atmospheric stability the model is able to determine plume rise and hence effective stack height, the mean wind at stack height and actual concentrations for varying time intervals. The plume size is dependent on the stability of the atmosphere and the dispersion of the plume in the horizontal and vertical directions (Tyson and Preston-Whyte, 2000; U.S.EPA, 2003).

It is based on the assumption that the plume concentration at each downwind distance has independent Gaussian distributions both in the horizontal and in the vertical axis; therefore the Gaussian formula describes a three dimensional concentration field generated by a point source under stationary meteorological and emission conditions (Boubel *et al*., 2004; Beychok, 2005). A simplified version of the Gaussian model, the Gaussian climatological model, can be used to calculate long-term averages (e.g. annual values) (Fourie, 2006).

The Atmospheric Dispersion Modelling System (ADMS 3) is one example of a steady-state Gausssian plume model. This dispersion model is capable of estimating pollutant concentrations emitted both continuously from point, line volume and area

sources or discretely from point sources. The model utilises algorithms which take into consideration complex terrain, wet and dry deposition, short term changes in concentration and chemical transformations (EPA, 2006). ADMS 3 is commonly processed with a sequence of hourly meterological conditions in order to predict concentrations at receptors for averaging times ranging from ten minutes up to a year.

The studies conducted by Pasquill (1961) and Gifford (1976) catagorise atmospheric stability for dispersion estimation and modelling into six classes (Table 2 and 3). The classification classes range from levels of instability (A) to stability (F) for both day time and night-time based on meteorological conditions.

Table 2: The Pasquill stability classes (Beychok, 2005)

Stability class	**Definition**
A	very unstable
B	unstable
C	slightly unstable
D	neutral
E	slightly stable
F	stable

Table 3: Meteorological conditions that define the Pasquil stability classes (Beychok, 2005)

Surface wind speed	**Daytime incoming solar radiation**			**Night-time cloud cover**	
m/s	Strong	Moderate	Slight	> 50%	< 50%
< 2	A	A – B	B	E	F
2 – 3	A – B	B	C	E	F
3 – 5	B	B – C	C	D	E
5 – 6	C	C – D	D	D	D
> 6	C	D	D	D	D

The work of Schnelle and Partha (1999) described the Pasquill-Gifford dispersion parameters as a function of atmospheric stability and downwind distance

from stack. The results showed that the horizontal dispersion coefficients increased as atmospheric conditions become less stable and that there is a greater impact on vertical dispersion than horizontal dispersion with respect to stability classes.

Gaussian plume models are based on the assumptions that there are no interaction between plumes which are important in modelling of urban scenarios (Jacobson, 1999), the emission rate is constant and continuous, wind speed and direction is homogenous over the modelling domain, plume range has a normal Gaussian distribution with the maximum concentration occurring at the centre of the plume and the plume edge is reflected from the ground without any pollution loss (Schulze and Turner, 1996).

Gaussian plume models are least applicable in areas with rapid time varying conditions, varying terrains, spatial scales greater than 50 km and where complex chemisty take place (Beychok, 2005; U.S.EPA, 2002).

GAUSSIAN PUFF MODEL

The Gaussian puff model assumes that a continuously emitted plume or instantaneous cloud of pollutants can be simulated by the release of a series of puffs that will be carried in a time and space-varying wind field. The model has the ability to account for complex flow scenarios because it makes provision for changing meteorological conditions across the modelling domain. The puffs are assumed to have Gaussian or bell-shaped concentration profiles in their vertical and horizontal planes (Scire *et al*., 2000a; Scorgie and Venter, 2005).

An example of a puff model is CALPUFF. It is a multi-layer, multi-species non steady-state Langrangian puff dispersion model which is able to simulate the effects of time and space-varying meterological conditions on pollutant transport for both gases and particulates from point, line, volume and area. It is widely used in applications involving long-range (> 50 km) transport of pollutants (Earth Tech, 2000; Scire *et al*., 2000a; Scorgie and Venter, 2005; Ministry for the Environment, 2004).

The capabilities of CALPUFF enable the model to account for a variety of effects such as spatial variability of meterological conditions, causality effects, dry depostion and dispersion over a range of spatially varying land surfaces, plume fumigation, calm and low wind-speed dispersion, pollutant transformation and wet removal (Earth Tech, 2000; Scire *et al*., 2000a; Barna and Gimson, 2002; Scorgie and Venter ,2005).

However, Calpuff does not perform well under conditions of extreme turbulence and the shortest averaging period is limited to a 1-hour average (Earth Tech, 2000; Godfrey and Clarkson, 1998; Holmes and Morawska, 2006).

3.3.1.2 Numerical Models

Numeric models are used in simulations for area source urban and industrial applications that involve reactive pollutants. These models are not widely utilised because they require extensive input databases and resources (Fourie, 2002).

Zannetti (1993) differentiates numerical models into four classes namely plume-rise, Eulerian, Lagrangian and chemical modules.

PLUME RISE MODELS

Plume rise models calculate the vertical displacement and general behaviour of the plume. This is affected affected by both thermal buoyancy and vertical momentum which tends to elevate the stack height.

EULERIAN AND LAGRANGIAN MODELS

The Eulerian model is represented as a fixed multi-box model, where the atmosphere in the modelling domain is divided into a grid of boxes and the flow of pollutants in the box is mixed vertically only and not horizontally (Johnson, 1976). These models use numerical terms to solve the atmospheric diffusion equation and are therefore able to model the transport of non-reactive pollutants (Fourie, 2002; Fourie, 2006).

The Lagrangian box approach allows for horizontal movement of the columns of air following the average wind speed and direction. The Eulerian box does not move horizontally according to the wind speed and direction (UNESCO, 1995). In a Lagrangian framework a specific parcel of air is followed in which concentrations of a pollutant is assumed to be homogeneously mixed.

CHEMICAL MODELS

Chemical models are air pollution models which contain a chemical component to simulate chemical transformations in the atmosphere. The type of chemical components used range from simple first order to complex photochemical reactions. Several reaction schemes have been proposed for simulating the dynamics of interacting chemical elements. These schemes have been implemented into both Langrangian and Eulerian photochemical models (Fourie, 2006; Ramadha, 2011).

3.3.1.3 Statistical/ Semi-Empirical Models

Semi-empirical models were developed mainly for practical applications and consist of a range of different types of models. Although there are conceptual differences between different models, overall semi-empirical models are distinguished by major simplifications and a high degree of empirical parameterisations. This category includes a variety of box and parametric models (U.S.EPA, 2004).

3.3.1.4 Physical Models

Physical models include the use of wind tunnelling or other fluid modelling techniques. This type of modelling is complex and requires high technical skills as well as access to the necessary facilities. It is used mainly for the modelling of complex flow scenarios from a source or group of sources in small domains (a few square kilometres) for example terrain or stack downwash conditions, plume impact on elevated terrains and diffusion in urban or complex terrains (Fourie, 2006; Ramadha, 2011).

3.3.1.5 Receptor Models

Receptor models start with observed concentrations within a receptor and endeavour to apportion the observed concentrations at a sampling point among the different source types (Moussiopoulos, 1997; Venkatram, 2003). This is done on the grounding of the known chemical composition of source and receptor materials. Receptor models are based on the principles of mass-bass equations and are essentially statistical as they do not include a deterministic relationship between emissions and concentration of a pollutant.

3.3.1.6 Stochastic Models

Stochastic models are based on statistical techniques which are used to analyse trends, periodicities, interrelationships of air quality and atmospheric measurements and to forecast the evolution of pollution episodes. The main limitation of stochastic models is the inability to establish cause-effect relationships however; these models can be efficiently used for applications in real-time short-term forecasting and have the ability to account for uncertainties in model components (Moussiopoulos, 1997).

3.3.2 AIR QUALITY MODEL PERFORMANCE EVALUATION

Generally model predictions are used to influence human health, social and economic decision making therefore it is important that air dispersion models be evaluated with observational data before their results can be utilised with confidence.

There are three components to the evaluation of air quality models namely scientific, statistical and operational. In a scientific evaluation, the model algorithms, physics, assumptions and codes are examined in detail for their accuracy, efficiency and sensitivity. This assessment requires an in depth understanding of the model. In statistical evaluations the model predictions are examined to see how well they match observations. It is also possible for a model to produce good outputs but as a result of compensating errors (Chang and Hanna, 2004).

Operational evaluations focus on issues related to the user-friendliness of the model, such as the user's guide and interface, error checking of the model inputs, diagnostics of the model calculations and processing and display of model outputs (Chang, 2002).

Dispersion is primarily a function of turbulence in the atmospheric boundary layer however turbulence is a random phenomenon and cannot be precisely described or predicted other than by use of statistical properties such as the mean and variance. As a result there are both spatial and temporal variability that occur in the observed concentration field. In contrast, uncertainty in the model outputs can also be attributed to factors such as errors in the input data, model physics and numerical representation. Due to the effects of uncertainty and inherent randomness, it is impossible for an air quality model forecast to be 100 % accurate. There is always a base amount of scatter that cannot be removed. Statistical evaluations produce a level of confidence which decisions can be made on (Chang and Hanna, 2004; U.S. EPA, 2007).

3.3.2.1 Model Evaluation Definitions and Methods

The aim of a model evaluation study must be well-defined. Different objectives could lead to the use of different variables to evaluate and different performance measures. Various model evaluation methodologies have been recommended and developed for different disciplines for example air quality and water quality models. Depending on the intended goals associated with each discipline, the focus and approach is different (Thunis *et al.*, 2012).

ASTM (2000) and US-EPA (2007) recommends performance measures such as the fractional bias, normalised mean square error, geometric mean, geometric variance, correlation coefficient and the fraction of predictions within a factor of 2 of observations for air quality and dense gas dispersion models. The bootstrap resampling method is utilised by Hanna (1989) and ASTM (2000) to estimate the confidence limits on the performance measures. Usually the methodology has been adopted to investigate whether air quality models can correctly predict the maximum concentration over an entire receptor study area, maximum concentration across a given sampling arc, the concentration integrated on a given sampling arc, or the cloud

width on a given sampling arc. However this methodology is generic and can also be applicable to other quantities for example wind speed and temperature and the stock price but the predictions and observations must be paired either in space only, time only or both space and time (Thunis *et al.*, 2012).

Generally model predictions are directly compared to observations however the ASTM (2000) authors recommend the proper averaging of observations prior to comparison as misleading results can be produced because air quality models typically predict ensemble means but observations represent single realisations from an infinite ensemble of cases under the same conditions and the uncertainties in observations and model predictions arise from different sources.

3.4 GEOGRAPHIC INFORMATION SYSTEMS

Geographic Information Systems (GIS) is a fast growing technological field that incorporates graphically referenced features with tabular data which can be utilised to evaluate real world problems. In simple terms location is linked to information to increase the value of this information. Air quality is recorded at specific sites across the Highveld region. Data collected over a period of time could be assessed to determine long term trends for the region or used to assess impacts on vegetation at specific locations.

A GIS is differentiated from other spatially related systems by its analytical capabilities, making it possible to perform modelling operations on the spatial data. Its power lies in the geo-processing functionality which has the ability to extract information from existing datasets, apply analytical functions, perform calculations and write results to a new dataset. A GIS can also depict two and three- dimensional characteristics of the earth's surface, sub surface and atmosphere (Bernhardsen, 1992).

The spatial data in GIS databases can be generated from remote sensing via the direct import of images and maps using photogrammetry. Other methods include downloading data from global positioning systems and physical capture. Remote

sensing data such as satellite images and aerial photography enable the mapping of changes in terrain properties, such as vegetation cover, water and land use both in space and time. Satellite images give a synoptic overview and provide very useful environmental information for a wide range of environmental studies for example water resources, air quality, topography, land cover and population location and dynamics (Skidmore, 2003). Power station emissions recorded at specific locations can be overlayed with aerial photography to determine potential risk to residential areas or in-land water areas.

3.4.1 COMPONENTS OF A GIS

A GIS consists of hardware, software, data, humans and a set of organizational procedures. All these components need to be in balance for the system to be successful. The process and development is iterative and ongoing The selection of hardware and software is the easiest step in the development of a GIS. Data collection and organisation, personnel development and the establishment of protocols for GIS use are often more difficult, time consuming and expensive (Lo and Yeng, 2007; Bolstad, 2008).

3.4.1.1 Hardware

Hardware consists of the technical equipment needed to run a GIS including a computer system with sufficient power to run the software, enough memory to store large amounts of data and input devices such as scanners, digitizers, GPS loggers and printers (Carver, 1998; DeMers, 2002).

GIS is unique in the volume of data that must be entered to define the shape and location of geographic features. Advances in computing technology during the 1990’s has lead to a substantial decrease of processing time, allowed for bigger storage space on computers and increased the methods for quicker capturing of large volumes of data (Bolstad, 2008).

3.4.1.2 Software

There are many different software packages widely available today. Their function is to provide capabilities for data input, storage, management, transformation, anlaysis and output but the apperance, methods, resources and ease of use of the various systems may be different. Both qualitative or quantitative information on non-spatial attributes of geographic features of interest can be captured. Software is required to view and edit these data, manipulate them to generate and extract the information that is required and produce the materials to communicate the information that has been developed (Lo and Yeng, 2007; Bolstad, 2008).

Different softwares offer different functionalities and the choice of software is dependent on what analysis the user needs to perform. The software is also chosen on the overall user friendliness of the product and the ease in which complex analysis can be performed.

3.4.1.3 Data

Data can be categorised as primary or secondary and it is the most time consuming and expensive component of a GIS. It is termed primary if collected in-house and secondary if purchased from a commercial data provider. The digital map base forms the basic data used in the GIS and tabular data related to the map objects can also be attached to the digital data. A GIS has the ability to integrate the spatial data with other data resources and database management systems, which are commonly used by organisations to maintain and manage their non spatial data (Goodchild, 1992; Lillesand *et al*., 2008).

It is crucial to check the data quality prior to accuring it. Errors in the data set can add extra costly hours to implementing a GIS and the results and conclusions of the analysis will be incorrect. The guidelines to consider prior to obtaining the data include lineage, positional accuracy, attribute accuracy, logical consistency and completeness (Guptill, 1995; Chrisman, 1999).

3.4.1.4 People

The people are the component who operate and make the GIS work. They include a range of people from managers to database administrators, application specialists, system anlaysts and programmers. They are responsible for the maintenance of the geograpic database and provide technical support. People associated with a GIS can be categorised into viewers, general users and GIS specialists. People also need to be educated in the understanding of the use of the software as well as principles of cartography and a set of protocols guiding the use of GIS in the organisation (Lo and Yeng, 2007).

3.4.1.5 Procedures

Procedures include how the data will be retrieved, input into the system, stored, manages, transformed, analysed and presented. The procedures are the steps taken to answer the questions that need to be resolved and the ability of a GIS to perform spatial analysis and answer these questions is what differentiates one system from the other (Carver, 1998).

The institutional context determines what spatial data are important, how these data are collected and used and ensures that the results are properly interpretted and applied. Failure to implement a GIS without adequate organisational commitment will result in an unsuccessful system (Lo and Yeng, 2007).

3.4.2 DATA MODELS

A spatial data model may be defined as the objects in a spatial database plus the relationships or rules between them. The purpose of a spatial data model is to provide a formal means of representing and manipulating spatially-referenced information. All spatial data models fall into two broad categories namely vector and raster data model. While either of these models can be used to represent the feature type, generally discrete features such as points, line and polygons are represented by vector models and continuous categories (i.e. cell matrixes that store numeric values) such as

soil type, rainfall, elevation and vegetation are represented by raster models (Wade and Sommer, 2006).

There are other hybrid data models as described by some GIS users or regarded as a different family of data models by others for example triangulated irregular network (TIN) and surface (Burrough and McDonnell, 1998). The TIN model is commonly used to represent surfaces such as elevations through a combination of point line and area features. Data models are also interchangable in that many features on the earth can be represented with either the vector or raster conceptualization approach for example elevation may be represented as a continous surface or as a series of lines representing contours of equal elevation. Data conversion from one model to the other entails costs both computationally and in data accuracy. The decision on which data model to utilise in a GIS depends on the type of operation that needs to be performed. The best data model for a given application depends mainly on the most common operations, the experience and views of the GIS user, the form of the available data and the influence of the data model on data quality (Goodchild *et al.*, 1992; Burrough and McDonnell, 1998; Bolstad, 2008).

Co-ordinates are used to define the spatial location and extent of geographic objects. A co-ordinate consists of a pair of numbrs that specify locations in relation to a point of origin. The co-ordinates quantify the distance from the origin when measured along a standard direction. Single or groups of co-ordiates are organised to represent the shapes and boundaries that define the objects. Co-ordinate information is an important part of the data model and models differ in how they represent these co-ordinates. Co-ordinates are usually expressed in one of many standard co-ordinate systems. The co-ordinates are based upon standardised map projections that unambiguously define the co-ordinate values for every point in an area (Chrisman, 1999; Bolstad, 2008).

3.4.3 SPATIALLY INTERPOLATED SURFACES

Interpolated models are widely used to review decisions on monioring network design and to predict the efficacy of emission control programs. Due to the limited number of ground monitoring sites across a region or country, there is a need to use

spatial interpolation techniques to predict ambient concentrations in unmonitored locations. The justification underlying spatial interpolation is the assumption that points closer togther in space are more related and likely to have similar values than points further apart. This is widely known as Toblers first law of geography (Miller, 2004). Spatial processes are an important modelling tool for many problems of environmental monitoring. Many of the techniques of spatial interpolation are two-dimensional developments of the one-dimensional methods originally developed for time series analysis (Fuentes and Smith, 2002).

The type of selection of an interpolation techniques is dependent on the nature of the data. Key to this choice is the understanding of the results and the data. Characteristics that are important to consider are spatial representativeness, temporal sampling frequency, measurement accuracy and existence of spatial relaionships at varying scales. The dataset needs to be understood to evaluate if there is a need to force the interpolated surface to pass through the measured values when there is a high degree of imprecision in the measured data, whether the data contains a global trend across the entire area of interest or whether short-range variation is significant. Such conditions may influence the decisions regarding the use of local or global interpolators (U.S.EPA, 2004).

3.4.4 SPECIFIC SPATIAL INTERPOLATION METHODS

There are several characteristics of spatial interpolation methods. These characteristics can be classified as point-based versus areal-based, global versus local, exactness versus approximate, stochastic versus deterministic, gradual versus abrupt and covariates (U.S.EPA, 2004; Li and Heap, 2008; Deligiorgi and Philippopoulos, 2011).

The analysis and interpretation of spatial datasets form an important part of geostatistics and is highly human dependent (Genton and Furrer, 1998). It is well known that different individuals will take different approaches, yielding many solutions to the same problem (Anderson, 2001; Azpuruna and Dos Ramos, 2010; Mooken *et al*., 2011). It is often a case where judgement, knowledge and experience play a key role in selecting the proper spatial interpolation technique for each

individual study (Englund, 1990). This can be attributed to the variety of available spatial interpolation methods, which range from simple intuitive predictions to more sphisticated and complex procedures (Cressie, 1991; Azpuruna and Dos Ramos, 2010; Mooken *et al.*, 2011).

3.4.4.1 Point-Based versus Areal-Based

Point-based interpolation methods predict values at specific points in space based on the values and locations of other discrete points in space for example the prediction of SO_2 concentration at a specific latitude and longitude based on the measurements from a monitoring network. On the other hand, areal interpolation methods estimate values for entire zones or areas based on data available for a different set of zones or areas for example many atmospheric dispersion models predict average pollution levels over grid cells (U.S.EPA, 2004; Li and Heap, 2008; Deligiorgi and Philippopoulos, 2011).

3.4.4.2 Global versus Local

Global interpolators develop and use only one function that estimates values for the entire sample area therfore changing one input data point affects the prediction for the entire area. Local interpolators break the sample area into smaller pieces that are evaluated individually by a particular function. With a local interpolator a change in at one data point affects only those areas that consider that point in the prediction algorithm. Local interpolation methods that consider a large percentage of the measured data points in each localised calculation become similar to global methods. An example of a global interpolator is a global polynomial interpolation. This method includes the fitting of a smooth surface based on one mathematical function over all the measured points. This type of interpolation is used when interpolating surfaces with gradual variation over the study area (U.S.EPA, 2004; Li and Heap, 2008; Deligiorgi and Philippopoulos, 2011).

3.4.4.3 Exact versus Approximate

Exact interpolators donot match the measured values on which the interpolation is based therefore the predicted surface must pass through each measured data point. Approximate interpolators utilise the measured values calculating the predicted surface, but the surface is not restricted to passing through the measured values at those locations. Approximate interpolators are used to produce a surface that avoids sharp peaks and troughs in the estimated surface and are commonly used when there is uncertainity about accuracy of the measured values. Exact interpolators are preffered when the user has confidence in the measured values (U.S.EPA, 2004; Li and Heap, 2008; Deligiorgi and Philippopoulos, 2011).

3.4.4.4 Stochastic versus Deterministic

Stochastic methods include the concept of randomness into the interpolation process. These methods allow the uncertainity of the predicted values to be calculated for example Kriging. Deterministic methods do not incorporate statistical probability theory into development of the predictions and utilise mathematical formulas or other relationships to interpolate values for example Inverse Distance Weighted. The advantage of stochastic methods is the abilitiy to provide estimates of uncertainity for the spatial interpolation model's output (U.S.EPA, 2004; Li and Heap, 2008; Deligiorgi and Philippopoulos, 2011).

3.4.4.5 Gradual versus Abrupt

A gradual interpolator produces surfaces with gradual, realively smooth changes whilst an abrupt interpolator produces a discontinous surface with sharp changes. The proximal "nearest neighbour" method which sets unknown points equal to the nearest measured point is an example of an abrupt interpolator. Local interpolators (describes above) can also produce discontinous surface with abrupt changes (U.S.EPA, 2004; Li and Heap, 2008; Deligiorgi and Philippopoulos, 2011).

3.4.4.6 Covariates

The inclusion of covariate analysis provides the ability of an interpolator to take account of additional variables other than distance between points in the interpolation process. In some cases the inclusion of other variables helps to identify highs and lows associtaed with the spatial process which otherwise could be over looked. It can also reduce the uncertainity of the interpolation model's output if the covariates explain some of the spatial variability in the process of interest. Elevation, topography and land use can bE utilised to explain spatial variation. When modelling air pollution, other covariates that might improve predictions include other pollutants (that are correlation with the pollutant of interest), meteorology and emissions information. If SO_2 concentrations are correlated with temperature, adding temperature to a SO_2 spatial interpolation model should improve the accuracy of the predictions (U.S.EPA, 2004; Li and Heap, 2008; Deligiorgi and Philippopoulos, 2011).

Common point based spatial interpolation methods that have been developed include polygonal (nearest neighbour), inverse distance weighted (IDW), splines, polynomial interpolation and kriging. These geostatistical functions are available in the Arcview 9.3 software as part of the spatial analyst extension.

3.4.5 SPATIAL INTERPOLATION MODELLING LIMITATIONS

Spatial interpolation provides a valuable tool for better understanding air quality, determining the extent of air pollution problems, highlighting relationships between different air pollutants and designing of ambient air monitoring networks. Interpolation is a method or mathematical function that estimates the values at locations where no measured values are available (Anderson, 2001; Azpuruna and Dos Ramos, 2010; Mooken *et al.*, 2011). The degree to which a spatial interpolation model can be successfully developed is strongly dependent on the atmospheric fate, transport of certain pollutants and chemical properties of the air pollutant. According to Main and Roberts (2001), a pollutant's residence time in the atmosphere, determines its range of transport. A residence time on the order of several days

generally yields long-range transport, which in turn leads to more uniform spatial patterns. More uniform spatial patterns may also be consistent with longer averaging times. Spatial interpolation models, model a specific point in time for a pollutant and do not necessarily take into account conditions as described above during a small scale spatial interpolation exercise. Different air pollutants may present different technical problems with respect to developing spatial interpolation models. The spatial interpolation modelling needs and the ultimate use of such models vary from pollutant to pollutant. These issues must be considered prior to choice of an interpolation method (U.S. EPA, 2004).

Depending on the size of the spatial domain to be interpolated, it can be important to consider different spatial scales in the modelling process. It is possible that air pollutants or other process being modelled exhibit differential behaviours at varying scales. For example, fine particulates and ozone may present relatively smooth varying large-scale trends at the regional level due to long-range transport, more textured variation at the urban scale due to the distribution of emission sources and further variation at the neighbourhood or micro scale due to terrain, surrounding infrastructure and other factors. It is important to model these different spatial scales of variation for the purpose of better understanding the impact of the various causal factors. Explicit modelling of such spatial effects may lead to increased accuracy in the resulting spatial predictions however this may lead to model overfitting which may lead to distortions and misinterpretation of data (Cressie, 1991; U.S.EPA, 2004).

One of the advantages of stochastic interpolation methods is their ability to provide uncertainty estimates along with their spatial interpolation predictions. A limitation of the uncertainty estimates provided by spatial prediction standard errors is that they are likely to underestimate the true uncertainty of the associated spatial predictions. This is due to the methods being a two-stage process, where a variogram model is estimated in the first stage and prediction and uncertainty equations are applied in the second stage. The second stage equations treat the first stage variogram model as true and known. However, it is only an approximation of the data's empirical co-variation. The variogram model itself is estimated with uncertainty. Thus, the spatial prediction uncertainty estimates output from kriging methods do not account for the inherent uncertainty in estimating the required variogram model.

These methods, therefore, are likely to underestimate the true uncertainty of their resulting spatial interpolation surface. Also, the estimated uncertainty of interpolated values can be quite sensitive to the variogram used to describe the spatial structure. This can be true even though the predictions themselves may be quite similar (U.S.EPA, 2004).

Monitoring network design is highly interrelated with spatial interpolation modelling, in that the ability to interpolate well depends strongly on the design of an existing network. Thus, the issue of network design cuts across all the limitations discussed above (pollutant and scale).

Spatial interpolation can be compared to "connecting dots" to complete a picture. The dots represent monitoring stations. All else being equal, the more space between "dots" or monitoring stations the more uncertainty there is with respect to the understanding of the picture for those areas filled in via spatial interpolation. Interpolation at larger spatial scales may require broad national or regional monitoring network data, while smaller scales may require dense urban or local networks. This statement is interrelated with the degree of spatial uniformity associated with different air pollutants. Monitoring network design usually encompasses the relative spatial density or sparsity of such "dots" along with other design issues (U.S.EPA, 2004).

A primary issue of concern with respect to a network of monitoring sites providing data for spatial interpolation modelling is the relative spatial density of the network. The more monitoring locations there are providing data within the domain of interest, the better. Consistent with Tobler's First Law of Geography, the common point based interpolation methods often assume greater spatial correlation with shorter distances between points in space. This translates to larger spatial prediction uncertainty at interpolation locations further from available monitoring data. Hence, more spatially dense monitoring networks tend to yield more certain spatial interpolation predictions throughout the domain of interest (US.EPA, 2004; Deligiorgi and Philippopoulos, 2011).

At some point, the relative spatial sparsity of a monitoring network can hinder a researcher's ability to construct a desired spatial interpolation surface based solely on

point based interpolation methods applied to monitoring data because monitoring sites are typically located to detect high concentrations and although such a configuration is appropriate for identifying the maximum potential exposure and risk, in many cases it fails to describe the spatial variability of air pollution (Lozano *et al*, 2009; Mofarrah and Husain, 2010). This is dependent on the application at hand and the desired quality of the resulting interpolated surface (US.EPA, 2004; Deligiorgi and Philippopoulos, 2011). No simple rule is available to determine whether a monitoring network's data are too sparse spatially to reliably apply the common point based interpolation methods for a given application. A formal evaluation process, such as the US.EPA recommended Data Quality Objective process , can be used to determine this. Such an evaluation may lead to researchers concluding that common point based methods and monitoring data alone are insufficient for their spatial interpolation needs. In this case, supplemental or new data might be pursued or a different interpolation approach might be considered for example co-kriging or kriging with external drift (US.EPA, 2004).

Aside from spatial density, which is obviously an important design component, one must take into consideration the many other facets of monitoring network design. In particular, the problem of selecting optimal sampling designs is complicated by considerations such as current pollution patterns, meteorology, cost, accessibility, security of sampling sights, and politics (US.EPA, 2004; Mofarrah and Husain, 2010; Deligiorgi and Philippopoulos, 2011).

3.5 AMBIENT AIR QUALITY GUIDELINES AND STANDARDS

South Africa is administrated by national policies and legislation for air quality management which has been shaped by international policies The country is a signatory to the Kyoto protocol, Viena Convention, Montreal Protocol and Stockholm Convention. Ambient air quality guidelines and standards are vital for effective air quality management as standards set encourage the protection of human health and ecosystems. There is an increasing societal awareness of global air quality and trans-boundary atmospheric pollution impacts. South Africa is also signatory to many multi-lateral environmental agreements (National Framework, 2007).

3.5.1 NATIONAL POLICY

South Africa's first endeavour to control air pollution came in 1965 with the enactment of the Atmospheric Pollution Prevention Act (45). The Atmospheric Pollution Prevention (APPA, Act 45 of 1965) was based on the best practical means approach to prevent and control air emissions while considering local conditions, technical knowledge, control options and the cost of abatement (Scorgie, 2007). This act was regarded as ineffective for a number of reasons. Some of the main reasons are that APPA was seen to have limited powers to enforce Act 24 of the South African Constitution, although APPA was guided by the best practical means approach to controlling air pollution it was considered ineffective, APPA was largely a point-source emission control that did not fully address the cumulative impacts of air pollution, allowed for the development of industries in areas of poor air quality, APPA did not set air quality standards and did not provide incentives for reducing emissions APPA also lacked transparency in the decision making processes (Department of Environmental Affairs and Tourism, 2009a).

In an attempt to address the short comings of APPA the Department of Environmental Affairs (DEA) published revised ambient air quality stanadards in 2006 for public comment. In December 2009 proposed ambient air quality standards were gazetted by the minister of Water and Environmental Affairs (Table 4 and Table 5) with compliance dates. The dates for both SO_2 and NO_2 were all for immediate compliance. The National Environmental Management Air Quality (NEMA) Act (39) 2004 came into full effect on 1st April 2010.

NEMA Act (39) 2004 was promulagated to give effect to section 24(b) of the South African Constitution in order to enhance the quality of ambient air for the sake of securing an environment that is not harmful to the health and well being of people. According to the National Framework (2007), two key princliples that support NEMA which are relevant to atmospheric pollution include:

i. *pollution avoidance or minimisation* – which states that pollution and degradation of the environment must be avoided, or, where it cannot be avoided, must be minimisised and remedied;

ii. *waste avoidance and consideration of life cycle assessment* – which states that waste must be avoided, or where it cannot be avoided, it must be minimised and re-used or recycled where possible or disposed of in a responsible manner.

The NEMA Act (39) of 2004 falls within the broad framework of NEMA, with the aim to manage air quality through the Best Practise Environmental Option approach in order to achieve the sustainable development principles outlined in NEMA (Diab and Zunckel, 2005; Ramandah, 2011). Violations of NEMA Act (39) of 2004 is prosecutable by law or substantial fines can be imposed. It is also a paradigm shift from previous national air pollution policies (Atmospheric Pollution Prevention Act (45) of 1965 and NEMA Act (107) of 1998) which were based mainly on source-based controls to decentralised air quality management through an effects-based approach. The emphasis has changed from exclusively managing air pollution by the control of emissions from individual point sources to a more inclusive approach based on controlling ambient concentrations in the receiving environment (Scorgie *et al.*, 2003, Ramandah, 2011).

Table 4: National ambient air quality SO_2 standards and compliance dates (Department of Environmental Affairs, 2009b)

Averaging Period	**Concentration (µg/m3)**	**Frequency of Exceedence**	**Compliance Date**
10 minutes	500	526	immediate
1 hour	350	88	immediate
24 hours	125	4	immediate
1 year	50	0	immediate

Table 5: National ambient air quality NO_2 standards and compliance dates (Department of Environmental Affairs, 2009)

Averaging Period	**Concentration (µg/m3)**	**Frequency of Exceedence**	**Compliance Date**
1 hour	200	88	immediate
1 year	40	0	immediate

Acess to air quality information was recently boosted with the launch of the South African Air Quality Information System (SAAQIS). SAAQIS is a web based interactive system that provides South Africans with information on the quality of the ambient air. SAAQIS has 40 monitoring stations across the country including full coverage of the national Priority areas.

SAAQIS is recogonised as a centralised, verified application for the practical implementation of the Air Quality Act to facilitate compliance with norms and standards by the different stakeholders. It is also seen as a vertical integration of the 3 spheres of government i.e national, provisional and local with respect to air quality information.

3.6 CONSEQUENCES OF ATMOSPHERIC POLLUTION

Knowledge of the effects of atmospheric pollution on human health and ecosystems on the Highveld is limited. Knowledge gained and experiences learnt from the Northern Hemisphere indicate the need for timely evaluation of atmospheric pollution impacts on the environment. Decision makers concerned with the compliance and control of atmospheric pollution or the sustainabilty and conservation of natural resources require a quantification of actual impacts and risks of impacts under different development scenarios.

3.6.1 EFFECTS ON HUMAN HEALTH

Air pollution seems to cause the largest and most widespread hazards and environmental problems as compared to other forms of pollution. The form of the air pollutant i.e. gas or particulate, produces different effects within the respiratory tracts. Humans inhale about 7500 litres of air each day and their lungs and respiratory system are in contact with and have the potential to retain harmful substances in the air (Lippmann and Schlesinger, 1979).

The effects of air pollutants can be classified according to the type of effect they can have on human health. According to Lippmann and Schlesinger (1979), pollutants

and their effects include chemical irritants, fibrotic response, asphyxiant response, allergic response, systemic reactions, and mutagenic, teratogenic and carcinogenic reactions.

While gaseous sulphur species are known to contribute to respiratory tract infections ((Balmes *et al*, 1989) atmospheric particulate sulphates are a more harmful secondary pollutant than other particulate matter for example pollens (Carmichael and Peters, 1984; Tuncel *et al*, 1985). Kitagawa (1984) reported severe cases of lung disease near a plant emitting sulphuric acid aerosols in Japan. The number of occurrences decreased with increasing distance away from the plant, and when sulphuric acid was removed completely from the emissions, the incidence of lung disease decreased sharply.

Controlled studies with exercising asthmatics indicate that some of them experienced changes in pulmonary function and respiratory symptoms after periods of SO_2 exposure as short as 10 minutes. Based on this evidence, the WHO recommended that the air quality guideline value of 500 $\mu g/m^3$ should not be exceeded over averaging periods of 10 minutes. Significant associations were found between SO_2 (at concentrations as low as 18 ug/m^3) and mortality in long term studies (WHO, 2005). A summary of health effects of SO_2 is provided in Table 6.

Table 6: Summary of SO_2 health effects (Raghunanadan *et al*., 2006)

Concentration (ppm)	Effects
0.3	Taste threshold
0.5	Odour threshold
1.5	Bronchiolar constriction
	Respiratory infection
2	ACGIH recommended TLV-TWA
3	Easily detected odour
12-Jun	May cause nasal and throat irritation
10	Upper respiratory irritation, nose bleeding
20	Eye irritation, development of chronic respiratory symptoms, respiratory protection is advised
50-100	Maximum tolerable exposures for 30-60 minutes
≥ 100	NIOSH recommended immediate danger to life

Studies on atmospheric pollution effects on human health in South Africa have produced confusing and ambiguous conclusions similar to conclusions arrived at from studies conducted by first world countries. The health effects of ambient atmospheric pollution are difficult to quantify as the effects are compounded with the effects of domestic coal or biofuel combustion, cigarette smoking, occupational exposure to pollutants and exposures in the home.

Research was conducted on a group of children attending Sasolburg primary schools to determine the effects of atmospheric particulates and SO_2 on the health of these children. The control group was made up of children attending primary schools from surrounding country towns. Both groups were exposed to different levels of smoke and SO_2 pollution. Although no significant differences were reported for respiratory illness and passive smoking influence, all lung functions were worse in the study group (Coetzee, 1986). A questionaire survey conducted on children from the Mpumulanga Highveld revealed that exposed children have increased frequencies of certain respiratory symptoms such as coughing and wheezing (significant amongst girls only) and certain respiratory illnessess such as asthma in boys and chest colds in

girls (not illnesses such as bronchitis and pneumonia). Subsequent lung function tests on both exposed and unexposed children showed no significant differences and therefore did not support the results from the questionaires (Zwi *et al*., 1987). These lung test results contradict those of Coetzee (1986). Contradictory results also indicate that more research is needed in this area and that a dose-response relationship needs to be established.

In population studies NO_2 has been associated with adverse health effects even when the annual average NO_2 concentration complied with the WHO annual guideline value of 40 μg/m^3. Also some indoor studies suggest effects on respiratory symptoms among infants at concentrations below 40 μg/m^3. However, NO_2 is an important constituent of combustion-generated air pollution and is highly correlated with other primary and secondary combustion products, it is unclear to what extent the health effects observed in epidemiological studies are attributable to NO_2 itself or to other correlated pollutants (WHO, 2005).

Many short term experimental human toxicology studies show acute health effects at levels higher than 500 μg/m^3, and one meta-analysis has indicated effects at levels exceeding 200 μg/m^3. However the WHO reports that current scientific literature has not accumulated evidence to change from the initial WHO-2000 guideline value of 200 μg/m^3 for 1-hour NO_2 concentration. In experimental studies the lowest level of nitrogen dioxide exposure reported in more than one laboratory shows a direct effect on pulmonary function in asthmatics at 560 μg/m^3. Studies of bronchial responsiveness among asthmatics indicate an increase in responsiveness at levels greater than 200 μg/m^3 (Updated Air Quality Guidelines for Europe, 1994; WHO, 2005).

Recently published studies document that NO_2, an indicator of a complex mixtures of traffic-related combustion pollution, can have higher spatial variation than particle mass. In addition, these studies reported adverse effects on the health of children living in the areas characterised by higher levels of NO_2 even when the

overall level was low. Furthermore, recent studies on indoor NO_2 concentrations have added evidence on adverse effects of NO_2 on respiratory symptoms in children (WHO, 2005).

3.6.2 EFFECTS ON VEGETATION

The Mpumulanga Highveld is South Africa's dominant forestry production area. These forests are mostly man-made forests of pine, *Eucalyptus* species and black wattle (*Acacia mearnsii*). More than 80 % of these commercial forests are located on the eastern region of South Africa and approximately 50 % lie in a zone potentially affected by industrial pollution from the Highveld (Tyson *et al*, 1988). Few studies have been conducted in South Africa on the impacts of species on non-commercial vegetation species (Van Tienhoven *et al*., 2003). More of these studies need to be undertaken in order to determine critical levels with confidence (Josipovic, 2009).

Gaseous pollutants such as NO_2, O_3 and SO_2 are absorbed through the stomata or damaged cuticles of trees. Effects on the leaf and its physiology may be biophysical through responses in the stomata. Biochemical effects arise through the direct uptake of pollutants in tissues or interactions with enzymes and proteins and changes to cell membranes especially where O_3 is concerned. These effects subsequently affect physiological processes such as photosynthesis (Winner *et al*., 1985; Kozlowski and Constantinidou, 1986). Responses to SO_2 by foliage are observable at concentrations of 35 ppb and less (Kozlowski and Constantinidou, 1986). Nitrogen dioxide is toxic to plants in short term exposures from concentrations of 120 $\mu g/m^3$. It will cause plant growth deficiency and hamper its regular growth progression (DEA, 2011).

In South Africa, fumigation experiments were conducted by Kelly (1986) with *Eucalyptus gradis, Pinus elliottii* and *Pinus patula* with exposure to SO_2 at concentrations of 50, 100, 500 and 1000 ppb respectively. The effects were assessed as visible damage. It was found that daily exposure for one to two hours (over 26 days) at concentrations of 50 and 100 ppb caused no damage to any of the species. *Eucalyptus gradis* showed damage after hourly exposures to 500 ppb for 26 days, and

both *Eucalyptus gradis* and *Pinus elliottii* were damaged by hourly exposures to 1000 ppb for the same time period. *Pinus patula* was not affected. *Pinus patula* and *Eucalyptus gradis* showed damage after a single 6 hour exposure at 500 ppb. *Pinus elliotii* showed slight damage after 6 hours but only showed significant damage after 3 consecutive weekly 6-hour exposures. Once damage was visible, subsequent exposures increased damage in all species concerned.

Mist precipitation frequently occurs on the Highveld and adjacent regions (Schulze, 1965). Acid mists with pH less than 3 have been noted to have negative effects on trees (Unsworth, 1984). This could reduce forest productivity.

The oxides of nitrogen seem to be less problematic and indirectly implicated in damage to trees. With nitrogen oxides and acid rain, synergistic effects with other pollutants have been reported in some experiments (Tyson *et al*., 1988). Sulphur deposition has been shown to increase frost sensitivity in trees and there is evidence that dry and wet deposition of nitrogen behaves in the same manner (Nihlgard, 1985; Unsworth and Crossley, 1985). Effects of this kind are pertinent to the Highveld area as periodic drought affects tree growth and the climate dictates the choice of species resistant to frost (Tyson *et al*., 1988).

The primary agricultural crops of the Highveld are annuals and are grown under dryland conditions. The agricultural sector produces maize, sunflower, potatoes and sorghum with maize being the major crop production (Department of Environmental Affairs and Tourism, 2003). Winner *et al*. (1985) have indicated that the maize crops examined in the early 1980's were relatively tolerant to ambient atmospheric levels of SO_2 at the time. The general assumptions are that maize is relatively sensitive to O_3 and more tolerant to nitrogen oxides, but further studies are required for adequate conclusions to be drawn. The second most important crop, sunflower, is relatively sensitive to SO_2 and nitrogen oxides and tolerant to O_3 (United States EPA Research Management Committee, 1981, 1982) whereas dry beans are sensitive to all three pollutants (Tyson *et al*, 1988). Marshall *et al* (1998) added that crops are at risk from O_3, but over a greater area than they are sensitive to SO_2

Engelbrecht (1987) conducted investigations on the effects of varying SO_2 concentrations on dry beans (*Phaseolus vulgaris*) in a non-filtered greenhouse. The study monitored effects from concentrations ranging from 50 ppb to 100 ppb. Exposure times ranged from 30 minutes to two hours. An extreme treatment was also administered where concentrations were increased to 3 000 ppb and exposure time to 8 hours. Responses in growth and yield to different SO_2 doses showed significant reductions in biomass and yield of pods relative to controls at low exposures (50 ppb). Doses of 3 000 ppb for 8 hours caused severe damage to leaves and reduced biomass considerably.

****

NO_X and SO_X pollutants have both natural and anthropogenic sources. The Highveld is seen to be one of the most polluted regions in southern Africa. The Highveld is the main coal producing region in South Africa and approximately 95 % of the country's electricity requirement is generated by coal fired-power stations (Department of Environmental Aaffairs, 2003; Department of Environmental Affairs, 2011). Besides power station and industrial uses coal is utilised for domestic heating and cooking in informal and township areas. Other near ground sources of air pollution include smouldering coal dumps, motor vehicles and emissions from airport activities. Lightning and biomass burning are also major contributors.

The oxides of nitrogen present in the atmosphere are N_2O, NO and NO_2. NO is emitted directly into the atmosphere via high temperature conbustion, where after it oxides into NO_2 it further oxides into NO_3. Gaseous sulphur in the atmosphere, exists mostly as sulphides and oxides. The common gaseous sulphur species found in the Highveld region are hydrogen sulphide and SO_2 from industrial sources. When sulphur, present in metal sulphides, oil or coal is burnt most of it is released as SO_2 . In a hot plume most of the SO_2 is quickly oxidised to SO_3. Water vapour which is also present in these plumes, hydrate the SO_3 to form H_2SO_4 (Warneck, 1988).

An atmospheric dispersion model is a mathematical simulation of the physics and chemistry determining the transport, dispersion and transformation of pollutants in the atmosphere (Pasquill and Smith, 1983) to improve the ability to characterise,

understand, predict and manage air pollution in the environment (Douglas, 1982). It is also utilised to assist in the design and assessment of various control strategies and abatement technologies for emission reductions through predictive and compliance assessment studies. There are many types of dispersion models which range from simple screening models that simulate air pollution behaviour in the ambient atmosphere in simple terrains, to more comples Gaussian plume and puff models which have the ability to simulate pollutant transformation, removal and transport over averaging periods for both steady state and spatiotemporal varying meteorology. Dispersion models can be classified into six generic types namely Gaussian diffusion, numerical, statistical or semi-empirical, physical, receptor and stochastic models.

GISs incorporate graphically referenced features with tabular data to evaluate real world problems. Data collected over a period of time could be assessed to determine long term trends for the region or used to assess impacts on vegetation at specific locations. Power station emissions recorded at specific locations can be overlayed with other datasets for example, wetlands, rivers and residential areas to determine potential risk to human health and ecosystems. A GIS is made up of five components namely hardware, software, data, humans and organisational procedures. Spatial data models are utilised to represent and manipulate spatially-refernced information and fall into two categories called vector and raster data models. There are other hybrid data models which are regarded by some GIS users as a different family of data models for example surface and TIN (Burrough and McDonnell, 1998).

Due to the limited number of ground monitoring sites across a region or area of interest, there is a need to use spatial interpolation techniques to predict ambient concentrations in unmonitored locations. There are several characteristics of spatial interpolation methods and these can be classified as point-based versus areal-based, global versus local, exactness versus approximate, stochastic versus deterministic, gradual versus abrupt and covariates (U.S.EPA, 2004; Li and Heap, 2008; Deligiorgi and Philippopoulos, 2011). There are a variety of spatial interpolation methods available which range from simple intuitive predictions to more sophisticated and complex procedures. It is well known that different individuals may choose different approaches to yield the same solution to a problem (Anderson, 2001; Azpuruna and

Dos Ramos, 2010; Mooken *et al*., 2011) however limitations to the use of spatial interpolation techniques must be fully understood.

South Africa is governed by national policies and legislation for air quality management which has been influenced at the international, national, provincial and municipal levels. Ambient air quality guidelines and standards are important for effective air quality management as limits and standards set encourage protection of human health and ecosystems. The knowledge of the effect of atmospheric pollution on human health and vegetation on the Highveld is limited. The effects of air pollutants can be classified according to the type of effect they can have on human health. According to Lippmann and Schlesinger (1979), pollutants and their effects include chemical irritants, fibrotic response, asphyiant response, allergic response, systemic reactions and mutagenic, teratogenic and carcinogenic reactions.

Gaseous pollutants such as NO_2, O_3 and SO_3 are absorbed through the stomata or damaged cuticles of trees. Effects on the leaf and its physiology may be biophysical through responses in the stomata or biochemical through the uptake of pollutants in tissues, interactions with enzymes and protein and changes to cell membranes. These effects subsequently affect phsiological processes such as photosynthesis (Winner *et al*., 1985; Kozlowski and Constantinidou, 1986).

Now that the literature of this study has been discussed the methodology utilised in this study is explained in the following chapter.

CHAPTER 4
DATA COLLECTION

This chapter presents the data and information that was collected and utilised in this study. The Eskom ambient air quality montoring network and data recorded at the Eskom ground based montoring stations are discussed in detail. The SCIAMACHY sensor, coverages, differential optical absorption spectroscopy (DOAS) method, nadir – limb geometries of SCIAMACHY and the non steady state of the CALPUFF suite of models are explained in this chapter.

4.1. INTRODUCTION

Data and information for this study was obtained from the Eskom air quality database of ground-based continuous measurements, the South African Weather Services (SAWS) meteorological data, Airshed Planning Professionals dispersion modelling studies conducted on behalf of Eskom and the European Space Agency's (ESA) SCIAMACHY retrievals. Only data that was recorded in 2003 for NO_2 and SO_2 concentrations were utilised.

4.2 GROUND-BASED MEASUREMENTS

Eskom began air quality monitoring on the Highveld in the late 1970's and has since compiled a comprehensive database (Rorich and Galpin, 1998). Both regional and compliance monitoring is undertaken at sites downwind of Eskom power stations to assess the compliance with DEAT ambient guidelines, the impact on air quality from power station emissions, regional impacts on air quality, long-term pollution trends and identify and quantify the contribution of pollution from various sources. The Eskom air quality datasets are also utilised to understand atmospheric chemistry and wet and dry deposition processes over the Highveld. Ambient monitoring provides a means of comparing power station impacts to local and international ambient guidelines and standards. Regional monitoring has been undertaken at Elandsfontein, Verkykkop, Makalu, Palmer and Leandra (Figure 10) which presents

ambient air quality data representative of the combined impacts from numerous sources in the areas of concern. Ambient concentrations of primary and secondary pollutants, such as SO_2, NO_2, O_3 and fine particulate matter (FPM) with a diameter less than 10 µm (PM_{10}), as well NO and NO_x are continuously monitored at these sites. In addition, meteorological parameters of wind direction, wind velocity, wind speed, sigma theta and ambient temperature are also monitored. Eskom installed an ambient monitoring site at Leandra to continuously monitor SO_2, FPM and meteorological parameters to assess the impacts on air quality resulting from the electrification of Lebohang Township located at Leandra (Rorich, 2005).

Compliance monitoring on the Mpumulanga Highveld is undertaken at Arnot, Camden, Kendal and Majuba power stations. Ambient air quality monitoring datasets from these sites are also utilised to assess pollution trends from emission control strategies and impacts from other sources (Snow, 2004).

The siting of ambient stations is influenced by: meteorology, air quality issues and resource constraints. The monitoring stations at Elandsfontein, Verkykkop, Palmer and Makalu are classified as rural – an open country location, in an area of low population density, distant as far as possible from roads, populated and industrial areas. The source influences at these sites are mainly long-range transport of urban and rural plumes. The monitoring station at Leandra is classified as urban-background – an urban location distanced from sources and therefore broadly representative of city-wide background conditions. The source influences being motor vehicles, commercial, domestic and space heating emissions. The Eskom monitoring stations and site locations are shown in Figure 10.

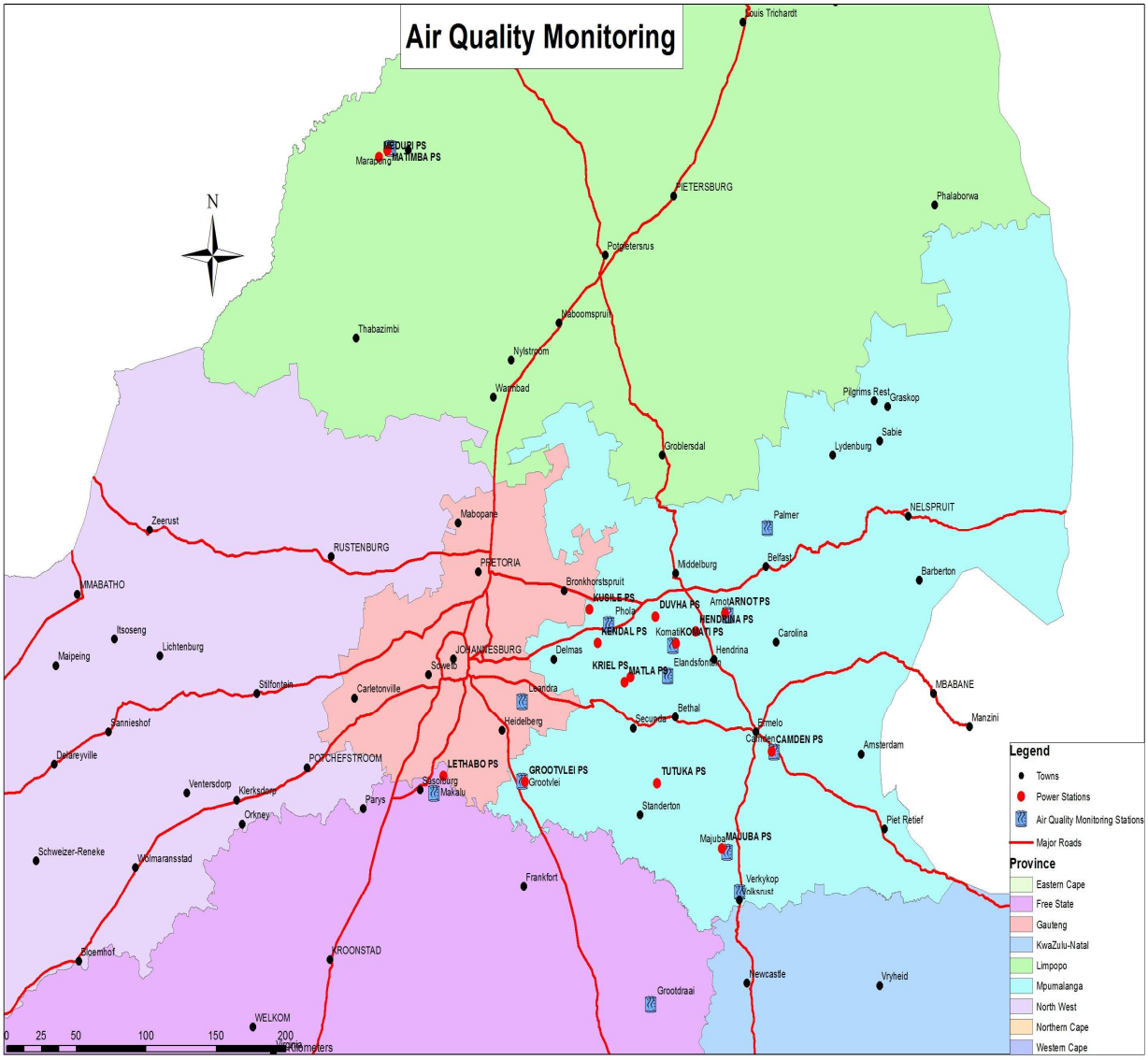


Figure 10: Eskom air quality monitoring network in relation to Eskom power stations

4.2.1 NETWORK RELIABILITY

The percentage data recovered at each Eskom monitoring station, together with the reliability of each parameter is presented in Table 7. Eskom utilises the South African National Accreditation System (SANAS) figure of 80% as a measurement standard for the representativeness of data captured since DEA has not published guidelines for the indication of network reliability.

The overall network reliability for 2003 was good, with a 83.2% data capture across all monitoring stations. The Camden monitoring station dataset was not utilised in this study as recording only began in July and the overall network reliability for this site was 49.4 %. The lowest site data capture of 72.1% was recorded at

Elandsfontein monitoring station resulting from only 42.6% of NO_2 data being recorded due to faulty instrumentation and a low site availability of 87% due to power outages. Palmer monitoring station also experienced numerous power outages resulting in only 79% site availability which affected the overall network percentage data capture. Other data loss on the network was largely attributed to instrumentation malfunction, power failures at sites and unavailability of spares for instrumentation (Rorich, 2005; Murray and de Beer, 2004).

Table 7: Percentage data capture

Monitoring Station	**NO_2**	**SO_2**	**Temperature**	**Wind Direction**	**Wind Speed**	**Data Capture**	**Site Availability**
Makalu	99.7	95.1	100	100	100	98.8	100
Elandsfontein	42.6	75.8	80.6	79.1	79.1	72.1	87.1
Leandra	Not Available	99.3	100	100	100	84.1	100
Palmer	77.9	78.1	79.4	79.4	79.4	77.7	79.4
Verkykkop	76	98	99.5	90.5	90.5	83.8	100
Majuba (J1)	Not Available	97	100	100	100	77	77.3
Majuba (J3)	Not Available	63.7	93.2	93.2	93.2	77	76.8
Kendal	98.3	98	100	100	100	95.0	86.2
Overall network data capture 83.2							

4.2.2 METEROLOGICAL OBSERVATIONS & AIR QUALITY AT GROUND MONITORING STATIONS

The distributions of wind direction and wind speed for daytime and night-time hours are summarised on polar diagrams for each ground monitoring station. The positions of the spokes show the directions from which the wind was blowing and the length of the segments indicate the percentage of the speeds in the various categories. The day time and night-time sector SO_2 and NO_2 exceedance roses describe the wind sectors in which the highest concentrations occurred. The centre of the wind rose depicts the position of the ambient air quality monitoring station.

4.2.2.1 Elandsfontein Monitoring Station

The Elandsfontein monitoring station is situated at the Elandsfontein micro-wave transmiting station, 25 km east of Kriel and Matla power stations and 38 km south of Duvha power station. Due to the central location of this monitoring station in the Mpumalanga industrial area and the large amount of historical data recorded, it is considered to be of prime importance to regional impact studies and long-term pollution trend analysis (Rorich, 2005).

METEROLOGICAL OBSERVATION

The diurnal winds are predominantly from the south-west to north (52.2%), east-north-east to east-south-east (23.6%) and infrequently 0.9% at 10 ms^{-1} (Figure 11). At night the wind direction was mainly from the north-east to east-north-east (50.3%) and north-west to north (19.8%) with lower wind speeds (4.4% > 7 ms^{-1}).

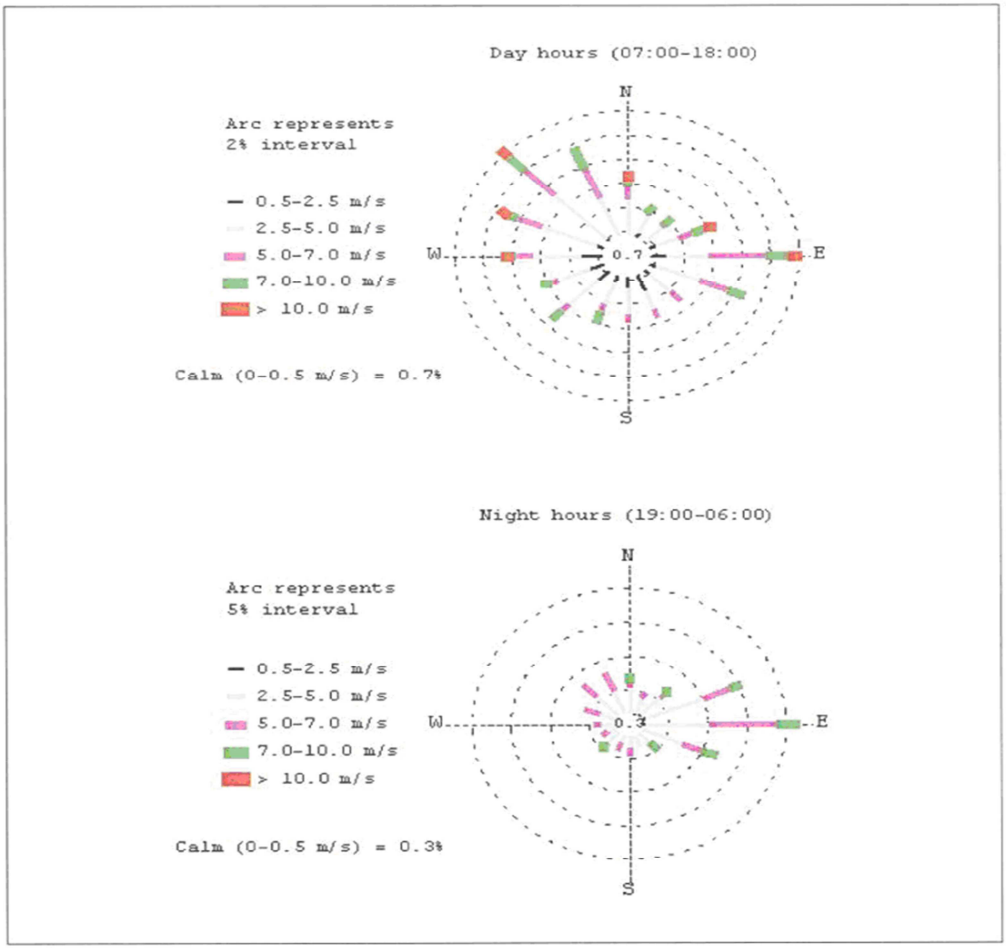


Figure 11: Daytime and night-time wind roses at Elandsfontein

The average diurnal wind speeds increase from 3.8 ms^{-1} at 07h00 to a maximum of 4.6 ms^{-1} at 11h00 (Figure 12). They remain fairly constant, decreasing in the late afternoon, then increasing throughout the evening and begin to drop once more during the early morning hours. This general pattern of diurnal wind speeds greater during the day and lower during the night-time period is observed at all Eskom monitoring stations. Exceptions occur when changing weather systems are passing. The increase during the day is due to the fact that under turbulent surface winds tend to couple with upper air winds. At night under inversion conditions the surface winds become decoupled and are not influenced by the upper air winds.

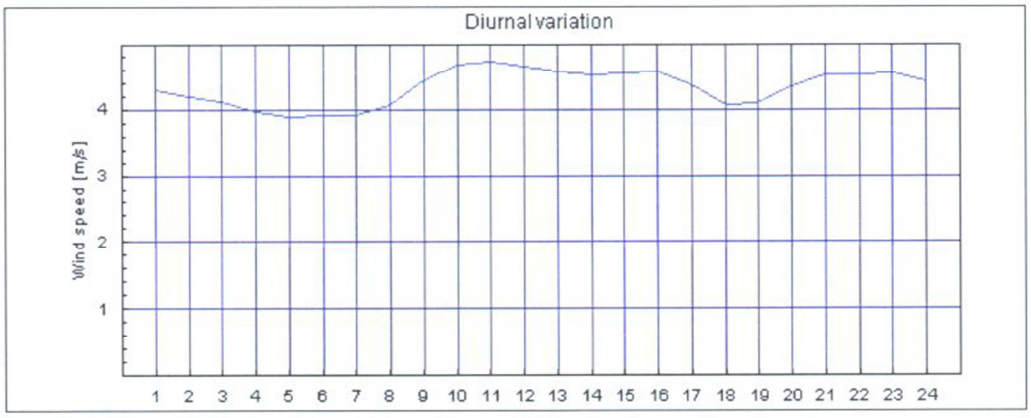


Figure 12: Diurnal variation of wind speed at Elandsfontein

The average daily wind speed graph for Elandsfontein (Figure 13) shows that the wind speeds are generally highest during August and September and lowest during June and July. The highest daily average of 9.9 ms^{-1} was recorded in September. The observation at all Eskom monitoring stations is that average daily wind speeds are different at all stations and the highest and lowest daily averages are recorded in different months for all stations suggesting that these differences are related to the predominant weather system in the area during these months.

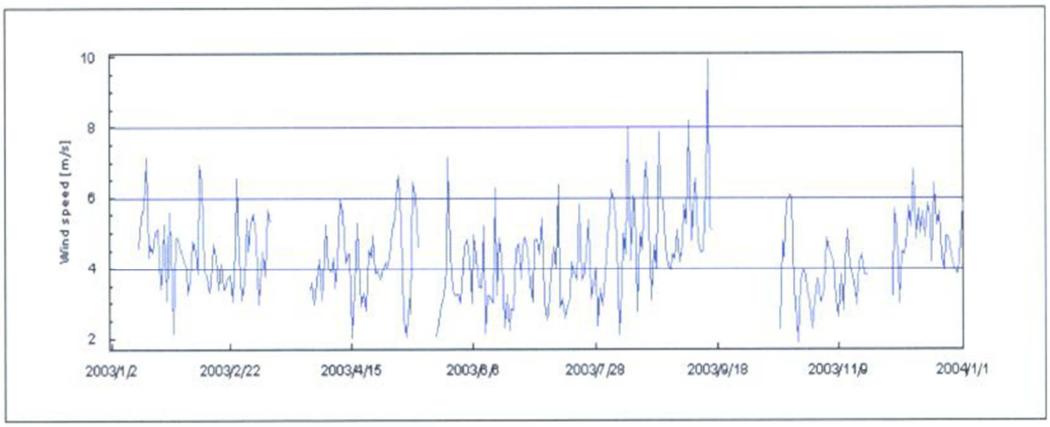


Figure 13: Average daily wind speed at Elandsfontein

The average temperature increases rapidly from 06h00 to a maximum of 27ºC at 13h00, then decreases during the afternoon and evening (Figure 14). As expected, the highest temperatures are recoded between 12h00 and 15h00. This pattern of hottest ambient temperatures experienced shortly after noon and coolest just before sunrise is observed at all Eskom monitoring stations.

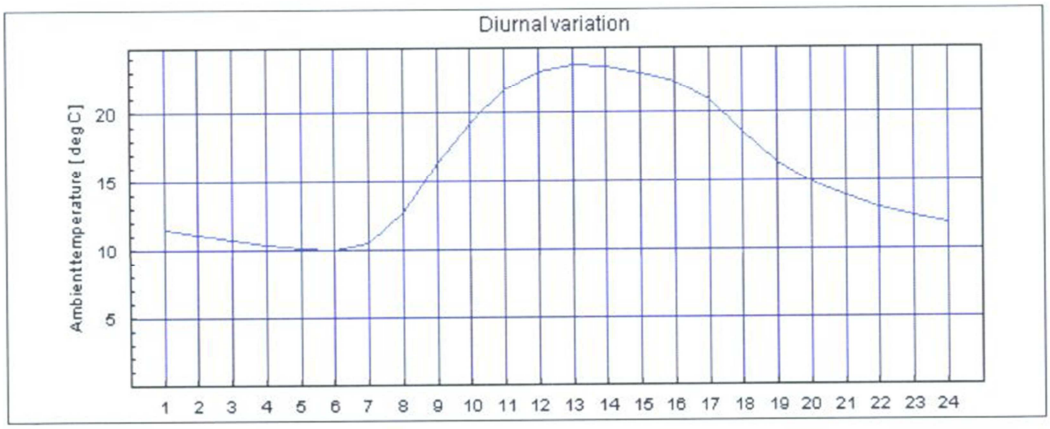


Figure 14: Diurnal ambient temperature at Elandsfontein

Daily average ambient temperature graphs at Elandsfontein (Figure 15) show that the temperatures are generally highest from December to February and lowest from June to August. The highest average hourly and daily temperatures of 34.1°C and 25.3°C respectively was recorded in January and the lowest average hourly of -5°C was recorded on 21 August whilst the lowest average daily temperature of 4.2°C was recorded on 18 October during an exceptional cold front. All Eskom monitoring stations recorded lower temperatures in the winter months as compared to summer.

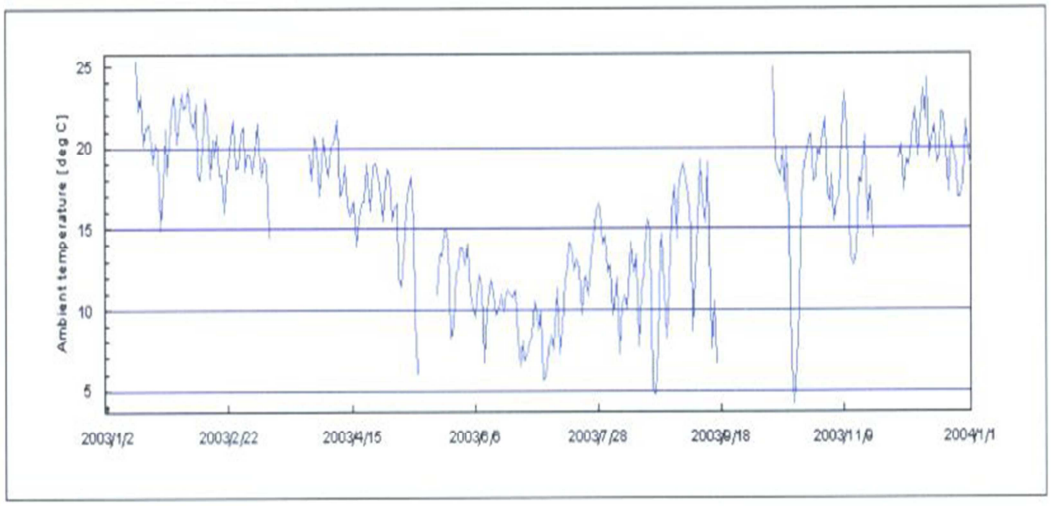


Figure 15: Daily average ambient temperature at Elandsfontein

SULPHUR DIOXIDE

The season variations in average hourly and daily concentrations (Table 8) indicate that the highest concentrations are generally during the winter months. A highest average hourly of 283 ppb was recorded in May.

Table 8: Highest average hourly, daily and monthly SO2 concentrations (ppb)

Month	**Highest Hourly Average**	**Highest Daily Average**	**Monthly Average**	**% Data Capture**
January	121	29.6	9.8	58
February	157	22	6.7	87
March	59.3	14.9	5.6	47
April	112	25.9	9.8	95
May	283	30	13.8	75
June	139	38	11.3	95
July	154	34.7	15.8	98
August	226	52.7	15.8	99
September	78.6	21.8	10.3	83
October	No data	No data	No data	0
November	57	13.2	2.8	62
December	146	18.2	9.1	93

NITROGEN DIOXIDE

The season variations in average hourly and daily concentrations are illustrated in Table 9. Comprehensive data analysis is not possible due to substantial data loss during the winter months. The highest average hourly concentration of 52 ppb was recorded in December and the highest average daily concentration of 13.5 ppb was recorded in August.

Table 9: Highest average hourly, daily and monthly average NO_2 concentrations

Month	Highest Hourly Average (ppb)	Highest Daily Average (ppb)	Monthly Average (ppb)	% Data Capture
January	34.2	11.3	5	58
February	19	4.6	2.5	54
March	No data	No data	No data	0
April	No data	No data	No data	0
May	No data	No data	No data	0
June	No data	No data	No data	0
July	No data	No data	No data	0
August	51.4	13.5	2.6	99
September	14.4	4.3	1.9	94
October	55.2	11.5	3.6	98
November	52.1	7.3	4.1	33
December	56.2	12.6	7.4	65

4.2.2.2 Verkykkop Monitoring Station

The Verkykkop monitoring station is located on a mountain top at Volksrust 35 km south of the Majuba power station and 70 km south-south-east of Tutuka power station. The site is approximately 130 km south-south-east of the central Mpumulanga industrial complex. The monitoring station was commissioned in 1984 to assess long-range transportation of power station plumes from central Mpumulanga, impacts from Majuba power station and theory of recirculation of pollutants back onto the Highveld.

METEOROLOGICAL OBSERVATIONS

During the day the winds are mainly from the west-north-west to north (48.2%) and south-south-east to south (27.3%) while during the night the winds are generally from the north-north-east to east-south-east (37.7%), north-west to north (24%) and south-south-east to south (21.3%). They frequently exceed 10 ms^{-1} during the day (22.4%) and night (18.2%), possibly due to the site's elevation of approximately 2 146 m above sea level (Figure 16).

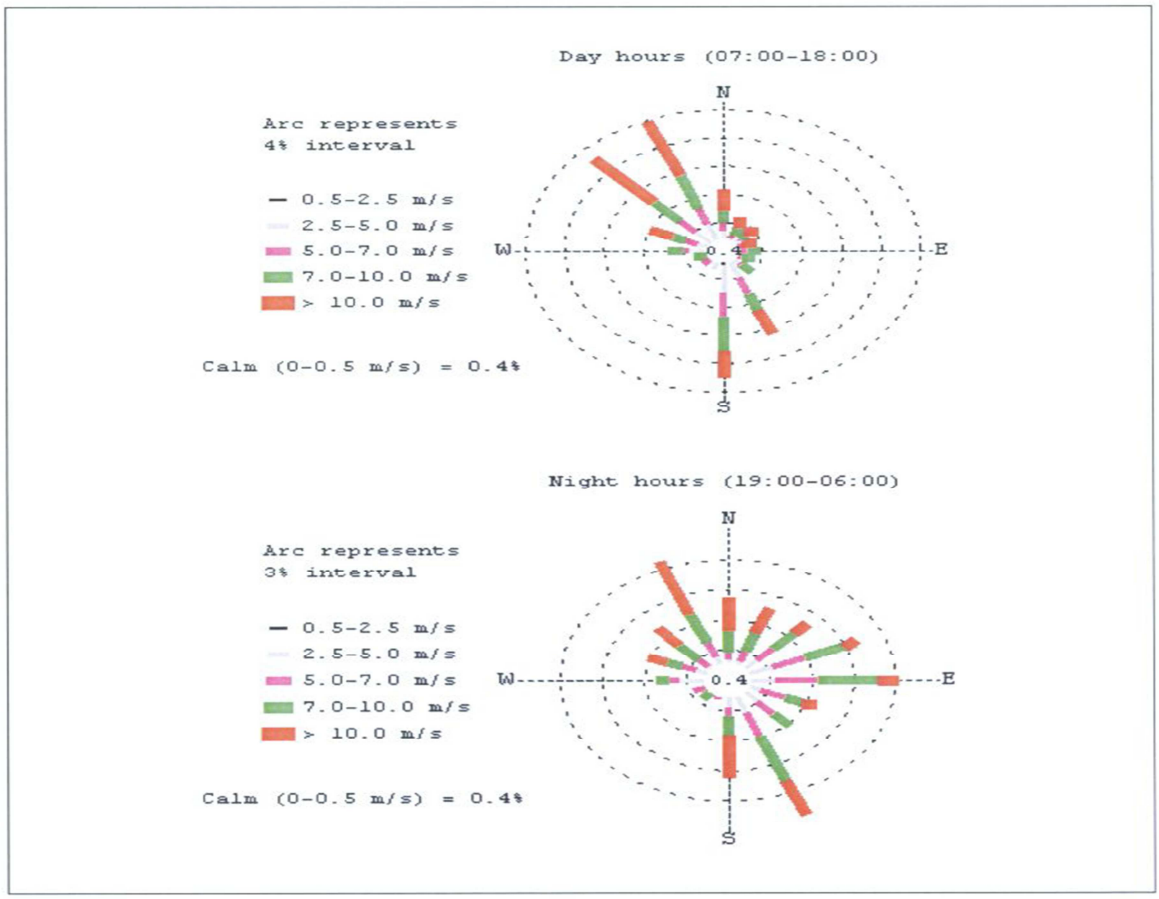


Figure 16: Daytime and night-time wind roses at Verkykkop

SULPHUR DIOXIDE

Although Verkykkop monitoring station is located on the boundary of southern Mpumalanga the diurnal variation is very similar to that of Elandsfontein monitoring station located in central Mpumalanga and shows the influence of tall stack emitters impacting at the site predominantly during the mid-day period. The average concentrations recorded are much lower than that of Elandsfontein monitoring station.

A highest average hourly of 140 ppb was recorded in December while the highest average daily of 29.8 ppb was recorded in November (Table 10).

Table 10: Highest average hourly, daily and monthly SO_2 concentrations (ppb)

Month	**Highest Hourly Average**	**Highest Daily Average**	**Monthly Average**	**% Data Capture**
January	49	12.3	4	97
February	123	20.1	3.7	89
March	57.2	11.7	3.4	99
April	58	10.2	4.4	94
May	70.6	23.4	5	100
June	101	15.2	4.5	95
July	68.1	20.6	6.4	100
August	67.1	15.8	5.8	96
September	110	19.3	7.4	93
October	125	15.2	6.2	98
November	129	29.8	7	92
December	140	15.6	5.4	100

NITROGEN DIOXIDE

The season variations in average hourly and daily concentrations are illustrated in Table 11. High concentrations were recorded during the summer months. The highest average hourly and daily concentrations of 60.6 ppb and 19.2 ppb respectively were recorded in November.

Table 11: Highest average hourly, daily and monthly NO_2 concentrations (ppb)

Month	Highest Hourly Average	Highest Daily Average	Monthly Average	% Data Capture
January	27.6	6.5	3.8	81
February	23.2	9.7	5.5	65
March	26	7.6	4.8	35
April	17.1	4.9	3.5	48
May	33.4	11.7	4.3	100
June	14.3	8.3	6.4	17
July	41.6	12.9	4.7	66
August	27.3	10.8	4.8	96
September	22	7.2	4.5	94
October	39.7	9.3	4.6	98
November	60.6	19.2	6.8	94
December	47.9	11.6	5.8	100

4.2.2.3 Palmer Monitoring Station

The Palmer monitoring station is approximately 2 015 m above sea level and is located 22 km north of Belfast and 50 km north-north-east of Arnot power station. The site was commissioned in 1989 to assess the impacts of plumes from central Mpumulanga on the eastern Escarpment forest plantations.

METEROLOGICAL OBSERVATION

During the day the most dominant wind directions (Figure 17) are from the south-west to north-north-west (44.3%) and north-east to east (31.5%). During the night the most dominant wind directs are north to east (59.2%) and west-north-west to north-north-west (26.2%). The wind speeds occasionally exceed $10ms^{-1}$ during the day (4.8%) and night (4.1%).

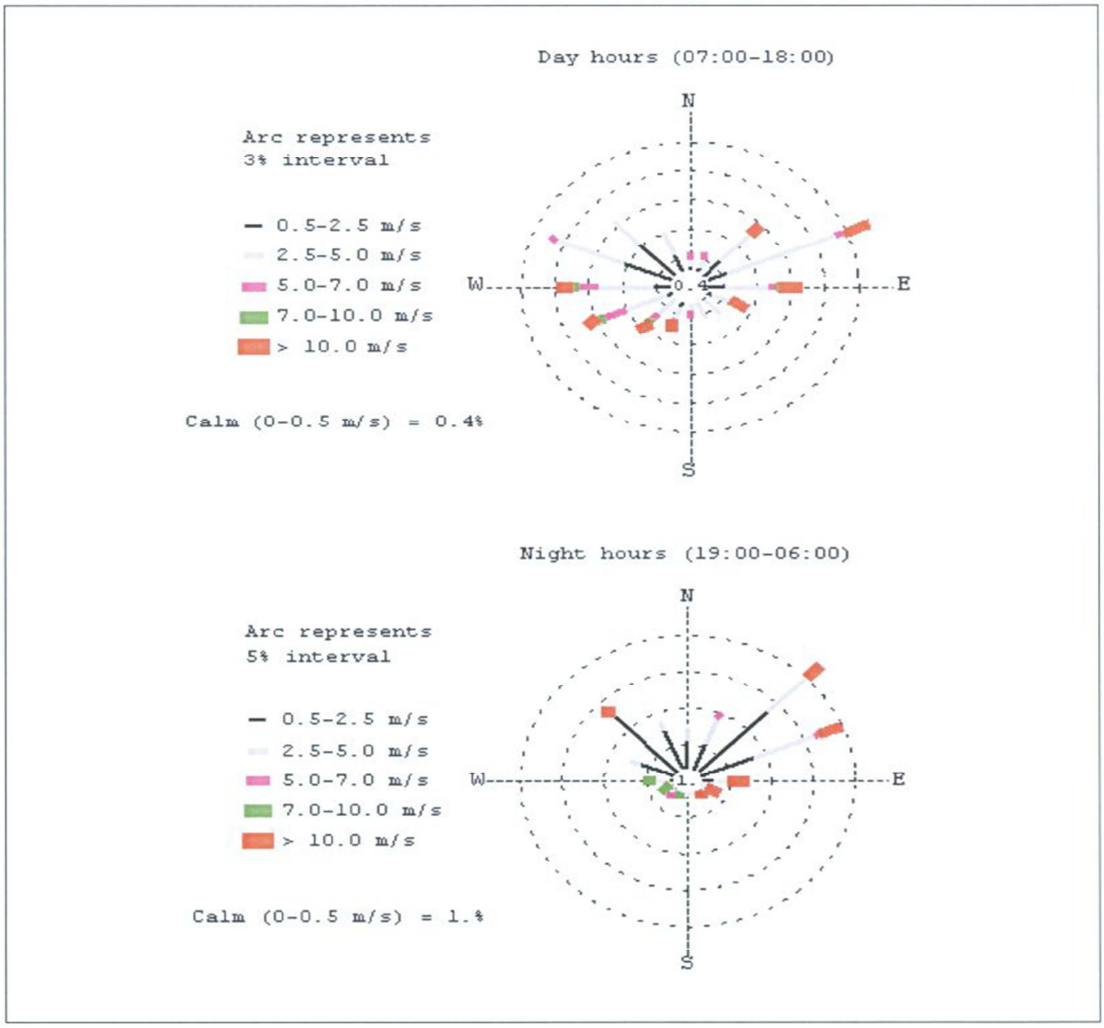


Figure 17: Daytime and night-time wind roses at Palmer

SULPHUR DIOXIDE

The average hourly and daily concentrations were higher during June to August (Table 12) which is attributed to the influence of domestic heating by coal and wood burning appliances during the winter months. This is common practice by residence in informal settlements across the eastern Highveld escarpment region. A highest average hourly and daily concentration of 156 ppb and 48 ppb was recorded in August and July respectively.

Table 12: Highest average hourly, daily and monthly SO_2 concentrations (ppb)

Month	Highest Hourly Average	Highest Daily Average	Monthly Average	% Data Capture
January	1.2	1	0.5	4
February	12.9	3.2	1.3	27
March	97.8	17.7	3.1	100
April	39.8	10	2.6	97
May	57.9	17.7	4.9	99
June	89.8	23.8	3.8	97
July	146	56.3	16.9	99
August	156	31.5	9.7	99
September	42.9	10.1	2.5	96
October	29.4	21.7	2.9	42
November	77.6	43	17.3	63
December	19.2	7.5	2.1	95

NITROGEN DIOXIDE

Although NO_2 average monthly concentrations are generally low, higher concentrations were recorded between May and August (Table 13). The highest average hourly concentration of 38.3 ppb was recorded in July, while the highest average daily concentration of 13 ppb was recorded in May.

Table 13: Highest average hourly, daily and monthly NO_2 concentrations (ppb)

Month	Highest Hourly Average	Highest Daily Average	Monthly Average	% Data Capture
January	1.5	0.6	0.4	4
February	6.1	1.5	1	26
March	31.6	7.1	1.6	100
April	9.7	2.6	1.3	97
May	25.7	13	2.5	99
June	25.4	11.3	1.9	97
July	38.3	10.3	3.9	99
August	33.2	9.4	2.6	99
September	15.6	4.7	1.1	96
October	12.3	3.9	1.4	42
November	20	4.6	1.5	62
December	8.2	2.5	0.9	96

4.2.2.4 Makalu Monitoring Station

Makalu monitoring station (approximately 1 500 m above sea level) is located 12 km south-south-west of Lethabo power station and 5 km east of the industrial area of Sasolburg. This site has been in operation since 1984 and was established by Eskom to assess impacts from Vaal and Highveld power stations which have since been decommissioned and the impacts from Lethabo power station which was being constructed at the time (Rorich, 2005).

METEROLOGICAL OBSERVATION

During the day the most dominant wind directions were from the west-north-west to north (27.8%), north-east to east (20.7%) and south-west to west-south-west (14.3%) with winds occasionally at 4.5% exceeding $7ms^{-1}$ (Figure 18). During the night the dominant wind directions are from the east-north-east to south-south-east

(47.6%), north-west to north (21.7%) and south-west (5.4%) with wind speeds much lighter, seldom exceeding 7 ms^{-1} (1.1%).

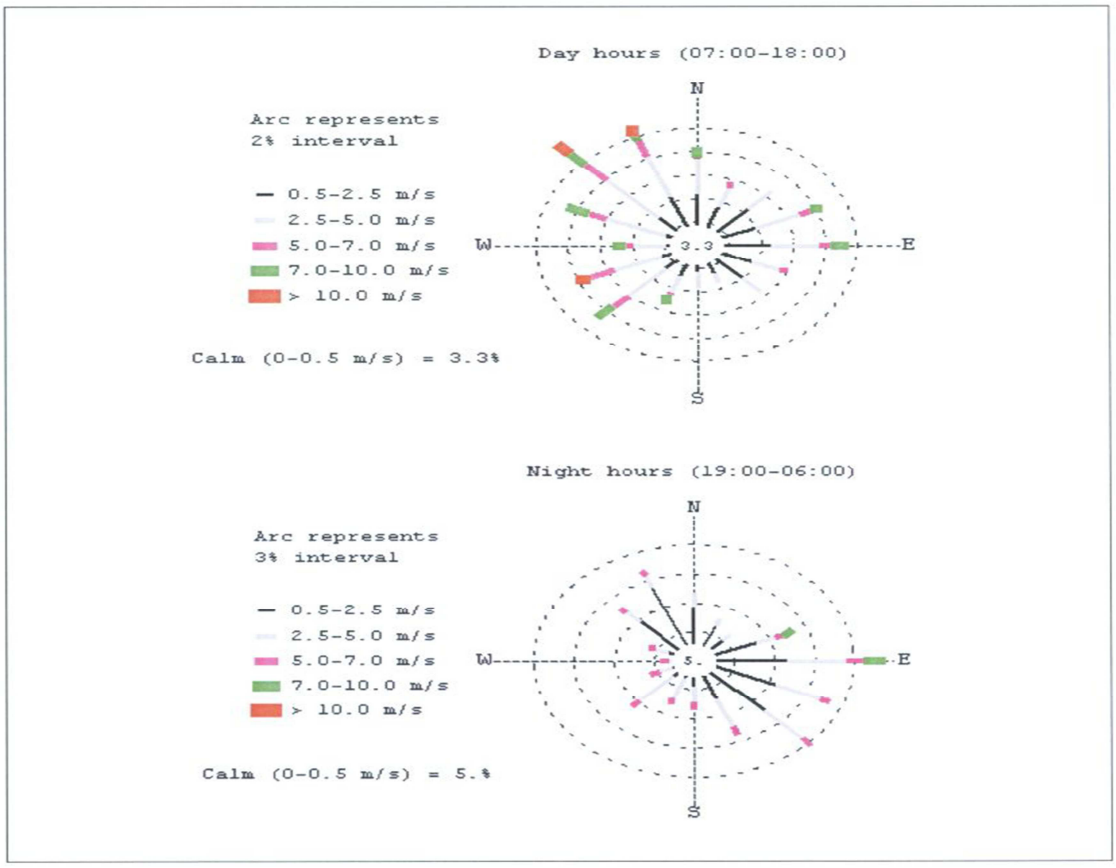


Figure 18: Daytime and night time wind roses at Makalu

SULPHUR DIOXIDE

There appears to be little seasonal influence on the SO_2 concentrations at this site (Table 14). A highest average hourly, daily and monthly concentration of 305 ppb, 38.6 ppb and 12. 1 ppb respectively was all recorded in July.

Table 14: Highest average hourly, daily and monthly SO_2 concentrations (ppb)

Month	Highest Hourly Average	Highest Daily Average	Monthly Average	% Data Capture
January	171	17.5	8.7	100
February	75	19.8	7.6	90
March	138	28.7	9	100
April	88	20.7	6.1	97
May	58.2	12.4	5.6	100
June	73.5	26.2	7.3	96
July	305	38.6	12.1	100
August	49.6	16.6	5.4	60
September	81.1	10.9	6.2	81
October	78.6	14.7	5.8	99
November	156	24	6.6	96
December	117	14.7	5.9	100

NITROGEN DIOXIDE

Average monthly concentrations were generally higher during winter and the transitional season months i.e. between May and September (Table 15). The highest monthly average of 12.2 ppb was recorded in July. The highest average hourly concentration of 46.5 ppb was recorded in October, while the highest average daily concentration was recorded in September.

Table 15: Highest average hourly, daily and monthly NO_2 concentrations (ppb)

Month	Highest Hourly Average	Highest Daily Average	Monthly Average	% Data Capture
January	23.9	8	5.1	100
February	28.2	10.2	5.1	90
March	31.9	9.8	5.8	100
April	37.6	14.4	6.7	97
May	45.2	15.1	8.3	100
June	39.9	17.1	8.1	96
July	44	20.7	12.2	99
August	32.9	18.6	9.2	99
September	39.8	23.2	8.4	97
October	46.5	16.8	8	99
November	31.8	13	7.3	97
December	34.3	11.1	6.8	100

4.2.2.5 Leandra Monitoring Station

Leandra monitoring station (approximately 1 706 m above seal level) is located at Leandra Junior School, 2 km north of the centre of the old Lebohang township and north-north-west of the new development township, which is rapidly growing towards the east. The monitoring station was commissioned in 1995 with the aim of assessing the air quality at Leandra and the impacts resulting from the electrification of Lebohang (Rorich, 2005).

During the day the dominant wind directions are from the west-north-west to north-north-west (39%), east to east-south-east (13.1%), south-south-east (5.5%) and south-west (5.3%) with wind speeds occasionally exceeding 7 ms^{-1} at 2.4% of the time (Figure 19).

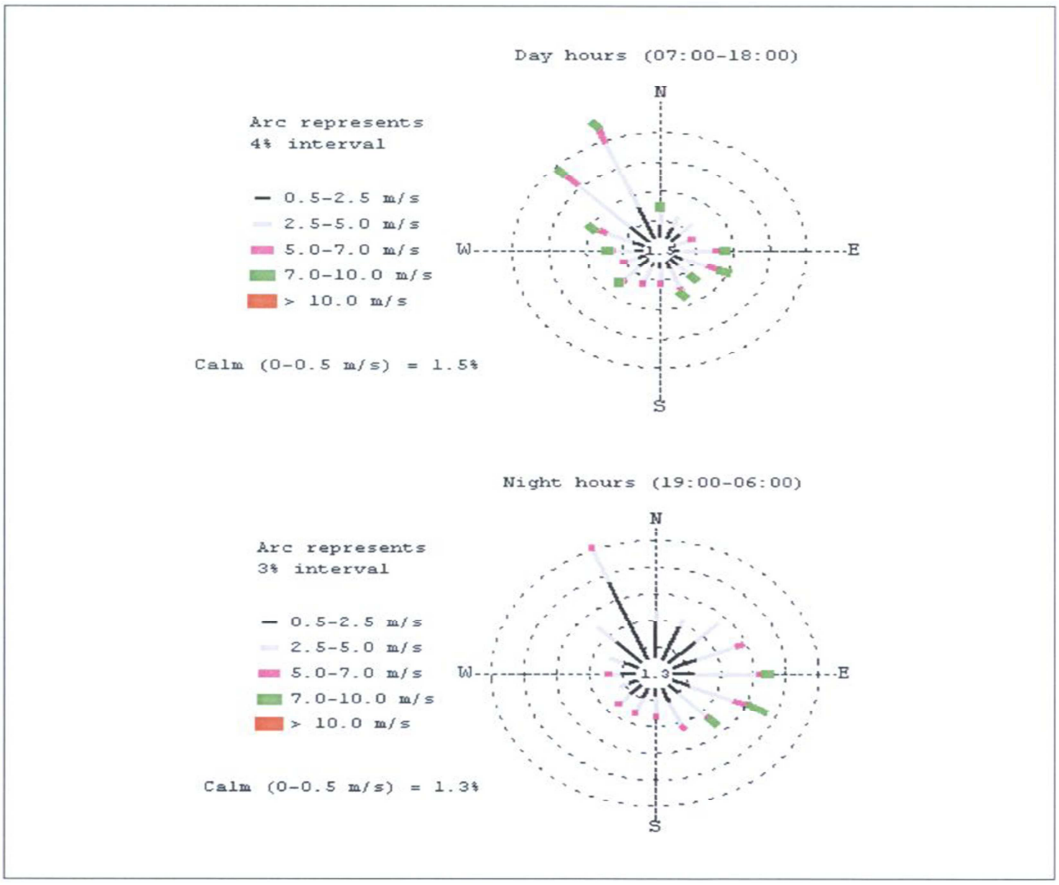


Figure 19: Daytime and night-time wind roses for Leandra

SULPHUR DIOXIDE

The average hourly, daily and monthly SO_2 concentrations (Table 16) are highest between April and July. A highest average hourly of 215 ppb and average monthly of 14.9 ppb was recorded in July while a highest daily average of 44.6 ppb was recorded in May.

Table 16: Highest average hourly, daily and monthly SO_2 concentrations (ppb)

Month	Highest Hourly Average	Highest Daily Average	Monthly Average	% Data Capture
January	114	17.9	5.5	100
February	149	30.9	8.1	90
March	160	27.5	8.3	99
April	161	39	10.9	96
May	170	44.6	10	99
June	207	39.6	3.4	96
July	215	41	14.9	99
August	132	25.1	7.6	99
September	117	16.2	6.5	96
October	85.8	15	4.8	99
November	176	35.4	6.9	95
December	177	28.7	6.3	99

4.2.2.6 Kendal Monitoring Station

Ambient air quality monitoring has been undertaken in the vicinity of Kendal power station since 1993. The monitoring is an integral part of the power stations environment management strategy and is seen as a vital link between power station operations and environmental management. The objective is to assess environmental impacts and compliance against the guidelines stipulated by the Department of Environmental Affairs. The monitoring station is situated 2 km south-south-east of the power station on the prevailing wind direction (Murray and de Beer, 2004).

METEOROLOGICAL OBSERVATIOS

The dominant wind directions during the monitoring period (Figure 20) were from the north to west (47.6%) and easterly to east-south-easterly (14.6%) sectors during the daytime. During the night the most frequent wind directions were from the east-north-earth to south-east (36.7%) and north-west to north-north-east (28.7%).

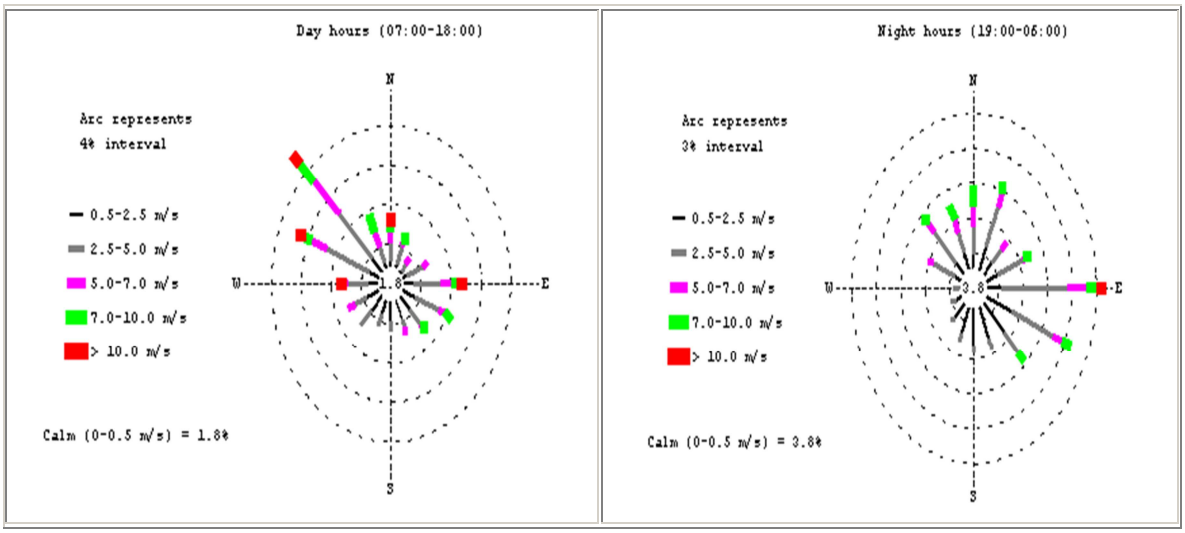


Figure 20: Daytime and night-time wind roses for Kendal

SULPHUR DIOXIDE

The highest average hourly, daily and monthly concentrations were all recorded in March (Table 17).

Table 17: Highest average hourly, daily and monthly SO_2 concentrations (ppb)

Month	**Highest Hourly Average**	**Highest Daily Average**	**Monthly Average**	**% Data Capture**
January	562	84.9	20	97
February	448	67.6	17.5	89
March	807	145.5	23.3	99
April	344	63.6	16.8	96
May	459	62	16.7	99
June	113	27.3	13.2	92
July	445	91.2	21.3	98
August	312	58.7	16.5	99
September	505	80.3	17.4	95
October	492	121.9	21.9	99
November	391	67.3	16.4	95
December	358	39.6	13.2	98

NITROGEN DIOXIDE

The average daily and monthly NO_2 concentrations (Table 18) are highest in the month of May. Although a highest monthly concentration of 10.8 ppb was recorded in both May and June, the month of May had a higher percentage of data capture. The highest average hourly of 65.5 ppb was recorded in October.

Table 18: Highest average hourly, daily and monthly NO_2 concentrations (ppb)

Month	**Highest Hourly Average**	**Highest Daily Average**	**Monthly Average**	**% Data Capture**
January	40.4	10.8	6.4	98
February	45.2	14.1	8.3	89
March	58.7	20.3	7.7	98
April	44.6	17.6	9.8	96
May	63.2	29.7	10.8	99
June	77	22.4	10.8	94
July	39.7	21.9	9.5	98
August	51.2	18	7.3	98
September	62.9	16	9.6	95
October	65.5	20.6	8.4	98
November	30.6	9.5	4.5	94
December	36.6	8.4	4	98

4.2.2.7 Majuba Monitoring Stations

Ambient air quality monitoring at Majuba power station is undertaken by Eskom to assess compliance to legislation and determine the local impacts on air quality from stack emissions and other activities such as coal stock piling and ash disposal. The monitoring forms an integral part of the power stations environmental management strategy and is seen as a vital link between power station operations and environmental management.

The ambient air quality monitoring stations J1 and J3, situated at the Majuba power station are equipped for continuous monitoring of SO_2 and fine particulate matter as well as meteorological parameters of wind velocity, wind direction and ambient temperature. J1 and J3 are situated 3 km south-east and 10.1 km west-north-west respectively of Majuba power station in the southern Mpumalanga Highveld. J1 was installed in December 1994 and J3 in January 2000.

METEROLOGICAL OBSERVATION

The dominant wind directions at J1 and J3 (Figure 21a and Figure 21b respectively) are from the west-south-west to north-north-west (47.68% and 42.74% respectively) and east-north-east to south-east (30.23% and 22.63% respectively) during the daytime and at night east-north-east to south-east (52.04% and 53.25% respectively). At night winds from the north-west sector reduce in frequency.

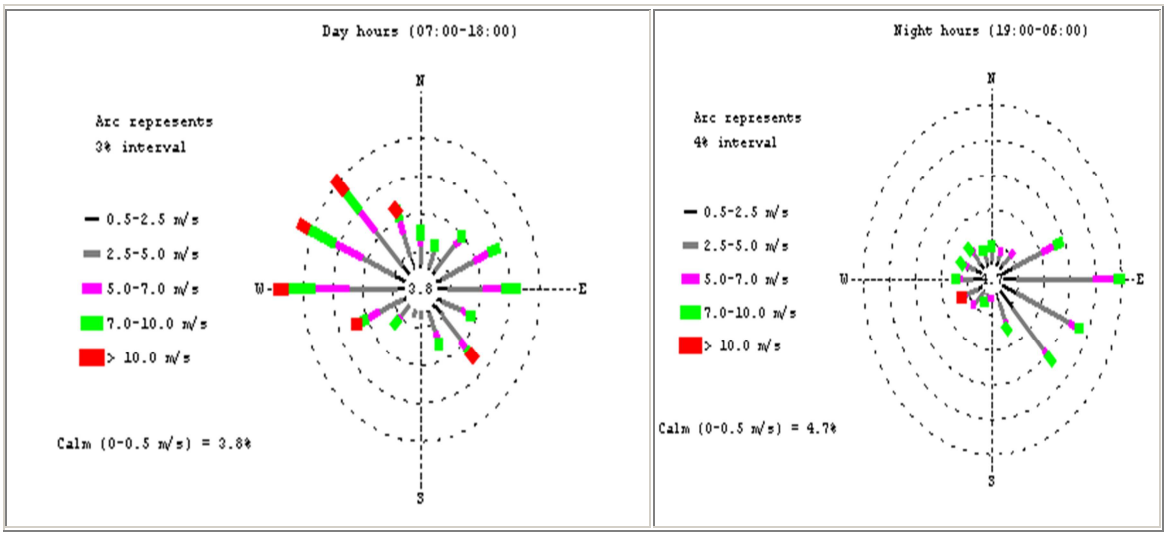


Figure 21a: Daytime and night-time wind roses for J1

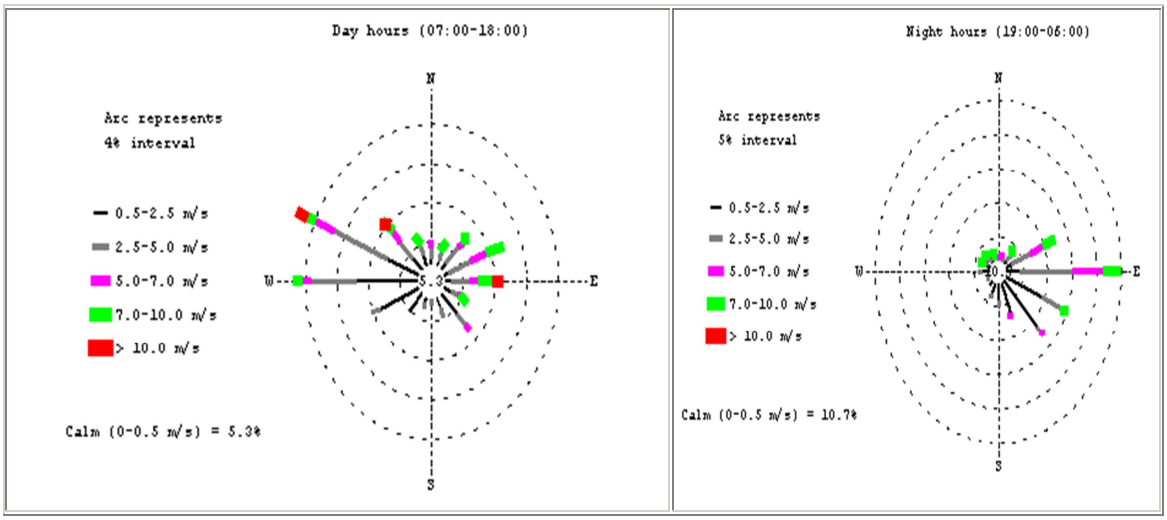


Figure 21b: Daytime and night-time wind roses for J3

SULPHUR DIOXIDE

The average hourly and daily concentrations were higher during July to August at J3 (Table 19). A highest average hourly and daily concentration of 164 ppb and 35.4 ppb was recorded in August and July respectively.

At the J1 monitoring station the average hourly and daily concentrations were higher during July and September (Table 19). A highest average hourly and daily concentration of 214 ppb and 49.4 ppb was recorded in September and July respectively.

Table 19: Highest average hourly, daily and monthly SO_2 concentrations [ppb] at J1 and J3

Month	Highest Hourly Average		Highest Daily Average		Highest Monthly Average		% Data Capture	
	J1	J3	J1	J3	J1	J3	J1	J3
January	190	48.5	30.1	11.1	5.5	3.9	99	54
February	150	35.8	29.6	5.9	6.1	4.5	79	9
March	147	69.2	30.8	13.2	4.8	5.1	98	53
April	148	120	16.3	15.1	4.4	5.1	96	96
May	112	77.8	24	17.7	4.4	4.2	99	99
June	109	78.7	18.9	14.2	4.7	4.6	95	71
July	195	106	49.4	30.8	7.5	9.1	98	98
August	173	164	25.9	35.4	9.8	7.7	99	99
September	214	86	32.2	16.6	10.5	7.4	94	52
October	202	71	23.3	9.8	7.5	4.5	94	40
November	184	46.6	23	9.6	9.3	4.2	92	78
December	152	3.3	21.3	1.3	8.1	1.3	99	4

4.3 MODELLED DATA

As discussed in Section 3.3 air dispersion modelling is a useful tool to establish the spatial and temporal patterns of ground level pollutant concentrations arising from the emission of various sources. Increasing reliance has been placed on ground level air pollution concentration estimates from models as the primary basis for environmental, health and risk assessments and determining emission control requirements (Scorgie and Venter, 2005; Davakis *et al.*, 2007, Zawar-Reza and Sturman, 2008). The modelled concentration fields which were utilised in this study were produced by Airshed Planning Professionals on behalf of Eskom. Although the modelling study was conducted to assess air pollution compliance of cumulative operations of current, return to service and proposed Eskom power stations located within the Mpumalanga and Gauteng provinces, the data utilised in this study is only of current baseline operations (Eskom power station and other sources).

4.3.1 SOURCE AND EMISSION DATA INPUTS

Emission rates for each pollutant and source were required as an input into the CALPUFF model. Source parameter requirements for input include stack height, stack diameter, exit temperature, exit velocity, elevation of stack base above sea level and source location (Scire *et al*, 2000a). The largest source of emissions at the Eskom power stations is the main stacks. The data for these parameters were provided by Eskom.

Although source and emissions data were collated by Airshed Planning Professionals for the Eskom current operating conditions (comprising emissions data for the years 2001, 2002 and 2003), future operating conditions and cumulative proposed scenarios only data for current operating conditions were utilised in this study.

Monthly emission variations were calculated based on the energy outputs per month for 2001 to 2003 from the current Eskom power stations. Eskom provided the data for energy outputs and the total emissions per year. Emission rates were varied diurnally for the simulations and a 'typical' diurnal variation for summer and winter based on energy output was utilised (Figure 22). During winter there is a distinct increase in electricity demand therefore there is an increased energy output during morning and evening hours. This trend is far less distinct during the summer months (Scorgie and Venter, 2005).

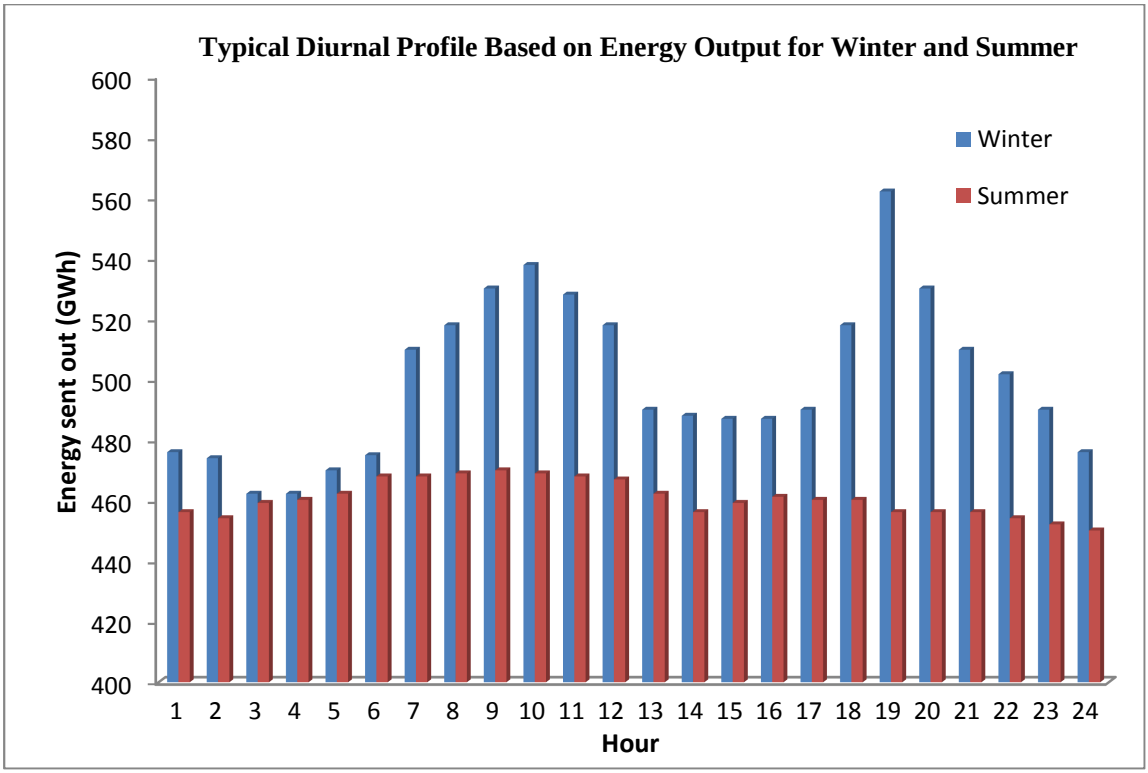


Figure 22: Typical diurnal profile based on the energy output for winter and summer (Scorgie and Venter, 2005)

Source and emission data for sources other than Eskom power stations which were available and in the public domain and/or for which permission had been obtained were included in the modelling simulations. Sources accounted for included road traffic (vehicle exhaust emissions), household fuel burning (coal, wood, paraffin and gas), industrial, commercial and institutional fuel burning (coal, wood, paraffin, heavy fuel oil and gas) and various industrial process emissions. Other significant sources not accounted for include fugitive dust (from industry, mining, vehicle entrainment and agriculture), agricultural and veld fire burning and aireborne aerosols from distant sources imported as a result of long-range transport (Scorgie and Venter, 2005).

4.4 SPATIAL DATA INPUTS

TNT mips a product of MicroImages as well as Environmental Science Research Institute's (ESRI's) Arcview 9.3, map and image processing softwares, were used as the tools for the analysis of the spatial information, advanced image

processing, desktop mapping, spatial database management and visual applications. TNT mips was employed mainly for the processing of the satellite data which is recorded in HDF format. The three air quality datasets (surface measurements, satellite retrievals and modelled concentration fields) as discussed in section 3.2, 3.3 and 3.4 were analysed, interrogated and integrated via an interpolation technique within Arcview to ultimately produce risk maps and improve the modelled outputs using measured concentrations.

The spatial datasets utilised in the GIS to output risk maps include, vegetation coverage, population density, residential areas, land cover, wetlands, towns, air quality monitoring stations and power stations.

The population density dataset was derived from the 2008 SPOT 5 building count dataset. The SPOT 5 building count dataset was a product of a South African government initiative which utilised the SPOT satellite imagery to map the location of all dwelling units and building structures in the country.

****

Data and information for this study was obtained from the Eskom air quality data base, the SAWS, Airshed Planning Professionals dispersion modelling studies conducted on behalf of Eskom and the European Space Agency's SCIAMACHY retrievals over the Highveld. Only datasets from year 2003 were utilised in this study.

Eskom began ambient air quality monitoring in the late 1970's for both regional and compliance monitoring down wind of Eskom power stations and to assess impacts from power station emissions. The Eskom monitoring stations that were used in this study included Elandsfontein, Verkykkop, Makalu, Palmer, Leandra, Arnot, Kendal, Majuba 1 and Majuba 3. The overall network reliability for data capture across all monitoring stations was 83.2%.

Although source and emissions data were collated by Airshed Planning Professionals for the Eskom current operating conditions (comprising emissions data for the years 2001, 2002 and 2003), future operating conditions and cumulative

proposed scenarios only data for current operating conditions were utilised in this study.

TNT mips and Arcview software were utilised for the analysis of satellite retrievals and modelled outputs. Spatial datasets utilised in the risk assessment aspect of this study included vegetation coverage, population density, residential areas, land cover, wetlands, towns, air quality monitoring stations and power stations . In this study three air quality datasets (surface measurements, satellite retrievals and modelled fields) have been statistically analysed and integrated using an interpolation technique in a GIS to produce a new set of "improved" modelled data of ambient NO_2 and SO_2 over the Highveld region.

The following chapter looks at the methodological framework for the study and discusses the assumptions made.

CHAPTER 5
METHODOLOGY

This chapter discusses the methodological approach for the study and states all the assumptions that were made. The method for the analysis and interrogation of SCIAMACHY retrievals, modelled output, statistical distribution at the tail of the modelled data, integration of measured and modelled datasets and the risk analysis for potential exposure to population and ecosystems are described.

5.1 INTRODUCTION

In air dispersion modelling, it is important to validate remotely sensed data as well as predicted concentrations from models with ground-based measuresments in order to acertain the level of confidence with which the results can be utilised in decision making. As discussed in section 1.2 the study area is often cited as a hotspot for SO_2 and NO_2 pollution (Figure 2) in satellite observations around the world. In this study an attempt is made to validate satellite-borne remote sensing observations (SCIAMACHY retrievals) from the Mpumalanga Highveld region and CALPUFF modelled outputs against measured ground-level concentrations of SO_2 and NO_2. Ground monitoring stations for ambient air quality only provide concentrations at a point whereas the use of satellite observations and modelled outputs provide coverages over a wider area.

Increasingly, modelled outputs are being overlayed with spatial datasets to determine potential risk to population and ecosystems. As discussed in Section 2.6 this is a useful method which can be used in AQMPs for an airshed.

5.2 SCIAMACHY

5.2.1 SCIAMACHY SENSOR & COVERAGE

SCIAMACHY was launched in March 2002 as part of the European ENVISAT space craft mission. The dataset is derived from an imaging spectrometer which records solar radiation transmitted, scattered and reflected in the ultraviolet, visible and shortwave infrared wavelength region (220-2 380 nm) at moderate resolution (0.2-1.5 nm). Scattered sunlight is measured in nadir and limb geometry, transmitted solar and lunar radiation in occulation geometry, and solar and lunar irradiance in occulation (Sierk *et al*., 2006). The extraterrestrial solar irradiance and lunar radiance is determined from observations of the sun and the moon above the atmosphere. The absorption, reflection and scattering behaviour of the atmosphere and the earth's surface is determined from comparison of the earth's sunshine radiance and solar irradiance. Inversion of the ratio of the earth's sunshine radiance and solar irradiance provides information about the concentration and distribution of selected atmospheric gasses and aerosols as well as knowledge about the pressure, temperature, radiation field, cloud cover, cloud top height and albedo of the earth's surface (Gurlit *et al.*, 2003; Bovensmann *et al.*, 1999).

A unique feature of the SCIAMACHY sensor is the ability of the instrument to alternate viewing geometries (Bovensmann *et al.*, 1999). In nadir mode (down-looking) column densities of trace gases are retrieved with a spatial resolution of 30 x 60 km using the Differential Optical Absorption Spectroscopy (DOAS) technique (Platt and Perner, 1983). In this mode the instrument scans the atmosphere underneath the space craft by sensing upswelling solar radiation that has been transmitted and scattered in the atmosphere and reflected towards the earths's surface. In the limb mode (in the direction of the flight) two mirrors direct the sunlight scattered by the atmosphere near the horizon into the spectrometer. During this scanning mode the vertical atmosphere is explored by changing the tangent height from the surface up to approximately 100 km (Sierk *et al*., 2006). The inversion of the combination of limb and nadir measurements enables the calculation of the NO_2 and SO_2 tropospheric column concentrations.

Attenuation processes mainly scattering and molecular absorption determine the intensity of the detected radiation at distinguishing wavelengths. Therefore the radiance measurements contain information on concentration and distribution of several trace gases showing distinct spectral absorption features in the observed wavelength (Bovensmann *et al*., 1999).

SCIAMACHY is able to observe the whole earth in a 100 minute orbital period. Measurements are made with a ground pixel size of 15 x 30 km^2, but due to the restricted bandwidth for data transmission, generally four observations are integrated on board, leading to a standard retrieved grouping pixel size of 30 x 60 km^2. The usage of alternating viewing geometries creates breaks along the track which forms a checkerboard pattern. The limb-nadir alternation is programmed in a manner such that areas which are missed during one scan are covered by the next overpass 3 days later. This permits SCIAMACHY to achieve a global coverage at the equator with a 6-day cycle (Beirle, 2004).

5.2.2 DIFFERENTIAL OPTICAL ABSORPTION SPECTROSCOPY (DOAS) ANALYSIS

SCIAMACHY utilises the DOAS method to determine concentrations of trace gases by measuring their specific narrow band absorption structure in the ultra violet (UV) and visible spectrum region (Platt, 1994; Platt and Perner, 1983). The DOAS instrument consists of a light source (generally the sun or scattered sunlight) and an optical setup which has the ability to send and receive the light through the atmosphere. After its path through the atmosphere, the light is spectrally analysed and the concentration of atmospheric constituents are calculated. In the atmosphere the light undergoes extinction processes by air molecules and aerosols, turbulence and absorption by many trace gases (Platt, 1994).

The objective of any spectroscopic method formulated for the atmosphere is to separate these effects in order to derive the concentrations of the atmospheric constituents. DOAS performs this by separating the cross sections of the trace gas absorptions into low and high frequency parts by specific numerical filtering methods. By applying the same filtering routine to the light intensity for a path of fixed length,

a new light intensity is created which contains the low frequency part of the spectrum (the exclusion of turbulence effects, as well as all broad band gas absorption structures). After the filtering DOAS only observes the narrow absorption structures and this is used to determine the trace gas concentrations (Platt, 1994).

Generally many trace gases absorb in the same spectral region. If this is the case then a numerical fitting procedure is used to separate them. Differential absorption cross-sections for some of the trace gases absorbing in the UV/visible wavelength spectrum that can be measured by DOAS are shown in Figure 23 The right axis describes the detection limits of the trace gases together with the typical light path lengths used to measure them (Stutz and Platt, 1997).

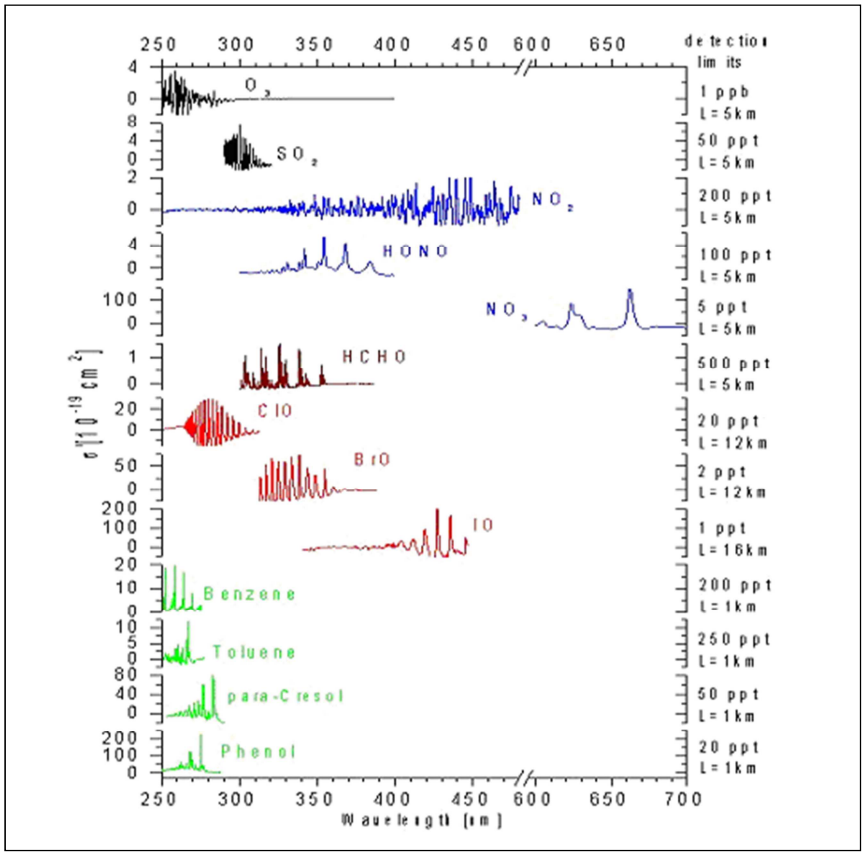


Figure 23: Differential absorption cross-sections of some trace gases absorbing in the UV/visible wavelength spectrum (Stutz and Platt, 1997).

5.2.3 SCIAMACHY LIMB AND NADIR MEASUREMENTS

Both the stratosphere and troposphere contains significant amounts of molecular NO_2 which plays an important role in the radiative transfer and the energy budget. As discussed in Section 2.2.1 and 2.3.1 NO_2 sources are both natural and anthropogenic.

The SCIAMACHY instrument was designed with the main aim of deriving tropospheric concentrations of trace gas species. This was achieved with the implementation of a spectrometer which continuously alternates between the limb and nadir geometries (Bovensmann *et al*., 1999). The viewing angles for the acquisition of limb spectra are adjusted to focus the tangent points as close as possible over the region, which is measured 7 minutes later in a nadir state. This provides the capability to infer vertical stratospheric concentration profiles directly over the region of the nadir measurement. Integrating these profiles from the tropopause upwards produces the stratospheric vertical column density above the target area (Sierk *et al.*, 2006 and Richter *et al.*, 2005).

Sierk *et al.* (2006) implemented the limb-nadir matching method to compute tropopause heights from meteorological model data. These data consisted of three-dimensional model calculations of pressure and temperature on a latitude/longitude grid of 1° resolution and 60 height levels up to approximately 60 km. A combination of two concepts is utilised to define the boundary between the troposphere and stratosphere. For the topics (± 20° latitude from the equator) a temperature gradient criterion is used which defines the tropopause at the point where the condition dT/dH > -2 k/KM (where T and H denote temperature and altitude, respectively) is satisfied. At the mid-latitudes, the calculated potential vorticity (PV) threshold of $3.5x10^6$ Km^2/(sec kg) is used to define the tropopause. In preparation for the application to SCIAMACHY measurements, the tropopause values were averaged within the nadir states to calculate the lower boundary for the numerical integration of the corresponding NO_2 limb profiles, and thus the stratospherical vertical column density (VCD).

The DOAS analysis of the nadir spectra yields the total slant column densities (SCDs) for the ground pixels, the stratospheric VCD is mapped to the nadir

observation geometry by transforming it to a corresponding stratospheric SCD. Using the airmass factor of the stratosphere (AMF_{strat}) component the difference from the SCD and VCD is exploited to obtain the tropospheric slant column density (SCD_{trop}) equation 26 (Sierk *et al*, 2006).

$$SCD_{trop} = SCD_{total,nadir} - VCD_{strat,limb} \times AMF_{strat,nadir} \qquad \text{equation 26}$$

5.2.4 SCIAMACHY ANALYSIS

SCIAMACHY observations are freely available on the European Space Agency's website. The daily individual overpass files from SCIAMACHY observations at Eskom monitoring stations were extracted from the TEMIS Website (http://www.temis.co.za). The extraction also included all SCIAMACHY observations for distances not greater than 200 km away from the Eskom monitoring stations. The scale of the SCIAMACHY pixel is larger than the scale that is required for ground observations. SCIAMACHY retrievals are based on gridded data at 1km x 1km resolutions.

The hourly average concentrations recorded at the Eskom ground based monitoring stations were compared with the satellite overpasses in order to validate the SCIAMACHY instantaneous retrievals. Within the study domain there are 67 SCIAMACHY pixels (30 km x 60 km) of imagery for year 2003 (Figure 39). A GIS polygon layer was created using these pixels. The co-ordinate data of the Eskom ground based monitoring stations were utilised to produce a GIS layer and the hourly, daily and annual concentration datasets per station was recorded as attribute data within this layer.

The SCIAMACHY sensor measures the total number of molecules of NO_2 gas in the whole depth of the atmosphere over the entire pixel area (30 km x 60 km).This is referred to as the total NO_2 column. An on board calculation is then utilised to automatically compute the concentration of NO_2 in the tropospheric layer and this is referred to as the tropospheric NO_2 column. Using assumptions, this integrated tropospheric NO_2 value needs to be converted to a representative single concentration value at a point. To perform this, it is assumed that a significant proportion of the NO_2

is in the mixing layer which is thoroughly mixed (Mijling, 2012) and the concentration value is constant (implying that the mixing layer is uniformly mixed). It is further assumed that the depth of the mixing layer is 800 m typically for the time of day that the satellite overpasses the Highveld (Tyson *et al*, 1998). This is an estimate which can be reviewed for future studies.

The extracted tropospheric NO_2 column retrievals were recorded by SCIAMACHY in molecules x 10^{15} / cm^2 and had to be converted to ug/m^3 to allow comparisons against Eskom ground measured data. This entailed the conversion from molecules per surface area into a mass per volume concentration (equation 27, equation 28, equation 29, equation 30, equation 31, equation 32 and equation 33).

The following calculation was utilised in the conversion:

number of moles = mass / molar mass equation 27

Molar mass [NO_2] = 14.007 + (15.999 x 2) g/mol equation 28
= 46 g/mol

NO_2 is not an ideal gas
1 mole of NO_2 = 6.02 x 10^{23} molecules (Avagadro's constant) equation 29
= 46 g

1 x 10^{15} molecules = 46g x (1 x 10^{15} molecules) / 6.02x 10^{23} molecules equation 30
= 7.641 x 10^{-8} g

Conversion from grams to micrograms:
7.641 x 10^{-8}g x (1 x 10^6) equation 31
=0.07641 µg

In terms of mass per area this is 0.07641 µg /cm^2. The mixing depth height is assumed at 80 000 cm.

Conversion from µg /cm^2 to µg /cm^3:

0.07641 µg /cm2 / 80 000 cm equation 32

$= 9.55125 \times 10^{-7}$ µg /cm^3

Conversion to µg /m^3:

$9.55125 \times 10^{-7} \times (1 \times 10^6)$ equation 33

$=0.955125$ µg /m^3

The value of 0.955125 µg /m^3 is the representative surface concentration of the NO_2 satellite retrieval at the measuring point on the ground. This constant value was multiplied to the NO_2 tropospheric column values which were retrieved by the satellite in order to estimate the point value on the ground.

The NO_2 data was in some instances negative in the overpass files. This can be attributed to the retrieval processes and is considered acceptable within error margins. In some instances the tropospheric NO_2 values were higher than the total NO_2 column. This is caused by the fact that both values are calculated in an independent manner, however the tropospheric value is believed to be more realistic (http://www.temis.co.za; pers com1) and this was utilised in the study.

SCIAMACHY retrievals for tropospheric SO_2 for years 2003 and 2004 are unavailable by ESA due to instrumentation noise (pers. com1) and therefore a validation of SO_2 retrievals could not be made in this study.

The overall limitations of using satellite retrievals for comparability and validation to monitored ground level concentrations are discussed in section 1.2.3.

5.3 THE CALPUFF MODELLING SUITE

The CALPUFF (California puff) modelling suite is a United States Environmental Protection Agency approved air dispersion model suitable for application in modelling domains of between 50 km and 200 km. The model is able to account for temporal and spatial variability of meteorological conditions, dry deposition and dispersion over a variety of spatially differing land surfaces. CALPUFF can also simulate plume fumigation, low wind speed dispersion and

determine first order chemical transformations for gas phase reactions of SO_2 and NO_x (Scire *et al*., 2000a; Scorgie and Venter, 2005; USEPA, 2005; Zhou *et al*., 2006).

CALPUFF is a non steady state regional Langragian Puff model comprising of three components namely: CALMET, CALPUFF and CALPOST (Figure 23). The model utilses three dimensional meterological fields developed by CALMET and a series of overlapping puffs to represent the spatial and temporal distribution of emisions from a source. CALPOST is then used as a post processor of the CALPUFF outputs to produce a summary of the simulations results (Scire *et al*., 2000a; SRC, 2008).

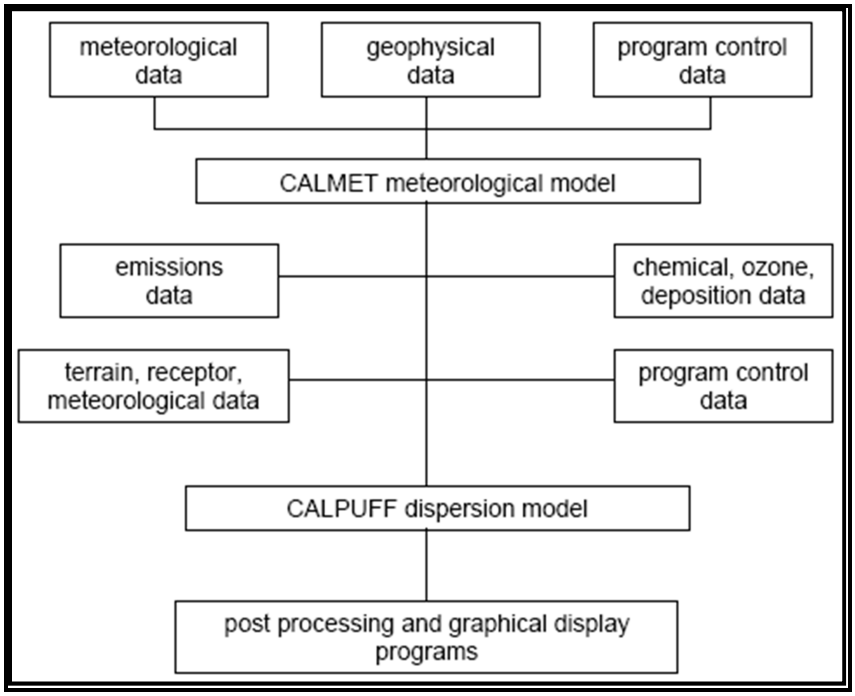


Figure 24: CALPUFF modelling system (SRC, 2008).

5.3.1 THE CALPUFF COMPONENT

The CALPUFF component recognises emissions as a series of continuous puffs. Each puff is simulated to move with the ambient wind flow. As the wind flow changes, the path of each puff is displaced in a Lagrangian manner while undergoing Gaussian dispersion. The model predicted concentrations are computed based on the contributions of each puff as it passes near and over a receptor point defined in the modelling domain (Scire *et al*., 2000a; SRC, 2008).

This CALPUFF component requires as a minimum the input of hourly average surface meteorological data. The CALMET component is utilised to generate the three dimensional wind fields for input into the CALPUFF component. In the study to assess air pollution compliance of cumulative operations of current, return to service and proposed Eskom power stations located within the Mpumalanga and Gauteng provinces, Airshed Planning Professionals utilised maximum hourly average, daily, and annual average concentrations to simulate the application of CALPUFF (Scorgie and Venter, 2005). This study utilises the results from the Airshed Planning Professionals study and is limited to the parameters set by these consultants.

CALPUFF allows for first order chemical transformation modelling in order to determine gas phase reactions for oxides of sulphur and nitrogen. Chemical transformation rates were computed internally by the model using the RIVAD/ARM3 Scheme. This scheme allows for the separate modelling of NO_2 and NO_2. The RIVAD/ARM3 scheme treats the NO and NO_2 conversion process in addition to the NO_2 and total NO_3 and SO_2 to SO_4 conversions, with equilibrium between gases HNO_3 and ammonium nitrate aerosol. The scheme uses user-input ozone data together with modelled radiation intensity as surrogates for the hydroxide concentration when gas phase free radical chemistry is active (Scire *et al.*, 2000; Scorgie and Venter, 2005).

5.3.2 THE CALMET COMPONENT

The CALMET meteorological model contains a diagnostic wind field module which requires input on terrain and kinematics effects, slope flows and terrain channelling. The wind fields are computed in a two step process. In the STEP 1 wind field, the initial guess wind field is adjusted for terrain effects. The user is prompted by the programme to input the vertical layers, through which the domain wind is averaged and calculated, and the upper air and surface meteorological stations are included in the interpolation to produce the spatially varying guess field. The Step 1, initial guess field and wind observational data are then weighted by allowing the user to input a radius of influence to the produce the Step 2 wind field. The programme excludes any observational data from the interpolation if the distance between the

source and a particular grid point exceeds the maximum radius of influence specified (Scire *et al.*, 2000b; SRC, 2008; USEPA, 2005).

CALMET was utilised in the Eskom study to simulate the meteorological field within the Mpumalanga Highveld, including the spatial (horizontal and vertical) and temporal variations in the wind field and atmospheric stability. CALMET required in put data for upper air parameters however there was no upper air monitoring stations available within the Mpumalanga Highveld therefore the nearest SAWS station located at Irene in the Tshwane Municipality was utilised. The SAWS ETA-Model data for twelve locations was used. Data were obtained twice daily for five sounding levels. The initial guess field in CALMET was determined as a combined weighting of surface winds at nine Eskom monitoring stations and ten SAWS stations, vertical extrapolation using Similarity Theory and upper air winds. Data was obtained from the Eskom monitoring stations at Verkykkop, Elandsfontein, Kendal 2, Leandra, Majuba 1, Majuba 3, Makalu, Palmer and Camden. The SAWS stations used in the study were located in Johannesburg, Irene, Vereeniging, Witbank, Leandra, Ermelo, Standerton, Newcastle, Verkykkop and Bethal (Scorgie and Venter, 2005).

The CALMET model requires average hourly surface data, wind speed, wind direction, mixing depth, cloud cover, temperature, relative humidity, pressure and precipitation as an input. The mixing depth is not measured at any monitoring station and had to be calculated based on available temperature and predicted solar radiation.

5.3.3 THE MODELLING DOMAIN AND RECEPTOR LOCATIONS

The modelling domain was defined to incorporate the existing, return to service and proposed Eskom power stations as well as the maximum impact zones of these stations. The three return to service power stations, namely Camden is located 22 km south east of Ermelo, Grootveli 18 km south west of Balfour and Komati 35 km south of Middelburg and approximately 40 km north of Bethal. The proposed new power stations namely Grootveli B, Kendal B and Lethabo B were located within a 2 km radius of the already existing and return to service power stations.

The meteorology was modelled and the dispersion of pollutants simulated for an area 160 km (east-west) by 108 km (north-south) with ambient ground-level concentrations and deposition level predicted for 17 280 receptor points. The resolution of the Cartesian receptor grid was 1 770 m by 1 770 m. Discrete receptor points were specified for each of the monitoring station locations to facilitate the simulation of concentrations and deposition at these locations (Scorgie and Venter, 2005).

5.4 ANALYSIS OF MODELLED OUTPUTS

The highest modelled hourly averages were statistically analysed and compared against the highest measured concentrations in order to validate the CALPUFF modelled outputs. This process provides us with an indication of the performance of the model. No attempt was made to pair the data in time and space. The measured hourly averages of SO_2 and NO_2 concentrations were extracted from the Environmental Database-driven Web-enabled Integrated System (EDWEIS) developed for Eskom's environmental observations and analysis. Values which indicate no data recorded for that hour were deleted. The data was ranked in ascending order and the percentile, at which the measured value was observed, was calculated. Comparisons between measured and modelled values were performed at the 99.99 percentile because in the study conducted by Airshed Planning Professionals to assess the impact on air quality of current, future and planned power station operations, the CALPUFF model was used to derive the highest predicted value (worst case scenario). All measured values were converted from parts per billion (ppb) to microgram per meter cube ($\mu g/m^3$) for comparisons.

The upper limit of the concentration values is calculated as twice the model value and the lower limit is half the model value at each monitoring station. The expected excursions depict the exceeded orders of magnitude between the measured and modelled values (equation 34).

Exceeded Order of Magnitude = (99.99 % - percentile of model values) x 100

equation 34

5.5 DISTRIBUTION TAIL ANALYSIS

The comparative analysis between the measured and modelled outputs revealed a significant difference between these two datasets therefore an attempt was made to statistically interrogate the modelled outputs in order to determine if there was bias in the model which could be corrected.

All missing values were removed from the measured dataset. The measured values were then sorted in ascending order. Data was multiplied by a factor of 2.62 and 1.89 in order to convert concentrations from ppb to ug/m^3 for SO_2 and NO_2 respectively. The cumulative distribution function (CDF) for each monitoring station was plotted for the ordered, converted values. The distribution fits were also performed to establish distribution characteristics, for example log normal. The tails of the distributions according to break points were examined. These were determined visually but a more vigorous analysis should be done to establish the threshold, however this was not required for this study (Coles, 2001; Gumbel, 2004; Sharma *et al.*, 2012).

5.6 INTEGRATION OF MEASURED AND MODELLED VALUES

The measured and modelled datasets were integrated to form a new dataset which could then be interrogated to produce a more accurate estimation of ground level concentrations of ambient SO_2 and NO_2.

The hourly averages recorded at all Eskom monitoring stations for SO_2 and NO_2 ambient concentrations in year 2003 were extracted from EDWEIS. All missing records were deleted and the highest daily, monthly and annual averages were calculated. A database was created for these averages and this database was used to create point layers within the GIS.

The CALPUFF model uses SURFER as the GIS application for spatially depicting pollution concentrations. However this application has limited

functionalities and did not possess the ability to process files in HDF format which is required for the validation and integration of the SCIAMACHY retrievals in this study. The functionalities within SURFER are basic and do not allow for sophisticated statistical analysis and easy integration of datasets. The output from the CALPUFF modelling study was exported to ARCVIEW for interrogation, refinement and integration. The exported modelled outputs from SURFER were in a format unrecognisable by ARCVIEW and needed to be transformed in order to allow for system compatibility.

The base map which was utilised in the CALPUFF model was geo-referenced within the ARCVIEW application and created as a layer. All the modelled values were imported into ARCVIEW in order to create a point layer. These points were spatially adjusted to fit the base map and the modelled points were geo-referenced to the monitoring stations. The modelled point layers were then interpolated to a continuous raster surface.

A model was developed within ARCVIEW to produce a new concentration raster dataset which utilises the ground based monitored values as the "truth" and calculates a new surface value for the modelled fields thereby improving the modelled concentration outputs. The model makes use of an inverse distance weighted interpolation function which estimates surface values for each pixel using the value and distance of nearby pixels.

5.7 HOT SPOT ANALYSIS

The new "improved" dataset was created into a point layer for hot spot analysis. Algorithms were formulated for different scenarios in order to assess impacts from SO_2 and NO_2 exposure on human health and ecosystems from power station emissions. Algorithms formulated for each scenario were utilised to create individual GIS layers.

In the SO_2 hot spot analysis, GIS layers were created to spatially depict areas where, the highest hourly average of 350 $\mu g/m^3$ which was exceeded more than 88

times a year, highest daily average of 125 µg/m^3 which was exceeded more than 4 times a year and annual average exceedence of 50 ug/m^3 for the protection of health, occurs.

In the NO_2 hot spot analysis, GIS layers were created to spatially depict areas where the annual average of 40 µg/m^3 and maximum 24 hour of 200 µg/m^3 were exceeded.

The frequency of exceedences for each point is an output from the CALPUFF model therefore the risk analysis is limited to the parameters which were used in the Eskom study conducted by Airshed Planning Professionals. Were possible DEA proposed standards for immediate compliance have been utilised to reflect current risk from power station operations (Discussion document, CD:AQM&CC/30/10/07/01).

The new "improved" air quality dataset was interrogated against DEA's, WHO's and EU's ambient air quality standards to map and identify potential risk to human health, vegetation and ecosystems from power station emissions.

The classification of health risks to SO_2 exposures was based on the work of Scorgie and Gruenewaldt (2008). The different thresholds that were utilised in the assessment are described in Table 20.

Table 20: Thresholds specified for health effects (Scorgie and Gruenewaldt, 2008)

Category of Risk	Maximum Hourly Average SO2 Concentration (µg/m³) (99th percentile)	Basis
Low	<660	California Acute Reference Level for Mild Respiratory Effects given as 660 µg/m³
Moderate	660 – 930	
High	930 – 1400	Upper range of UK's "high" band (i.e. 708 µg/m³ for 15 minute average – projected as 934 µg/m³ for a 1-hourly averaging period) (a). Coincides closely with the dose-response threshold at 916 µg/m³ given for increased airway resistance in asthmatics at exercise
Very high	>1400	UK's "very high" band (i.e. 1064 µg/m³ for 15 minute average – projected as 1404 µg/m³ for a 1-hourly averaging period)(b)

(a) "High" band expressed by UK Department for Environment, Food and Rural Affairs (DEFRA) as "significant effects may be noticed by sensitive individuals and action to avoid or reduce these effects may be needed (e.g. reducing exposure by spending less time in polluted areas outdoors). Asthmatics will find that their 'reliever' inhaler is likely to reverse the effects on the lung".
(b) "Very high" band expressed by UK DEFRA as follows: "the effects on sensitive individuals described for 'High' levels of pollution may worsen".

The annual SO_2 and NO_2 modelled concentrations were overlayed with vegetation, wetland and land cover datasets to highlight areas likely to be impacted from power station emissions. The thresholds utilised in the risk assessment were generated based on the work of Scorgie and Gruenewaldt (2008) whom classified the potential for harm to vegetation from SO_2 exposures into three distinct categories (Table 21).

Table 21: Thresholds specified for potential harm to vegetation (Scorgie and Gruenewaldt, 2008)

Category of Risk for Vegetation Injury [(a)]	**Maximum Annual Average SO_2 Concentration (µg/m³)**	**Basis**
Low	< 20 µg/m³	EC annual SO_2 limit given as 20 µg/m³ for the protection of ecosystems WHO guideline for annual SO_2 given as in range of 10 – 30 µg/m³ depending on sensitivity of receiving environment
Moderate	20 – 30 µg/m³	
High	> 30 µg/m³	

The census 2001 enumerated area dataset could not be utilised for the calculation of population density because the areas represent a size of land enumerated by one census fieldworker in the allocated census period for the data capture. The enumerated areas are not uniform and cannot be amalgamated to reflect the density of a municipality or district.

The SPOT 5 Building Count dataset was used for the calculation of population density. In the SPOT 5 Building Count dataset every dwelling in South Africa was captured as a point. As recommended by StatsSA (2012), an estimate of 1,6 was multiplied to each dwelling to estimate the number of households in the country. A house hold is defined by STATS SA as a group of people that form a nuclear family. An estimation of 3.6 people per household (StatsSA, 2012) was utilised to calculate a new population density dataset

****

In this study an attempt is made to validate satellite-borne remote sensing observations (SCIAMACHY retrievals) from the Mpumalanga Highveld region and

CALPUFF modelled outputs against measured ground-level concentrations of SO_2 and NO_2.

The daily individual overpass files from SCIAMACHY observations at Eskom monitoring stations were extracted from the TEMIS Website (http://www.temis.co.za). The hourly average concentrations recorded at the Eskom ground based monitoring stations were compared with the satellite overpasses in order to validate the SCIAMACHY instantaneous retrievals.

The highest modelled hourly SO_2 and NO_2 averages were statistically analysed and compared against the highest measured concentrations in order to validate the CALPUFF modelled outputs. The comparative analysis between the measured and modelled outputs revealed a significant difference between these two datasets and an attempt was made to statistically interrogate the tail of the distributions of the modelled outputs in order to determine if there was biasness in the model.

A model was developed in ARCVIEW to produce a new air quality dataset whereby the measured data was integrated into the modelled dataset to produce a more accurate estimate. The model was run for different scenarios utilising the "new" dataset in order to assess impacts from SO_2 and NO_2 exposure on human health and ecosystems from power station emissions.

The results from the analysis of SCIAMACHY retrievals, modelled SO_2 and NO_2 outputs, analysis of tail distributions and risk to human health and ecosystems from power station emissions will be presented in the following chapter.

CHAPTER 6
RESULTS AND DISCUSSION

This chapter examines and discusses the statistical analaysis of the modelled, measured and remotely sensed air quality datasets, refinement of modelled outputs and the quatification of impacts on human health and ecosystems from power station emissions.

6.1 VALIDATION OF SCIAMACHY NO_2 RETRIEVALS

The processing of raw data obtained from the TEMIS website for NO_2 retrievals from the SCIAMACHY satellite, produced 67 pixels of imagery within the study domain for the year 2003 (Figure 25). Analysis of these retrievals revealed that the Arnot and Elandsfontein monitoring stations had the highest number of image pixel intersects. The nature of the SCIAMACHY imaging over the Highveld for the year 2003 was such that insufficient satellite retrievals were available to conduct any quantifiable analysis at Kendal, Camden, Palmer, Verkykkop and Makalu ground monitoring stations i.e less than 2 image coverages were available at these ground monitoring stations . Unfortunately in year 2003, Eskom recorded data at the Arnot monitoring station only in November and December and this corresponded to 2 image coverages which limits quantifiable analysis at this monitoring station. Therefore the Elandsfontein monitoring station was the only station with data suitable for analysis of measured NO_2 concentrations against SCIAMACHY retrievals.

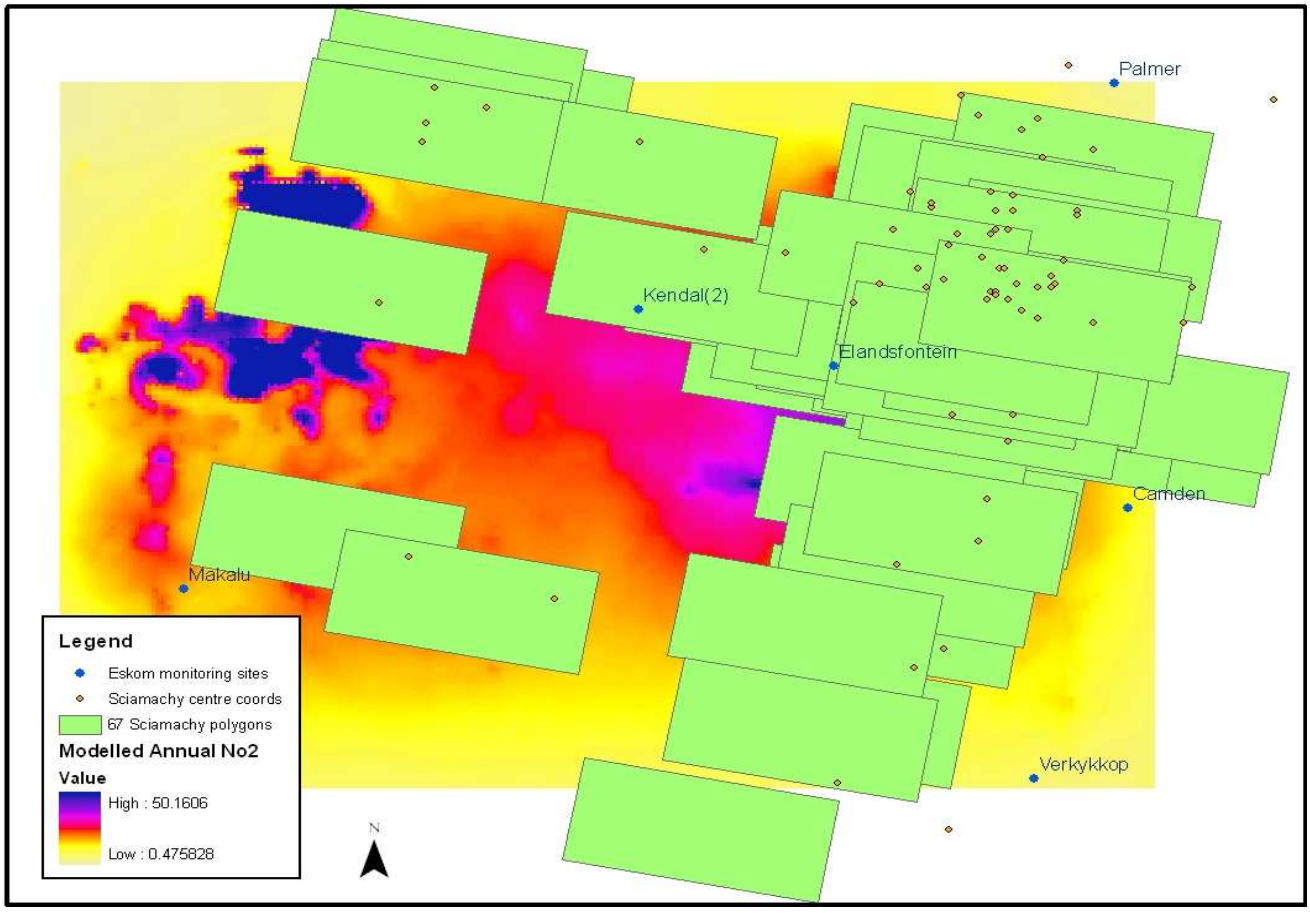


Figure 25: Available SCIAMACHY data within study domain

The 6 records for which both measured data and corresponding SCIAMACHY NO_2 retrievals occur are indicated in Table 22. The Eskom measured values at 10:00 were utilised in this evaluation as Eskom records hourly average concentrations and the SCIAMACHY satellite overpasses the Highveld between 09:30 and 10:30.

Table 22: Comparison of measured hourly average concentrations and SCIAMACHY retrievals at 10:00

Elandsfontein monitoring station				**Measured hourly average concentration**		**SCIAMACHY retrieval**
Year	Month	Day	Hour	NO_2 (ppb)	NO_2 ($\mu g/m^3$)	NO_2 ($\mu g/m^{3)}$
2003	1	16	10	2.12	4.01	4.68
2003	1	19	10	6.19	11.70	7.38
2003	1	29	10	7.85	14.84	21.13
2003	8	5	10	2.21	4.18	9.69
2003	10	1	10	1.13	2.14	5.53
2003	10	7	10	3.82	7.22	6.92

The SCIAMACHY sensor measures the total number of molecules of NO_2 gas in the whole depth of the atmosphere over the entire pixel area (30 km x 60 km) referred to as the total NO_2 column value. An independent calculation is further utilised on board to derive the tropospheric NO_2 column for the pixel area. Using assumptions as discussed in Section 4.2, representative single near ground-level concentration values at a point were estimated from these integrated values. A good correlation (R^2 = 0.76), that is 76% of the variance explained by the model was estimated to exist between measured concentrations and the SCIAMACHY data at 10:00 (Figure 26) indicating a linear relationship.

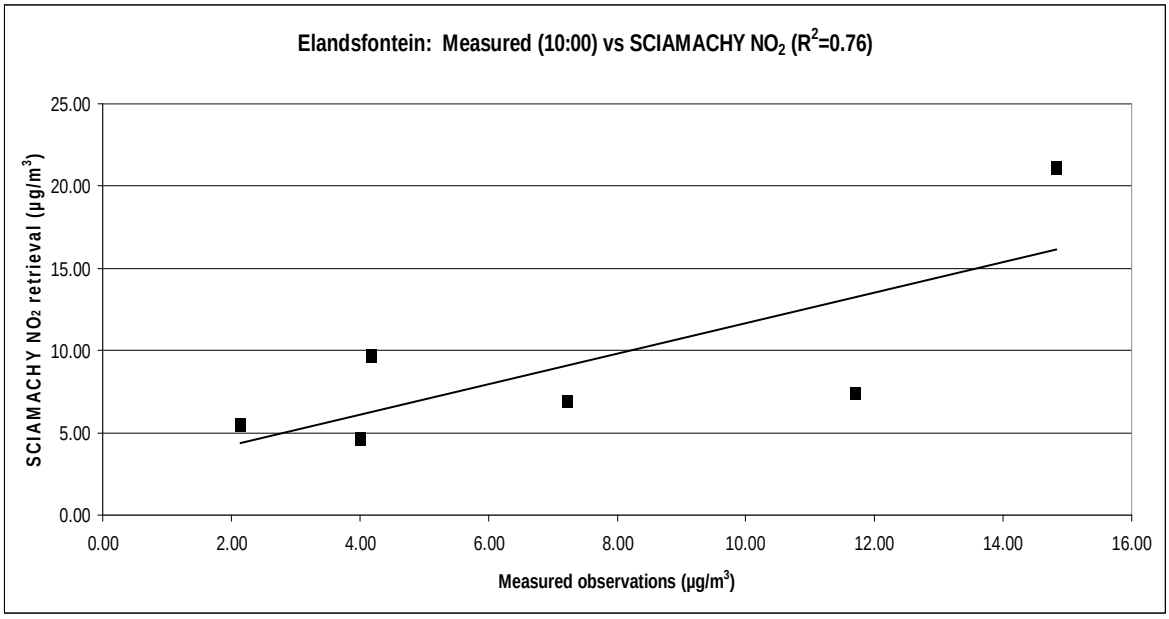


Figure 26: Correlation of measured ground concentrations and SCIAMACHY retrievals at 10:00

The satellite derived NO_2 concentration value is observed to be greater than the values measured on the ground because SCIAMACHY records the total concentration in the atmosphere over a pixel (60km x 30 km) were as the monitoring station records the concentration at a point. Also the SCIAMACHY measurement is an instantaneous value whereas the measurment from the monitoring station is a hourly average value. The assumptions made in the conversion of the tropospheric NO_2 column to indicate a ground concentration may not be robust enough to reflect a true representation. There may be a possibility that the satellite is not specifically calibrated for Southern Africa

and the airmass factor used in the calculation of the light path in the satellite could be different for Southern Africa as compared to other regions in the world.

The regression analysis of measured concentrations on the ground and SCIAMACHY retrievals at 09:00 (Figure 27) revealed a poor correlation ($R^2 = 0.18$).

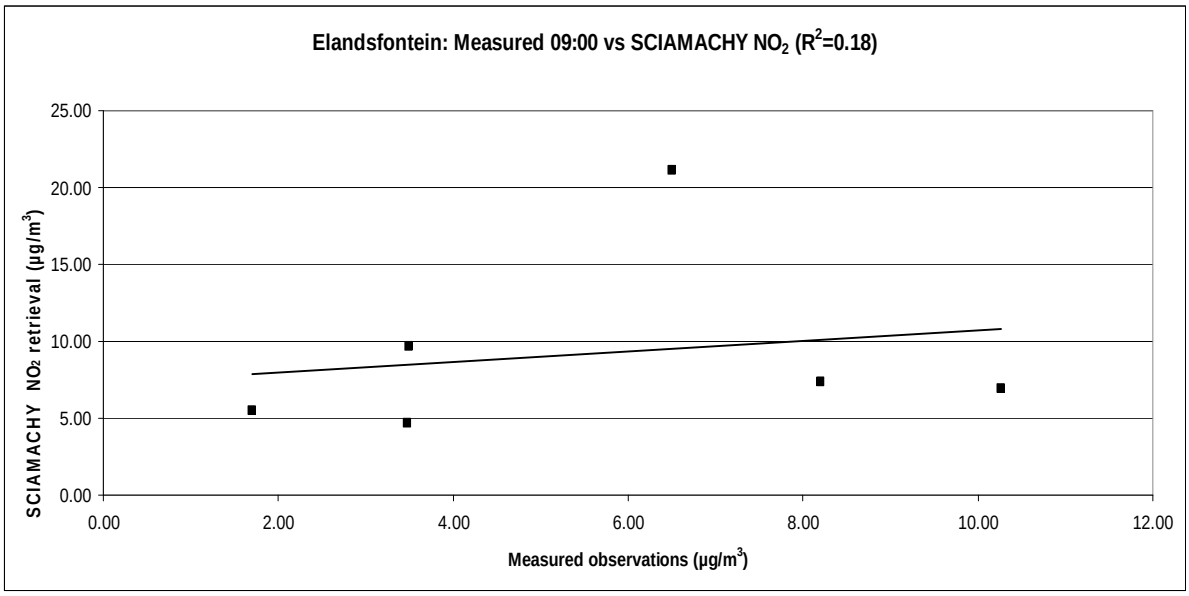


Figure 27: Correlation of measured ground concentrations and SCIAMACHY retrievals at 09h00

The values retrieved by the satellite for NO_2 at 09:00 are higher than the measurements recorded on the ground (Table 23) which can be expected, as instantaneous values at a point are always going to be higher than hourly mean values in a real situation. Whilst the analysis of measured observations with satellite retrievals has been severly restricted due to gaps in the measured data that coincide with high temporal resolution satellite overpasses, these results show that there is potential for analysis with a more complete dataset.

The sample size (6 records) was too small to determine any statistically significant bias.

Table 23: Comparison of measured hourly average concentrations and SCIAMACHY retrievals at 09:00

Elandsfontein monitoring station				**Measured hourly average concentration**		**SCIAMACHY retrieval**
Year	Month	Day	Hour	NO_2 (ppb)	NO_2 ($\mu g/m^3$)	NO_2 ($\mu g/m^3$)
2003	1	16	9	1.84	3.48	4.68
2003	1	19	9	4.34	8.20	7.38
2003	1	29	9	3.44	6.50	21.13
2003	8	5	9	1.85	3.50	9.69
2003	10	1	9	0.9	1.70	5.53
2003	10	7	9	5.43	10.26	6.92

6.2 VALIDATION OF THE CALPUFF MODEL

6.2.1 SO_2 STATISTICAL ANALYSIS OF MEASURED AND MODELLED CONCENTRATIONS

US-EPA (2007) and Chang and Hanna (2004) accepts modelled predictions within a factor of 2 of observations as one of the statistical validation methods utilised for air dispersion modelling. Given that the US EPA gives the acceptable range of uncertainty in dispersion model results as being –50% to 200% only model predictions falling outside of this range when compared to measured concentrations, were flagged as being unrepresentative (i.e. measured to modelled ratios of <0.5 or >2.0). Flagged values are indicated in red font in tables 24 and 25. Based on this premise the upper limit of the concentration values represent twice the model value and the lower limit is half the model value at each monitoring station.

Statistical evaluations of the SO_2 measured and modelled concentrations indicate that out of eight monitoring stations the model under predicts at five monitoring stations (Elandsfontain, Verkykkop, Leandra, Makalu and Palmer) and over predicts at the other three monitoring stations (Kendal, Majuba 1 and Majuba 3) (Table 24). The model has a calculated reliability of 62%. The comparison of the measured value to the upper and lower limits of the model also indicates that the model does not conform at Majuba1, Majuba3 and Palmer monitoring sites. Under

predictions at Palmer monitoring station could be attributed to the location of this station on the periphery of the modelling domain with not all sources contributing to this site having been quantified and included in the simulations.

There is no constant value by which the model under predicts as demonstrated in the expected excursions. The expected excursions indicate the number of times exceeded if the model value was accepted as the threshold (99.99 percentile). The values indicated in the percentile of the model column indicates the actual percentile

Table 24: Comparison of modelled and measured highest hourly SO_2 concentrations (after Scorgie and Venter, 2005)

MODEL @ 99.99th percentile			**99.99th percentile**		
Lower limit	**Upper limit**	**Monitoring stations**	**Highest hourly measured concentration ($\mu g/m^3$)**	**Highest hourly modelled concentration($\mu g/m^3$)**	**Expected excursion**
119.3	477.2	**Verkykkop**	366.80	238.62	14.00
244.8	979.2	**Elandsfontein**	741.46	489.58	4.00
1215.1	4860.6	**Kendal**	2114.34	2430.28	0.00
181.2	724.8	**Leandra**	563.30	362.42	17.00
691.1	2764.4	**Majuba1**	560.68	1382.20	0.00
503.5	2014.0	**Majuba3**	429.68	1007.02	0.00
352.7	1410.7	**Makalu**	799.10	705.34	3.00
37.5	149.9	**Palmer**	408.72	74.94	577.00

6.2.2 NO_2 STATISTICAL ANALYSIS OF MEASURED AND MODELLED CONCENTRATIONS

Statistical evaluations of the NO_2 measured and modelled concentrations indicate that the model both under and over predicts for 50 % of the time (Table 25). The comparisons of the measured value to the lower and upper limits reveal that the modelled values do not conform at Camden and Palmer monitoring sites. Again, under predictions at Palmer monitoring station could be attributed to the location of this station on the periphery of the modelling domain with not all sources contributing to this site having been quantified and included in the simulations. Camden power station was not operational in year 2003 as it was being prepared for return to service

and under predictions at this modelling domain could be due to the model under predicting for low level sources in the area. The expected excursions indicate that there is no constant bias in the model for which corrections could be easily applied.

Table 25: Comparison of modelled and measured NO_2 highest hourly concentrations (after Scorgie and Venter, 2005)

MODEL @ 99.99th percentile		**Monitoring stations**	**99.99th percentile**		**Expected excursion**
Lower limit	**Upper limit**		**Highest hourly measured concentration ($\mu g/m^3$)**	**Highest hourly modelled concentration ($\mu g/m^3$)**	
33.49	133.94	**Verkykkop**	114.53	66.97	28
22.18	88.70	**Camden**	94.88	44.35	5
68.87	275.48	**Elandsfontein**	106.22	137.74	0.00
86.14	344.56	**Kendal**	145.53	172.28	0.00
83.22	332.90	**Makalu**	87.89	166.45	0.00
13.48	53.92	**Palmer**	72.39	26.96	16

6.2.3 DISTRIBUTION TAIL ANALYSIS

The analysis of measured and modelled values showed large discrepancies as discussed above. From the preliminary results there was an indication that what was observed from the model and the results obtained from the empirical fit of the data yielded different probability values at the tail. A break in the quantile graph is observed as illustrated in Figures 28 and 29. This indicates that there is a different behaviour in the tail of the distribution i.e the bulk of the distribution seems to behave differently to the distribution at the tail which is where the extreme values are located. Cumulative Distribution Function graphs were plotted for all monitoring stations for both SO_2 and NO_2 and these graphs indicate that the CALPUFF model appears to predict the highest values based on calculations from the bulk of the distribution rather than the unique distribution at the tails. This could possibly account for the large variance between measured and modelled values.

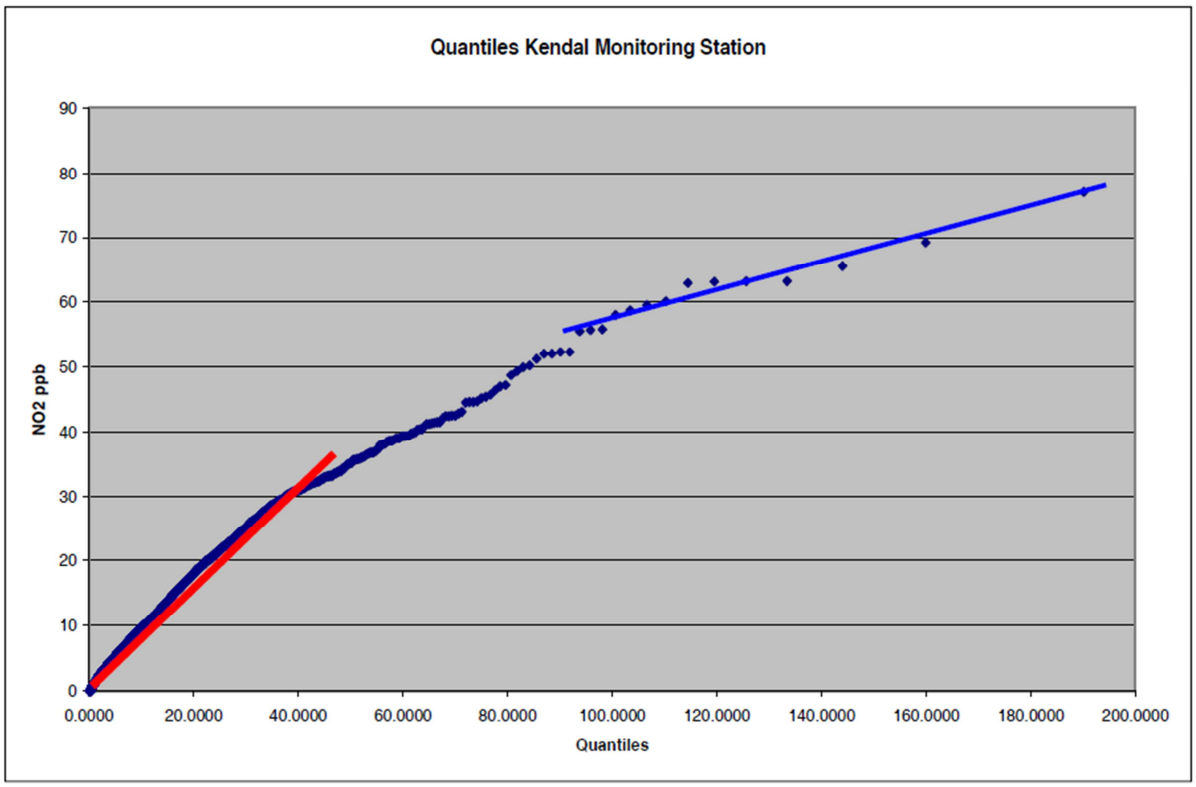


Figure 28: Cumulative distribution function graph of NO_2 concentrations at Kendal monitoring station

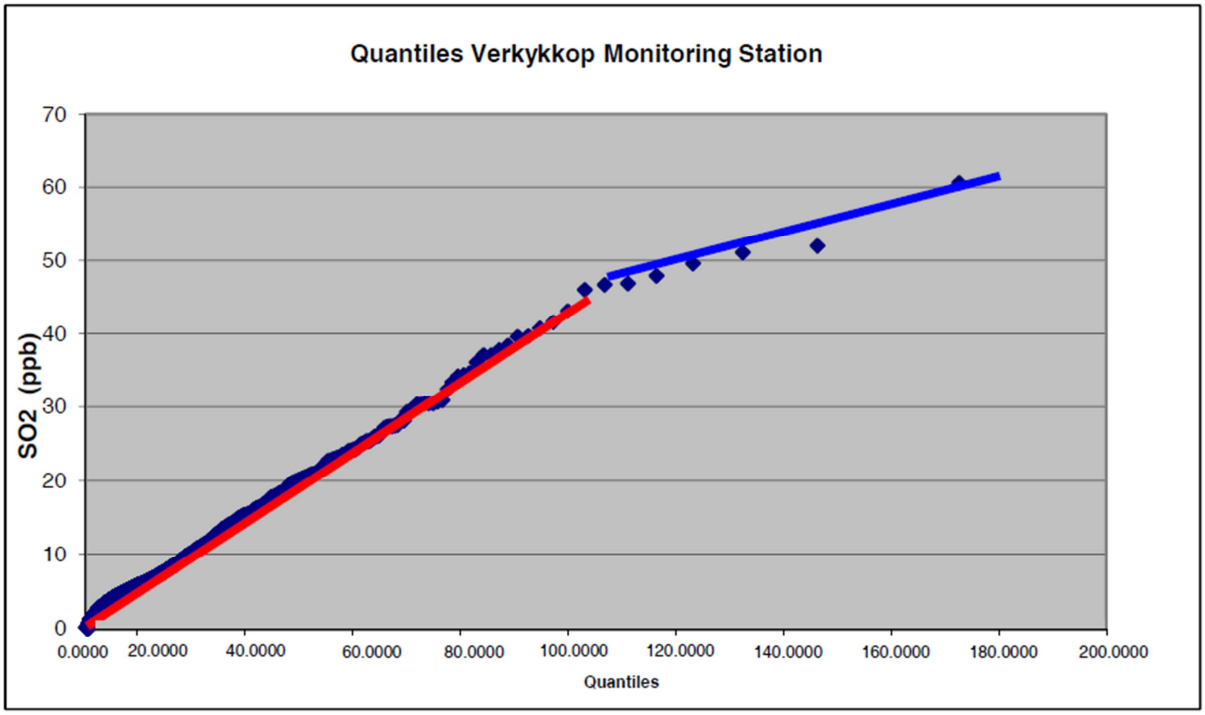


Figure 29: Cumulative distribution function graph of SO_2 concentrations at Verkykkop monitoring station

6.3 POTENTIAL FOR HEALTH AND VEGETATION IMPACTS

A risk assessment is a tool used in risk management to estimate the increased risk of health problems in people who are exposed to varying amounts of toxic substances . A risk assessment for an air pollutant combines results of studies that estimate the level of people's exposures at different distances from the source of the pollutant. Hotspot analysis is a widely utilised risk assessment tool by national and international agencies to inform environmental policies, quantify the impact of air pollution on human health and vegetation and weigh options for pollution control.

The CALPUFF modelled data was "improved" as described in section 5.6. This new "improved" air quality dataset was further interrogated against DEA's air quality standards and the risk thresholds based on the work of Scorgie and Gruenewaldt (2008) to map and identify potential risk to human health, vegetation and ecosystems from power station emissions. The risk categorisation for the hotspot analyses has been described in Tables 20 and Table 21.

6.3.1 COMPARISON OF SOUTH AFRICAN AMBIENT AIR QUALITY STANDARDS TO INTERNATIONAL BEST PRACTISES

The 1st of April 2010 marked a significant milestone for air quality management in South Africa when the new National Air Quality Act came into full effect and the old Atmospheric Pollution Prevention Act of 1965 was repealed. The air quality limits issued in South Africa (Table 26 and 27) were compared with limits from the World Health Organisation (WHO), International Finance Corporation (IFC), European Community (EC) and United States Environmental Protection Agency (US-EPA) for bench marking and hot spot analysis. Generally the South African ambient air quality SO_2 and NO_2 standards seem to be in line with those of the IFC, WHO, US-EPA and EC except for SO_2 were the WHO for maximum 24 hour averages is stricter (20 $\mu g/m^3$) . This limit of 20 $\mu g/m^3$ is set as the limit for the protection of human health by the WHO.

With regards to US-EPA the annual average and maximum 24 hour average for SO_2 seems to be more relaxed however, the US-EPA allows only one exceedence a year for the maximum 24 hour average. The South African limit is much lower (125 $\mu g/m^3$) with and allowance of 4 exceedences. The ECs annual average for SO_2 is much stricter as the Commission utilises this value of 20 $\mu g/m^3$ for the protection of ecosystems.

Table 26: Comparative ambient air quality standards for SO_2 (adapted from Scorgie and Venter, 2005)

Averaging Period	**South African Air Quality Act µg/m³**	**IFC (2007) µg/m³**	**WHO (2005) µg/m³**	**US-EPA µg/m³**	**EC (2003) µg/m³**
Annual Average	50	50	50(1) 10-30(2)	80(4)	20(6)
Max 24-Hour Average	125	125	120(1)	365 (5)	125(7)
Max 1-Hour Average	350	-	350(3)	-	350(8)
10 Minute Average	500	-	500(1)	-	-

(1)Air quality guidelines issued for Europe for the protection of human health

(2) Represents the critical level of ecotoxic effects issued for Europe; a range is given to account for different sensitivities of vegetation types

(3) WHO 1994

(4) Arithmetic mean

(5) Not to be exceeded more than 1 day per year

(6) Limited value to protect ecosystems

(7) Limit to protect health, to be complied with by January 2005 (not to be exceeded more than 3 times per year)

(8) Limit to protect health, to be complied with by January 2005 (not to be exceeded more than 4 times per year)

Table 27: Comparative ambient air quality standards for NO_2 (adapted from Scorgie and Venter, 2005)

Averaging Period	South African Air Quality Act µg/m^3	WHO (2005) µg/m^3	US-EPA µg/m^3	EC (2003) µg/m^3
Annual Average	40	40	100(1)	40(2) 30 NO_X (4)
Max 24-Hour Average	-	150	-	-
Max 1-Hour Average	200	200	-	200(3)

(1) Arithmetic mean

(2) Annual limit for the protection of human health to be complied with by 1 January 2010

(3) Not exceeeded more than 18 times per year. This limit to be complied with by 1 January 2010

(4) Annual limit for the protection of vegetation

6.3.2 ANALYSIS OF POTENTIAL RISK FROM SO_2 CONCENTRATIONS

The SO_2 diurnal variation graphs at all Eskom monitoring stations utilised in this study generally depict a build-up of SO_2 concentrations in the early morning, climbing rapidly from 07h00, peaking just before noon and then dropping off sharply to reach back ground levels again about 22h00 (Figure 30). The standard deviation gives an indication of the worst case scenario. Generally there is a another small peak in the afternoon around 18h00 due to coal fires for domestic heating and cooking. The high concentrations recorded during the mid-day period are typical, of emissions from high-level sources as a result of strong daytime convective air turbulence experienced on the Highveld, which tend to bring stack emissions to ground level, while the emissions are buoyed above the surface inversion during night-time.

The SO_2 diurnal variation shows the influence of tall stack emitters impacting at sites predominantly during the mid-day period due to atmospheric instability. Concentrations are comparatively lower during the evening and early morning period, suggesting little influence from tall stack sources.

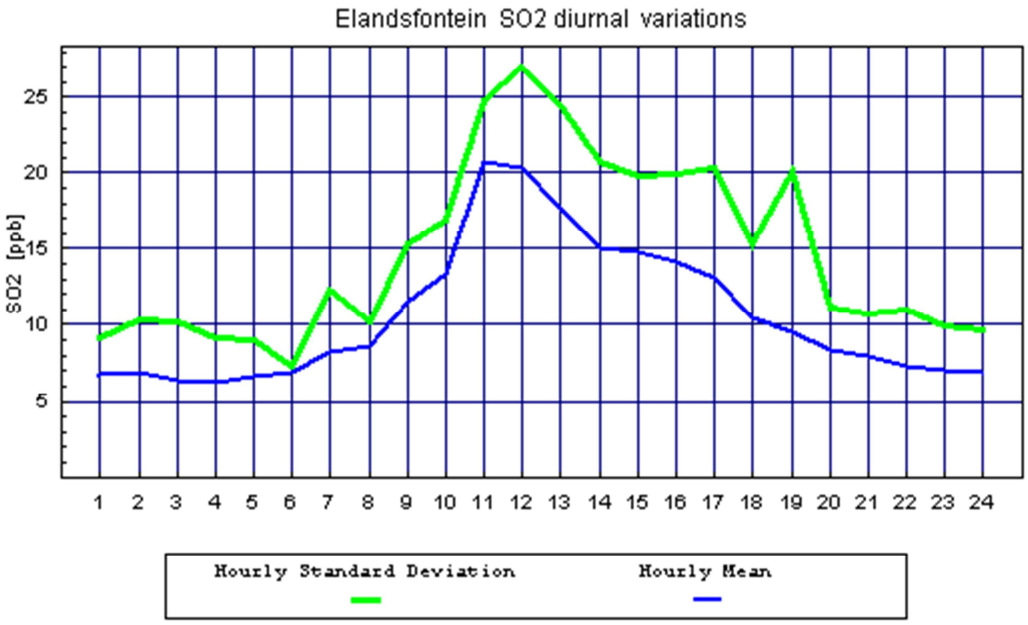


Figure 30: SO_2 diurnal variation at Elandsfontein

6.3.2.1 Sector Exceedance Roses

ELANDSFONTEIN MONITORING STATION

The daytime sector exceedance rose indicates the prevalence of sources to the south-south-west (Figure 31) which indicate Sasol Secunda, the west-south-west and west sectors indicating Matla and Kriel power stations respectively. All these sources are tall stack emitters. The night-time sector exceedance rose shows dominant sources in the west-north-west and north-west sectors, most likely associated with low level emitters. This plot shows little influence from tall stack emissions suggesting that these plumes are buoyed above the night-time surface inversion.

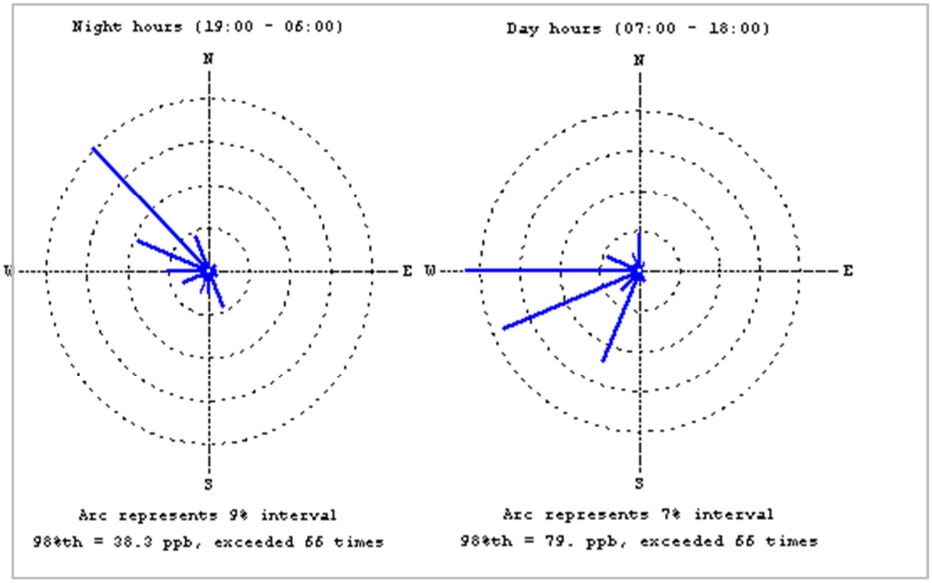


Figure 31: SO_2 daytime and night-time sector exceedance roses

VERKYKKOP MONITORING STATION

The daytime sector exceedance rose (Figure 32) indicates prominent sources to the north-north-west of which Majuba power station is likely to be the most dominant and to a lesser degree to the north. The night-time sector exceedance rose for which the 98 percentile value is half of the daytime value, indicates the same sectors but with the north more prominent. Due to the site's altitude, the power station plumes may be impacting on this site during the night-time period. The source to the north is most likely from low level emissions at Amersfoot town that would be enhanced during the evening.

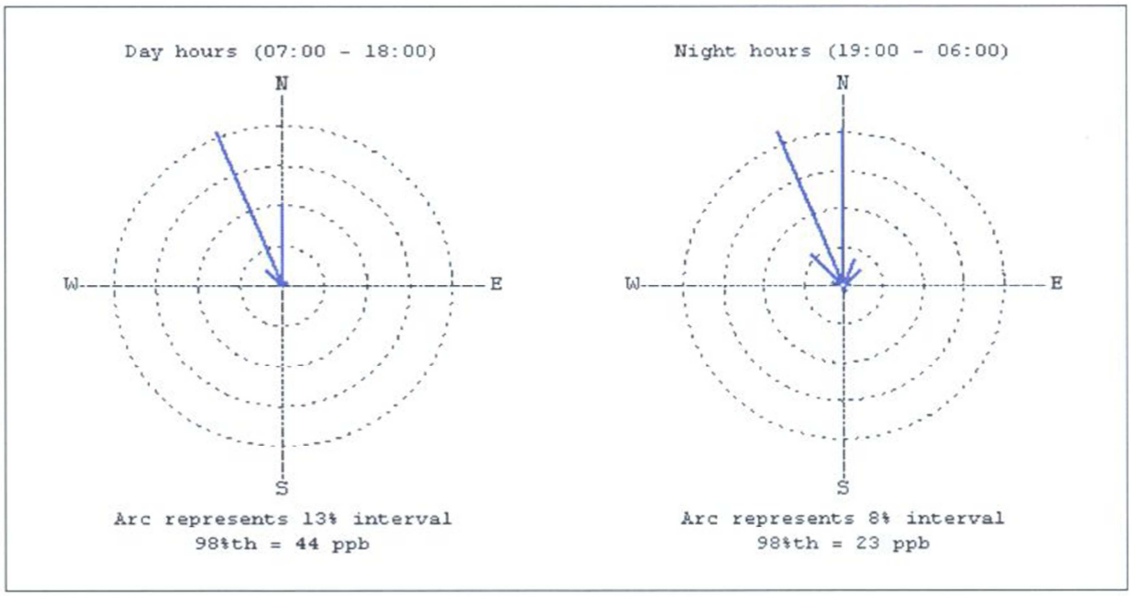


Figure 32: Daytime and night-time SO_2 sector exceedance roses

PALMER MONITORING STATION

The daytime sector exceedance rose (Figure 33) indicates the prevalence of sources in the south-south-west to west-south-west and west-north-west to north-west sectors. Most of the power stations as well as other tall stack emitters in Middelburg and Witbank lie south-south-west to west-south-west of the site. The sources in the west-north-west to north-west sectors are industry and low level sources. The extreme night-time concentrations are similar to those of the daytime values. The night-time sector exceedance rose shows the dominance of sources in the north-west and north-north-east to east-north-east which are low level sources in the area.

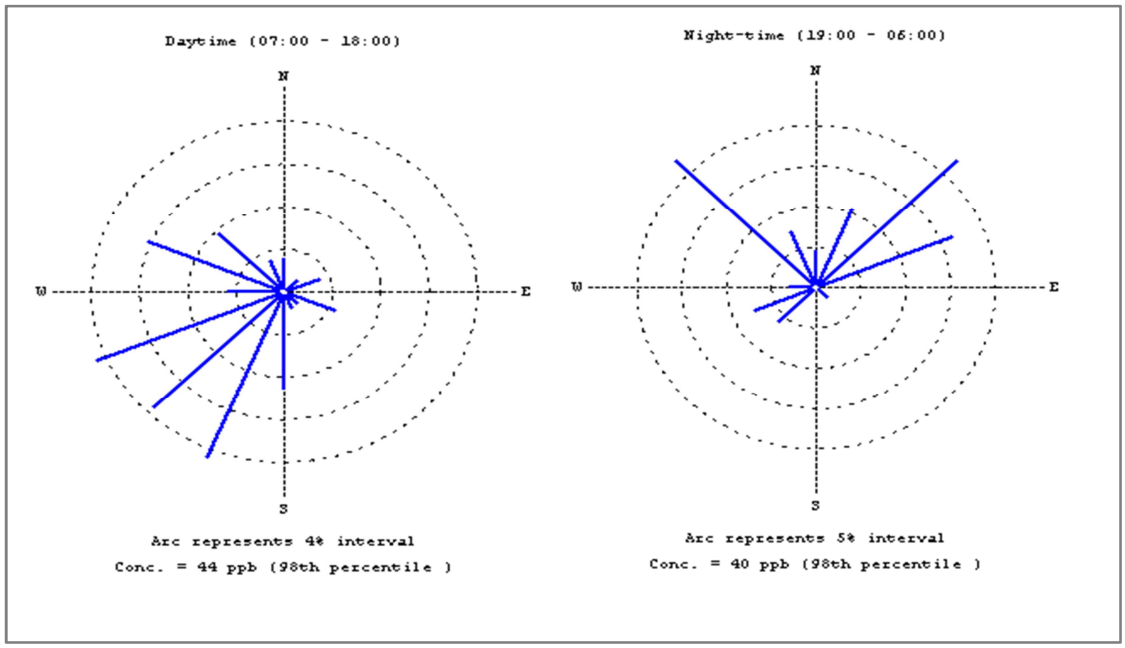


Figure 33: SO_2 daytime and night-time sector exceedance roses

MAKALU MONITORING STATION

The daytime sector exceedance rose (Figure 34) indicates the prevalence of sources in the north-north-east to east-north-east sectors which would indicate the impact from Lethabo power station which lies to the north-north-east. The night-time sector exceedance rose shows the dominance of low level sources in the north-west to north-north-west and south-south-east sectors. There is little influence from Lethabo power station in the north-north-east at night.

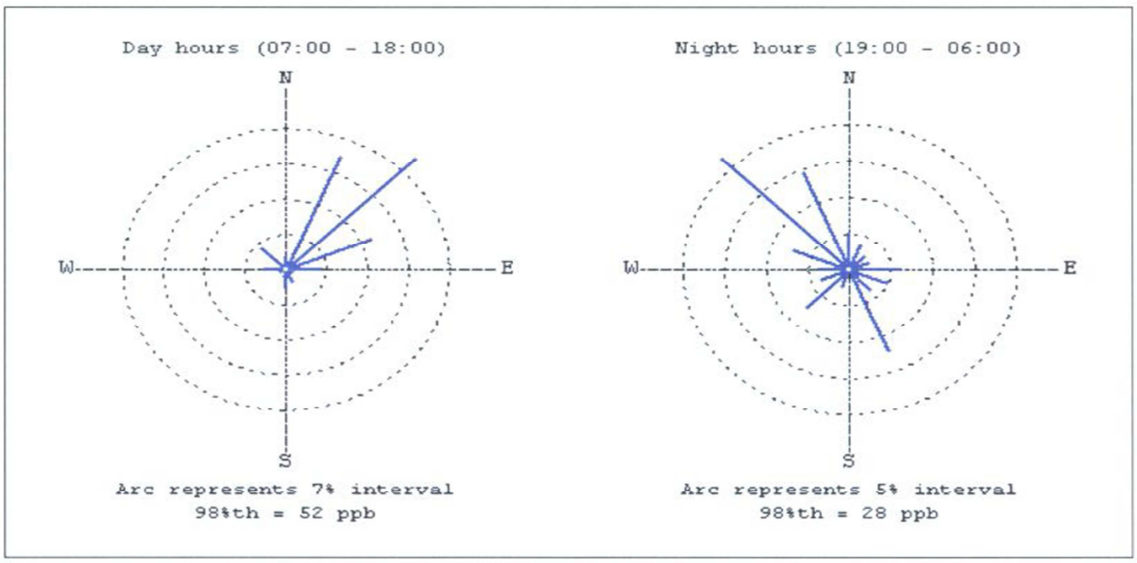


Figure 34: SO_2 daytime and night-time sector exceedance roses

LEANDRA MONITORING STATION

The daytime sector exceedance roses (Figure 35) show the prevalence of sources in the north-east to south-east sectors, with the east-north-east most dominant. Kriel and Matla power stations lie to the east-north-east and Sasol Secunda lies south-east of the site.

The night-time sector exceedance roses show sources in the majority of sectors but most dominant in the north-north-east to east-north-east and south-east to west sector which may be related to numerous low level sources in these areas. The lower income housing at Lebohang is located south-east to west of the monitoring site, while the new development of housing stretches east towards Kinross. The majority of these homes use coal or wood on occasion for space heating and cooking.

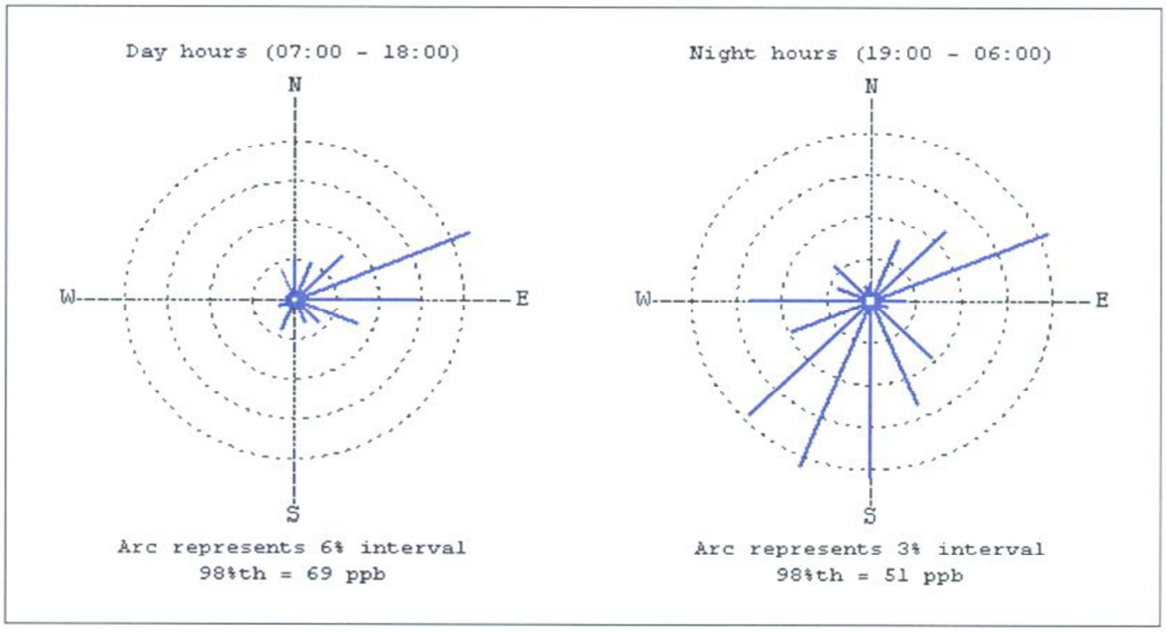


Figure 35: SO_2 daytime and night-time sector exceedance roses

KENDAL MONITORING STATION

The SO_2 daytime sector exceedance rose (Figure 36) indicates lobes distributed between the north west and north sectors indicating Kendal power station stacks as the source. The SO_2 diurnal variations show that these exceedances occurred mostly

between 10:00 and 17:00 which is indicative of tall stack emissions being brought to ground level by convective air turbulence. The night-time sector exceedance rose indicates a weak low level source to the east.

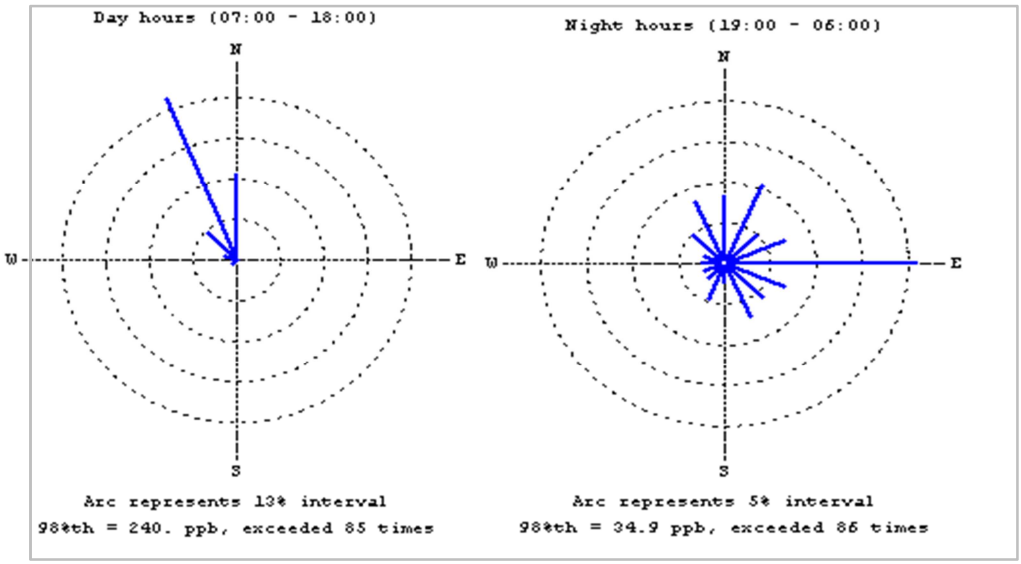


Figure 36: SO_2 daytime and night-time sector exceedance roses

MAJUBA MONITORING STATION

The daytime sector exceedance roses at J1 and J3 show that there is a lobe indicating main sources distributed between the north-west and west-north-west (Figure 37a and 37b), indicating emissions from Majuba and Tutuka power stations. The night-time sector exceedance rose indicates emissions from low level sources at both monitoring stations.

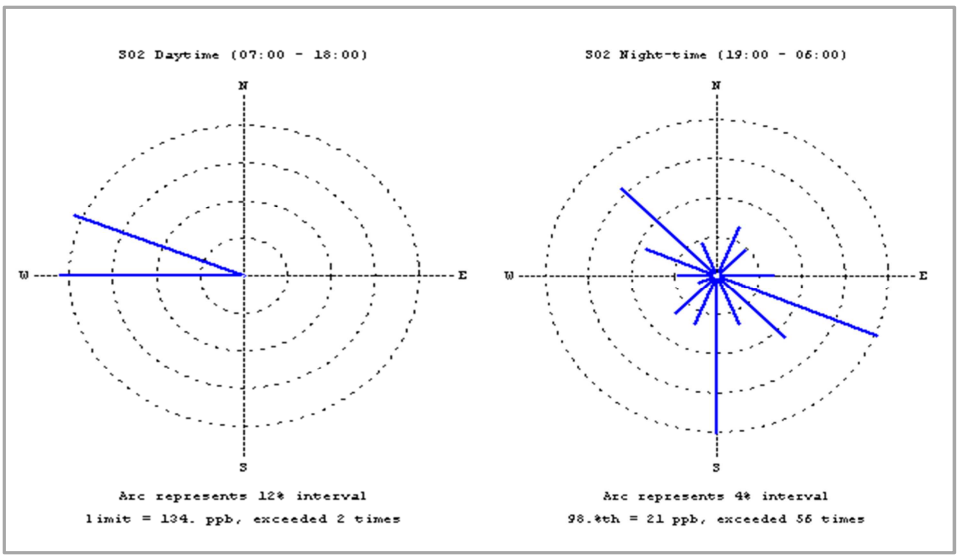


Figure 37a: SO_2 daytime and night-time sector exceedance roses at J3

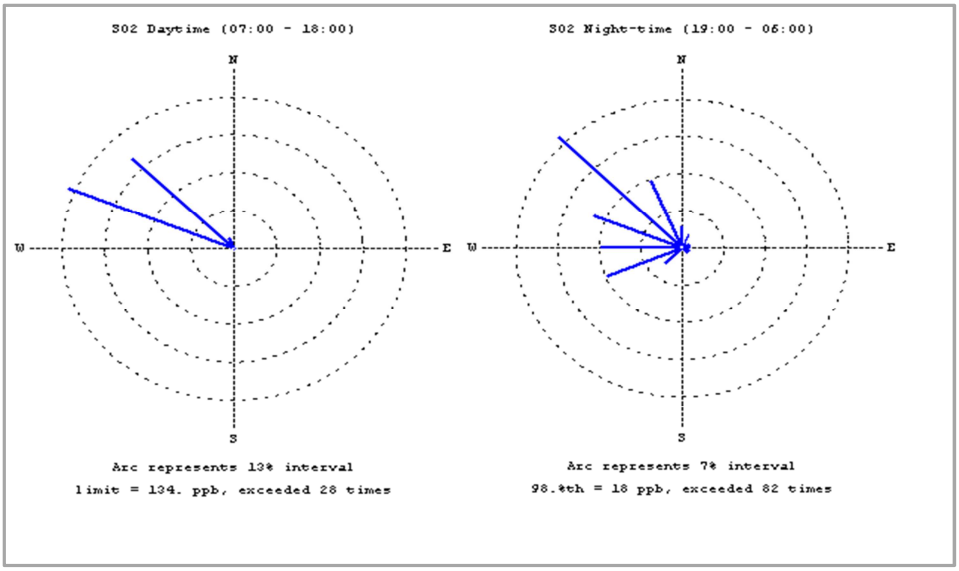


Figure 37b: SO_2 daytime and night-time sector exceedance roses at J1

6.3.2.2 SO_2 Hot Spot Analysis

HEALTH RISK ASSESSMENT

The DEA ambient air quality standard for hourly SO_2 concentration has been gazetted at a tolerance of 350 ug/m^3 with a permissible frequency of 88 exceedances for immediate compliance (DEA, 2009). The assessment of the modelled spatial distribution of impact on population agglomerations (Figure 38), show that exceedances occur at both relatively sparse and densely populated areas. The areas where the DEA standards for immediate compliance are exceeded are generally of population agglomerations 0 to 1 000 per km^2 located in areas close to Matla, Kriel and Kendal power stations in the central Highveld. The hot spot near Vanderbijilpark in the Vaal Triangle is located in a more densely populated area of 2001 to 5000 per km^2. The hotspot to the west of Tembisa extends over population agglomerations 1001 to 2000, 2001 to 5000 and 5001 to 10 000. Diepsloot which is an informal settlement is located in this area. The analysis also revealed that high concentrations of SO_2 occur in areas which are located close to Hendrina power station and west of Sebokeng.

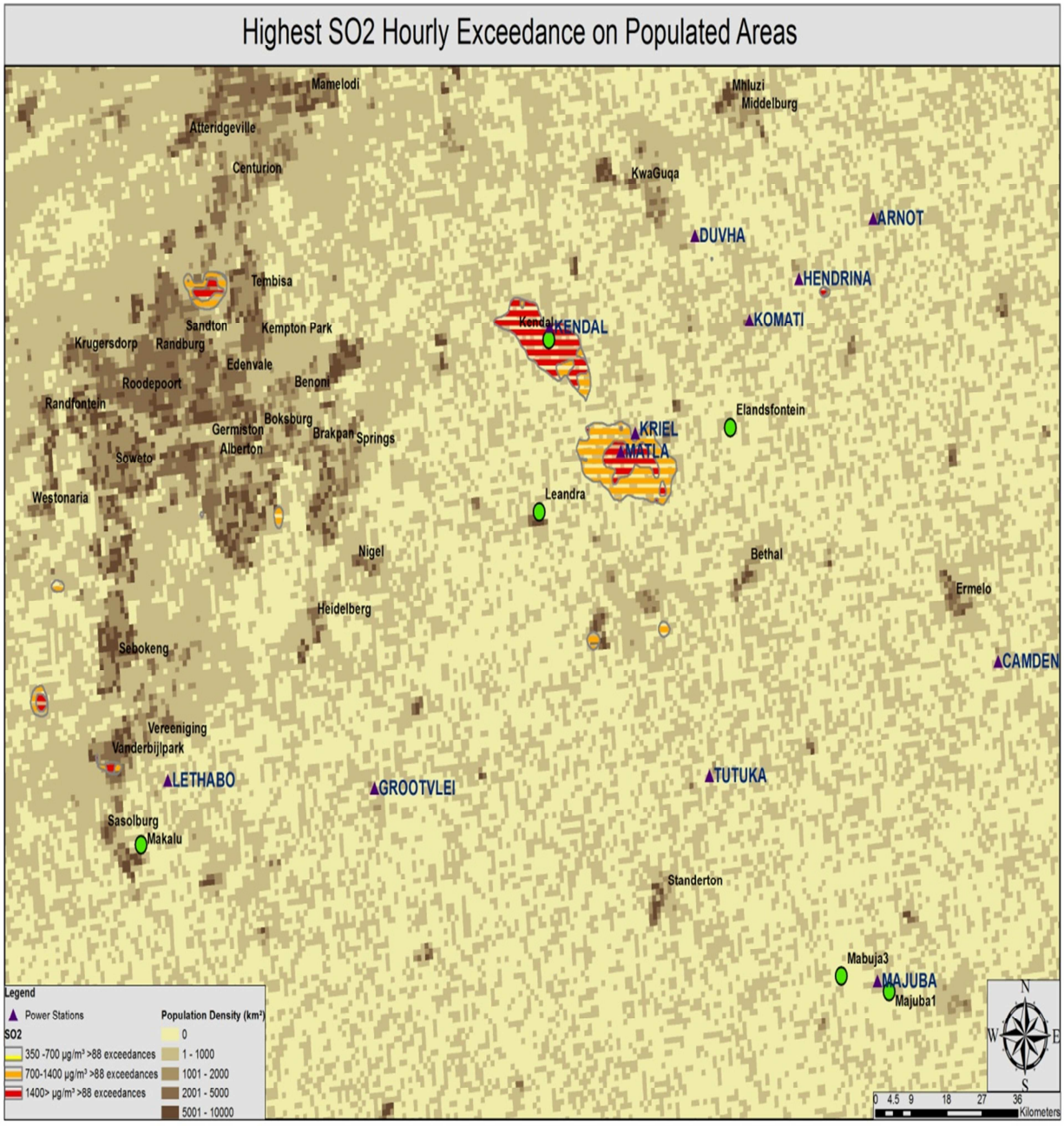


Figure 38: Highest SO_2 hourly average exceedances on populated areas

Hotspots for potential high to very high risk to human health are observed around all power stations (Figure 39) except Grootvlei and Camden which were not operational in 2003. Generally the category of very high risk near power stations seem to be located in areas with population agglomerations between 0 to 1000 per km^2 except for areas around Vanderbijlpark and Sasolburg which have population agglomerations between 2001 to 5000 and 5 001 to 10 000 per km^2.

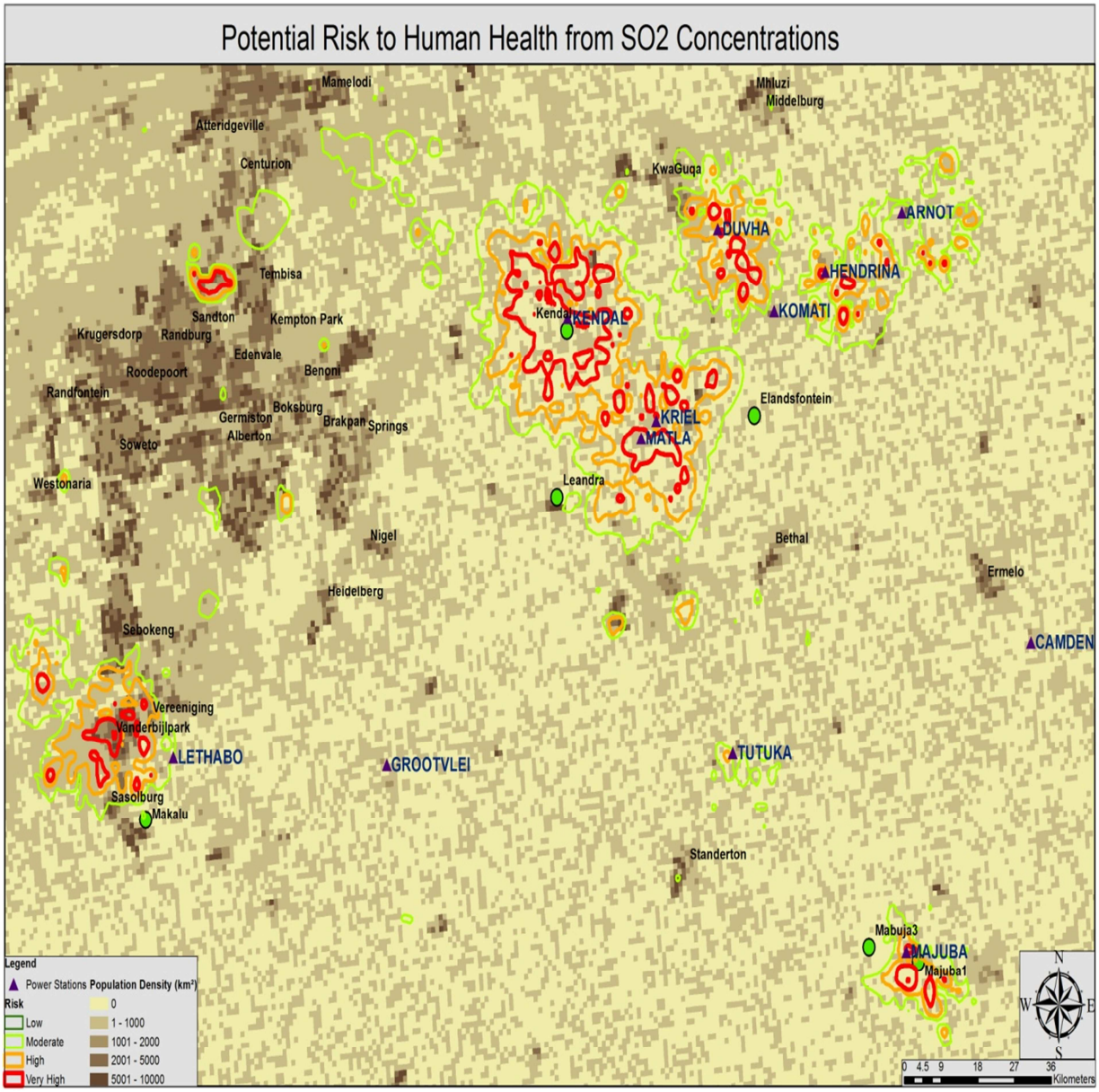


Figure 39: Potential risk to human health from highest hourly SO_2 concentrations

The DEA ambient air quality standard for daily SO_2 concentration has been gazetted at a tolerance of 125 ug/m^3 with a permissible frequency of 4 exceedances for immediate compliance (DEA, 2009). Analysis of modelled outputs on population density show hotspot areas around the Kendal, Matla, Kriel, Hendrina, Duvha and Arnot power stations (Figure 40). The impacts are generally on population agglomerations of 0 to 1 000 per km^2 except for areas close to Standerton and Vanderbjlpark which impact on agglomerations between 2 001 to 5 000 per km^2 and

5001 to 10 000. Generally the areas of risk extend from Middelburg in the north to Standerton in the south and Westonaria in the west.

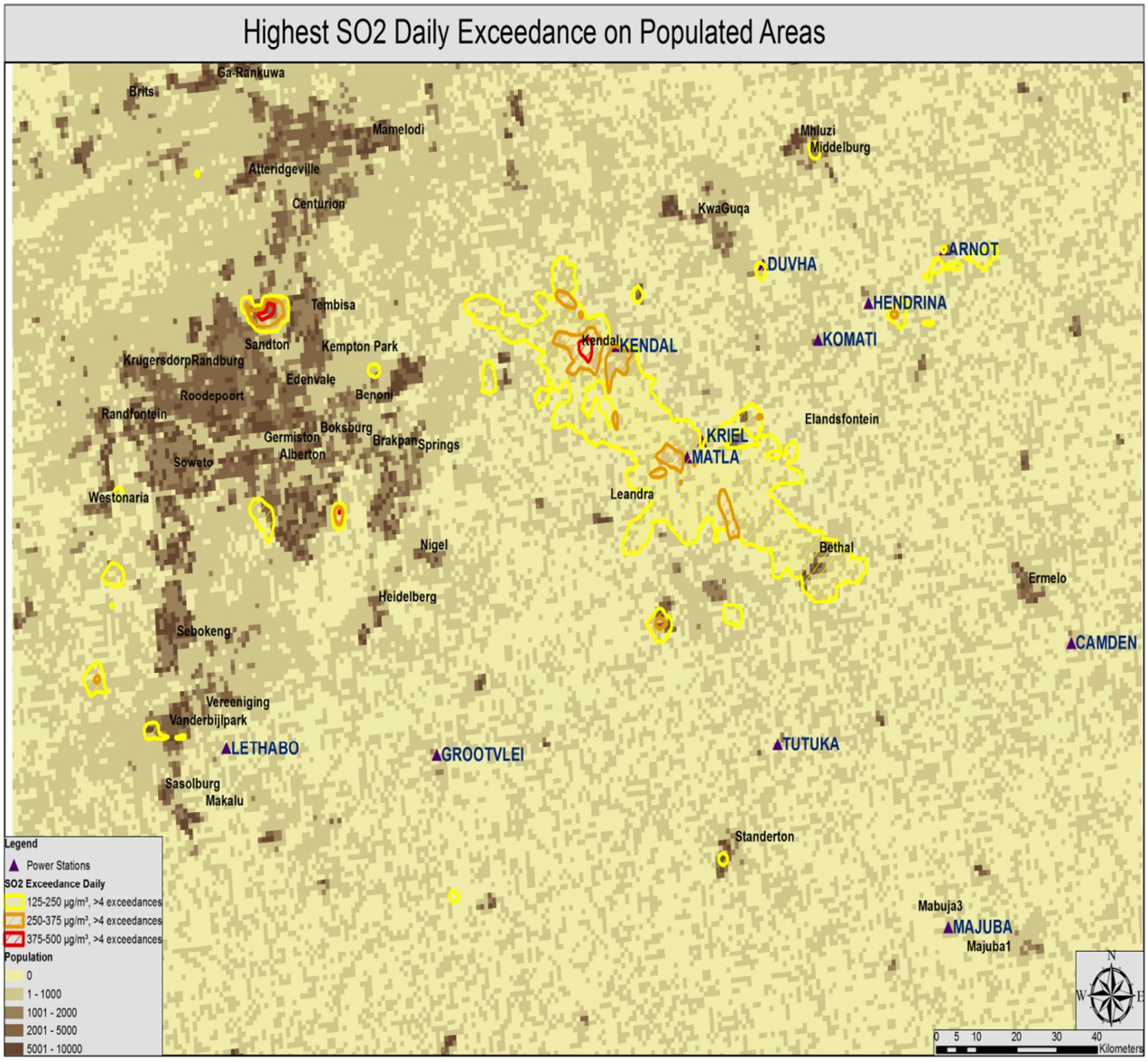


Figure 40: Highest SO_2 daily average exceedance on populated areas

The DEA ambient air quality standard for annual SO_2 concentration has been gazetted at a tolerance of 50 ug/m^3 with no permissible exceedances for immediate compliance (DEA, 2009). An assessment based on these parameters show that there are no impacts from power station emissions (Figure 41).

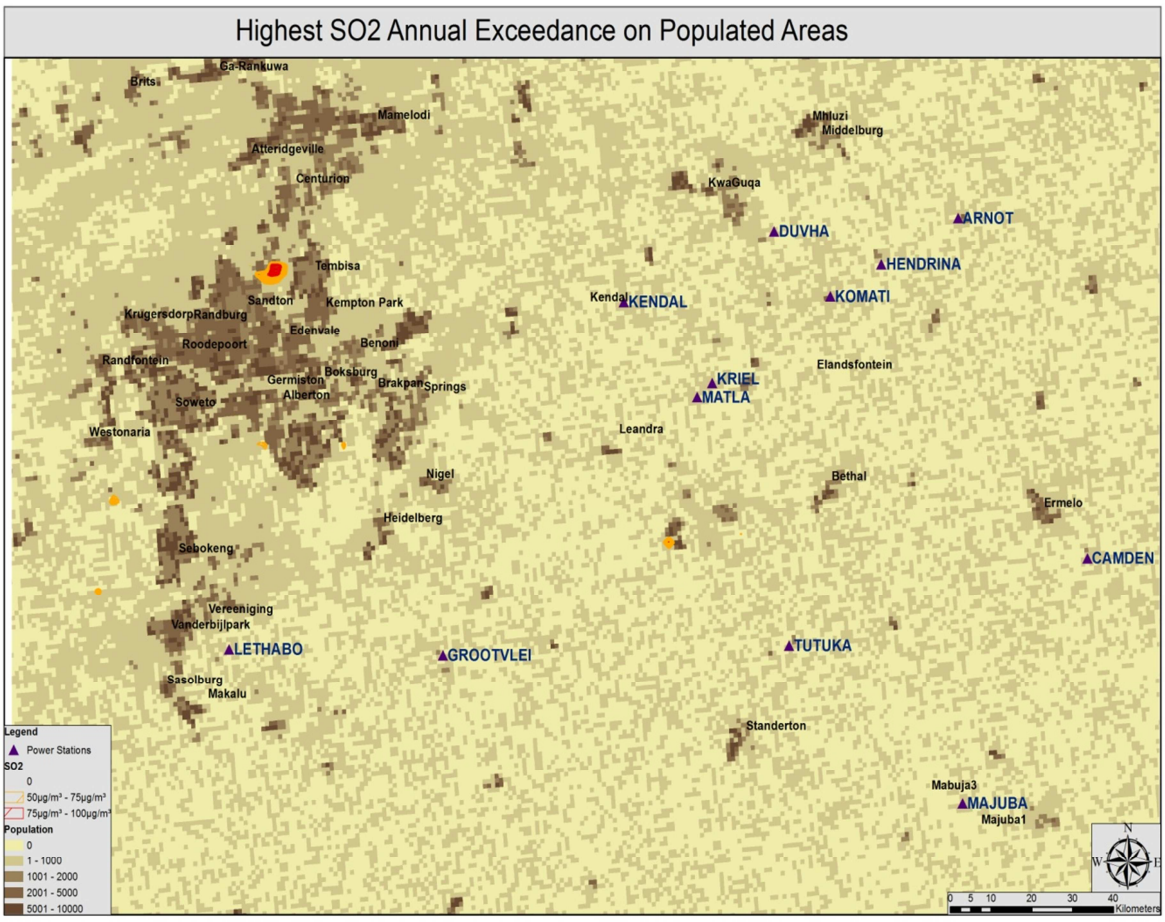


Figure 41: SO_2 annual average exceedance on populated areas

ECOSYSTEM RISK ASSESSMENT

Several high risk areas for potential harm to ecosystems can be seen on the Highveld (Figure 42) with a large extent around Kendal, Matla and Kriel power station. Generally the potential high risk areas extend from Standerton in the South, to Middelberg in the North and the Vaal Triangle in the west and south west. There are several informal settlements located in the west and south west areas.

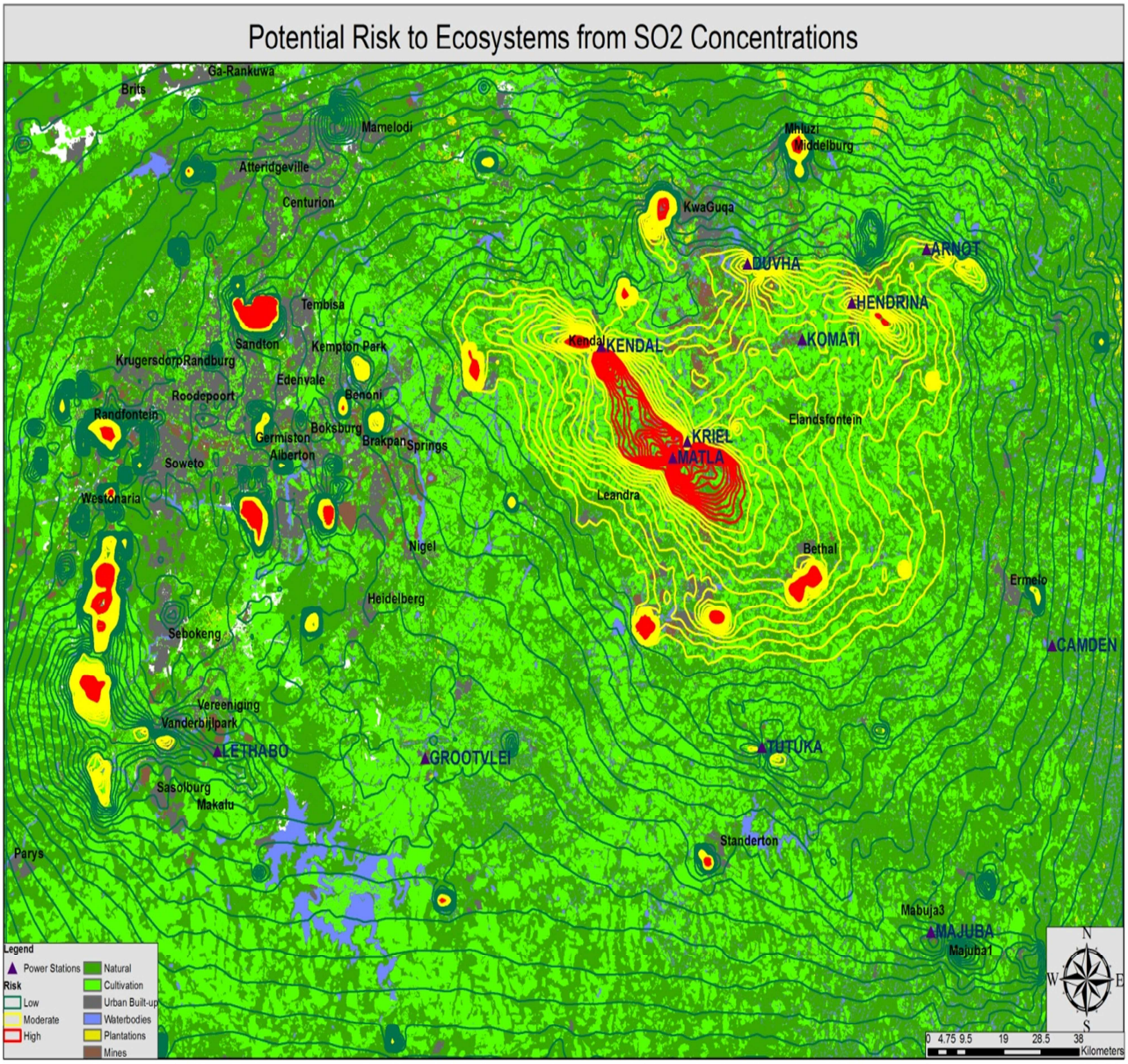


Figure 42: Impact on ecosystems from SO_2 concentrations

There are approximately 26 837 wetlands in the study area with 871 being located in areas categorised as high risk. The seven types of wetlands found on the Highveld can be described as channelled valley-bottom, depression, flat, flood plain, seep, unchannelled valley-bottom and valleyhead seep. The impact of emissions from the Kendal, Matla and Kriel power stations seem to have the largest spatial extent (Figure 43).

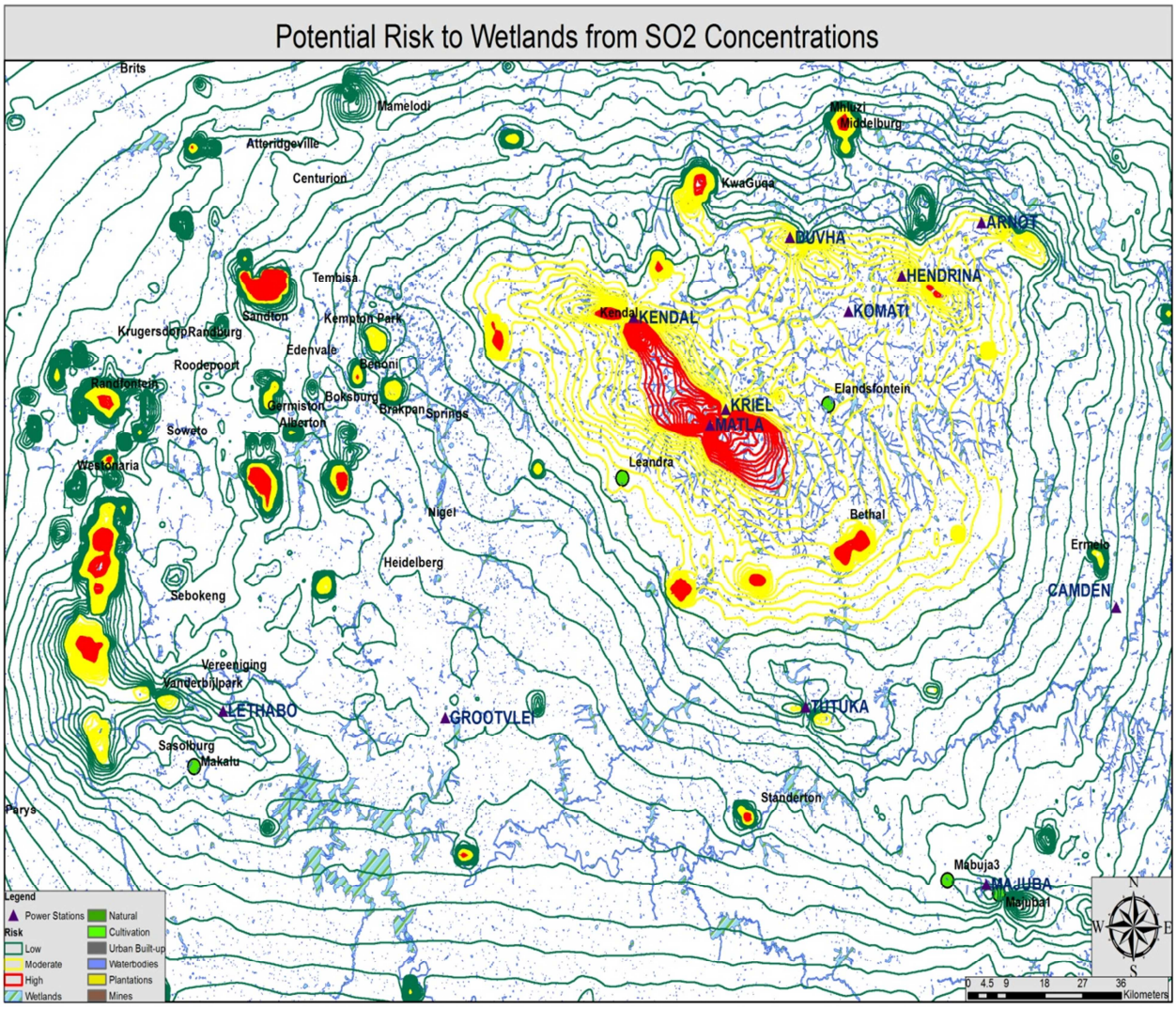


Figure 43: Impact on wetlands from SO_2 concentrations

According to the map (Figure 44) of potential risk to vegetation from SO_2 emissions there seems to be a potential for high risk to the Eastern Highveld , Soweto Highveld and Rand Highveld grasslands as well as the Egoli Granite, Cartonville Dolomite, Tsakane Clay and Gold Reef grasslands. The Gold Reef and Andesite Mountain bushvelds are also located in high risk areas.

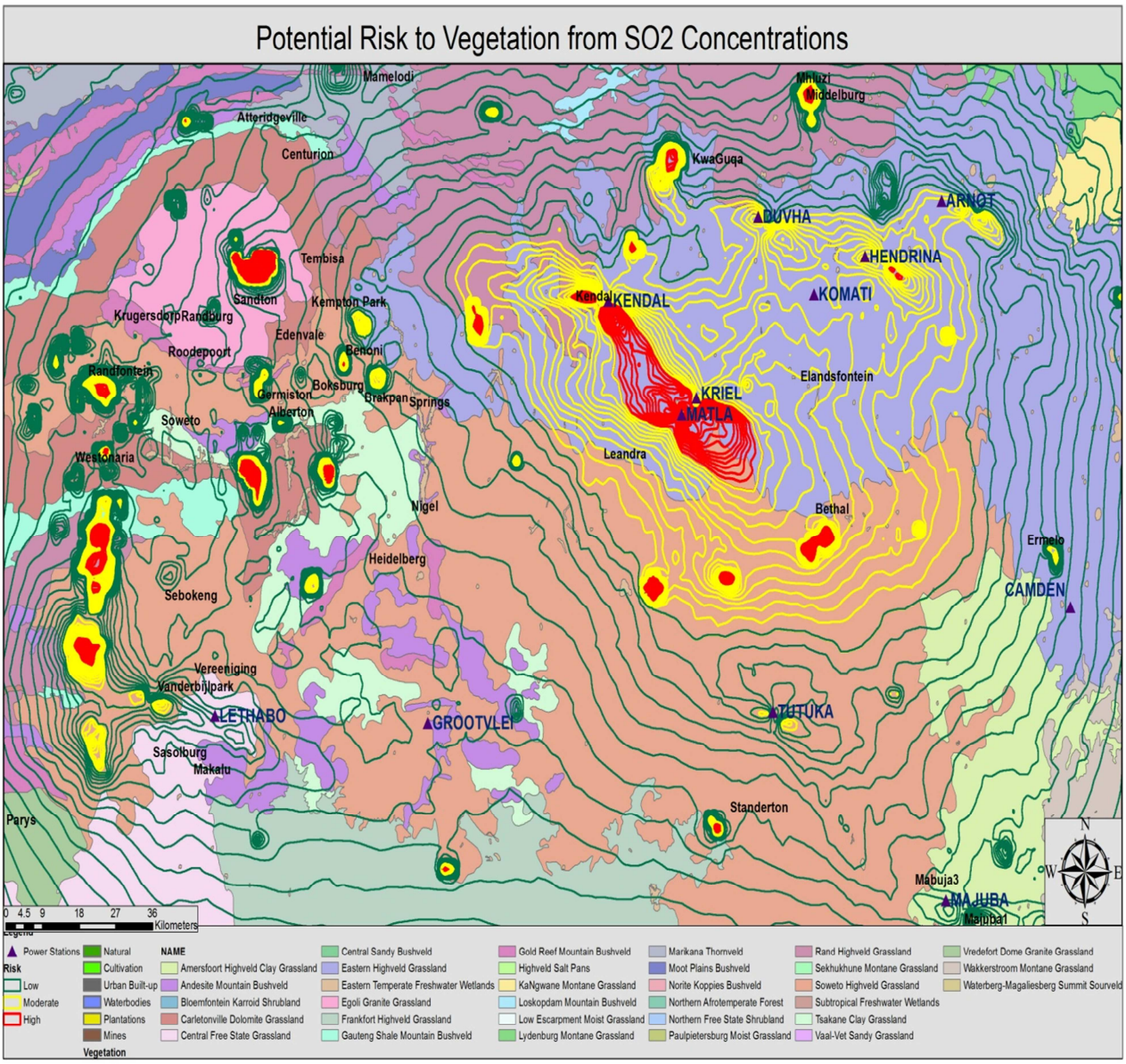


Figure 44: Impact on vegetation from SO_2 concentrations

6.3.3 ANALYSIS OF POTENTIAL RISK FROM NO_2 EMISSIONS

The NO_2 diurnal variation graph shows the influence of tall stack emitters impacting at the site predominantly during the mid-day period due to atmospheric instability and low level sources to a smaller extent between 06h00 to 08h00 and 15h00 and 18h00 due to motor vehicle emissions (Figure 45). Generally this distinct signature is observed at all monitoring sites. The standard deviation gives an indication of the worst case scenario.

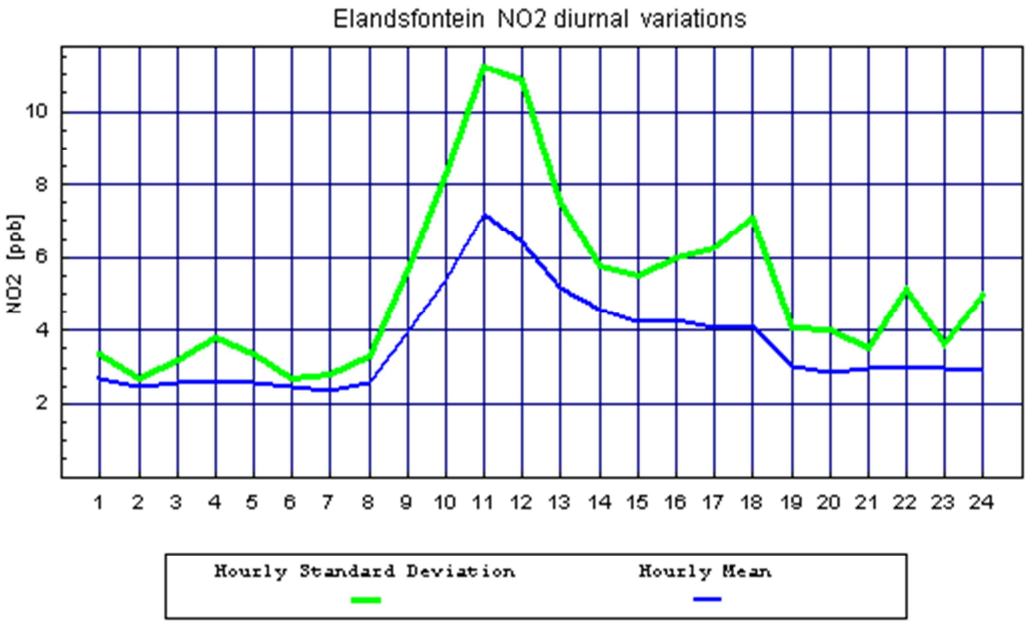


Figure 45: NO_2 diurnal variation at Elansfontein

6.3.3.1 Sector Exceedance Roses

ELANDSFONTEIN MONITORING STATION

The daytime sector exceedance rose indicates prevalent sources to the west, which indicate Kriel and Duvha power station to the north (Figure 46). The impact from Matla power station in the west-south-west is negligible.

The night-time sector exceedance rose indicates much lower concentrations were recorded during these hours. The dominant sources were in the north-north-east, south-south-east, south-south-west and north-west sectors. These sources are most likely related to motor vehicle emissions in neighbouring towns. This plot shows no influence from power stations, suggesting that these plumes are buoyed above the night-time surface inversion at this site.

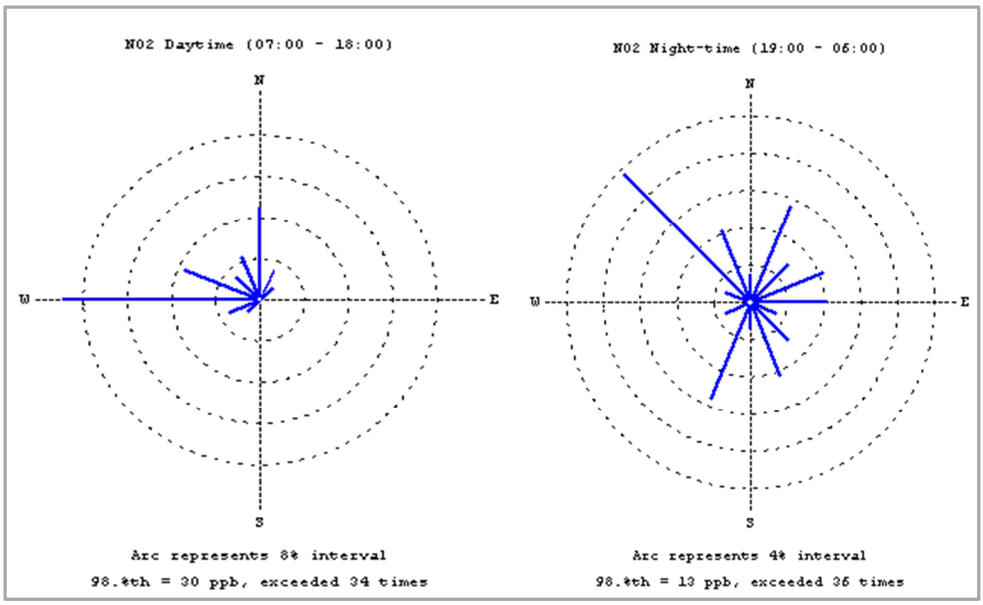


Figure 46: NO_2 daytime and night-time sector exceedance roses

VERKYKKOP MONITORING STATION

Both the day-time and night-time sector exceedance roses (Figure 47) show the prevalence of sources to the north-north-west and north, with the north being more dominant at night. This suggests that in both instances as with the SO_2 concentrations, the highest concentrations are likely to be related to Majuba power station in the north-north-west and Amersfoort in the north.

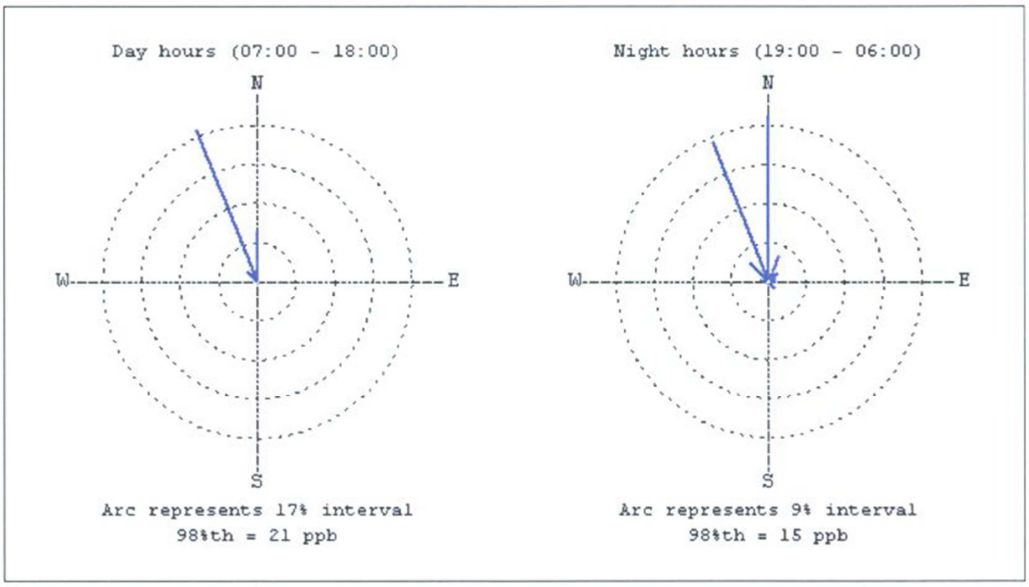


Figure 47: Day time and night-time NO_2 sector exceedance roses

PALMER MONITORING STATION

Both the daytime and night-time sector exceedance roses (Figure 48) indicate the prevalence of major sources in the south-south-west to west-south-west sectors. Arnot power station lies south-south-west while Hendrina, Duvha, Kriel and Matla power stations all lie south-west to west-south-west of the monitoring station, as do the towns of Middelburg and Witbank.

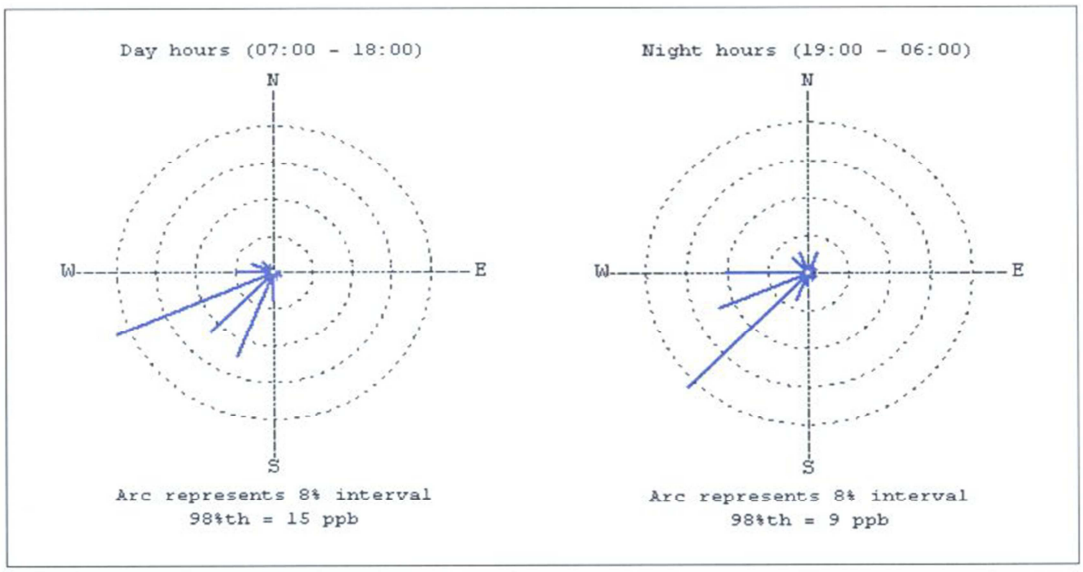


Figure 48: NO_2 daytime and night-time sector exceedance roses

MAKALU MONITORING STATION

The daytime sector exceedance rose (Figure 49) shows the prevalence of sources in the south to north-east sectors, with the north-west and north-north-west sectors as most dominant. Sasolburg lies to the west, Vanderbijlpark to the north-west and Vereeniging to the north. The night-time sector exceedance rose shows dominant sources in the west and north-north-west sectors.

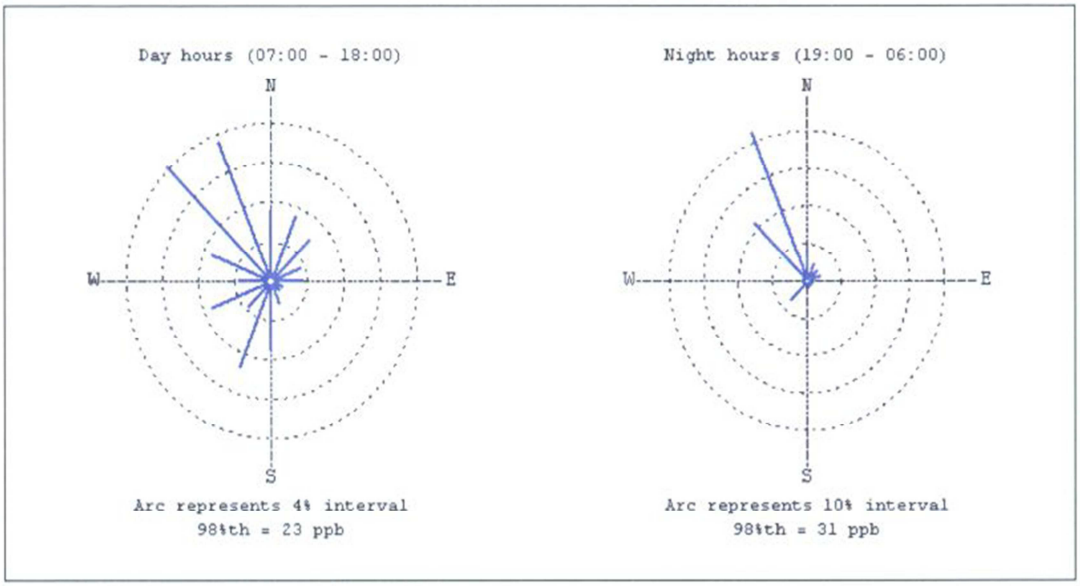


Figure 49: NO_2 daytime and night-time sector exceedance roses

KENDAL MONITORING STATION

The day and night time sector NO_2 exceedance roses at the Kendal monitoring station(Figure 50) show sources in majority of the sectors but most dominant occur in the South East, South West and North West sectors which may be related to numerous high level sources in the vicinity.

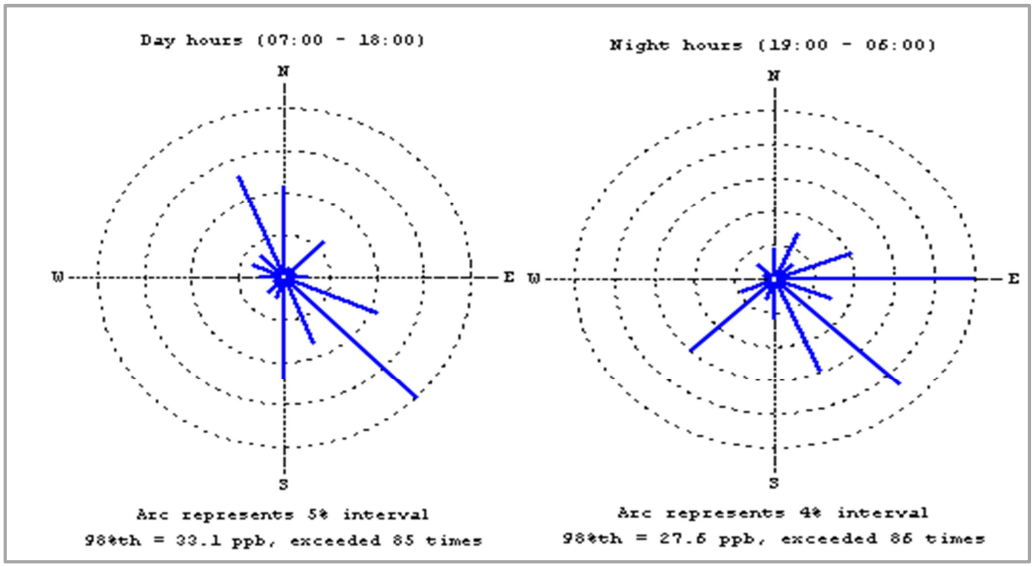


Figure 50: NO_2 daytime and night-time sector exceedance roses

6.3.3 ANALYSIS OF POTENTIAL RISK FROM NO_2 CONCENTRATIONS

Results from the analysis of the NO_2 annual average for a tolerance of 40 ug/m^3 for the protection of human health (DEA, 2009) and 30 ug/m^3 for the protection of vegetation (EC guideline) show no areas of potential concern around power stations. The highest measured annual average concentration for the year was recorded at 26.99 ug/m^3.

Eskom records from ground monitoring stations indicated that there were no stations which exceeded the 200 ug/m^3 highest hourly average more than 88 times a year as stipulated by DEA's national ambient air quality standards. The highest hourly average was recorded at 145.5 ug/m^3 at Kendal monitoring station.

****

Elandsfontein was the only monitoring station suitable for analysis of measured NO_2 observations against SCIAMACHY retrievals. A fairly good correlation seems to exist between measured observations and SCIAMACHY data.

Statistical evaluations of the SO_2 measured and modelled concentrations indicate that out of eight monitoring stations the model under predicts at five and over predicts at the other three. The calculated reliability of the model for SO_2 modelled concentrations are 62%. The comparison of the measured value to the upper and lower limits of the model also indicate nonconformity at three monitoring stations.

Statistical evaluations of the NO_2 measured and modelled concentrations indicate that the model both under predicts and over predicts for 50% of the time. The comparison of the measured value to the upper and lower limits of the model also indicate nonconformity at two monitoring stations. There appears to be no constant biasness in the model for both SO_2 and NO_2 outputs.

The results on the statistical distribution of the modelled outputs seem to indicate that the CALPUFF model predicts the highest values based on calculations

from the bulk of the distribution rather than the unique distribution at the tails. This could possibly account for the large variance between measured and modelled values.

Hotspots for high to very high risk to human health from SO_2 emissions occur around all power stations. Generally the category of high risk around power stations seems to be located in areas with population agglomerations between 0 to 1 000 and 2 001 to 5 000 per km^2.

Several high risk areas for potential harm to ecosystems from SO_2 emissions can be seen on the Highveld with a large spatial extent around Kendal, Matla and Kriel power station. Approximately 871 wetlands fall within the high risk areas. The vegetation risk map indicates a high risk to several grassland and bushveld types. There seems to be no potential risk to human health and ecosystems from emissions of NO and subsequent conversion to NO_2 in the atmosphere.

The following chapter discusses the conclusions of this study and outlines the recommendations and opportunities for future research.

CHAPTER 7
CONCLUSION & SUMMARY

This chapter discusses the extent to which the results have addressed the study objectives and outlines the recommendations and opportunities for future research.

7.1 SUMMARY OF RESULTS

The overall aim and objectives of this study were described in Section 1.3. The main objective of this study is to improve SO_2 and NO_2 modelled air quality predictions using measured data in order to credibly predict concentrations without reference to fixed ground based monitoring stations.

The study utilised data for the year 2003 from the Eskom air quality database of ground-based continuous measurements, the South African Weather Services meteorological data, Airshed Planning Professionals dispersion modelling studies conducted on behalf of Eskom and the European Space Agency's SCIAMACHY retrievals. Measured, modelled and remotely sensed air quality data was validated, interrogated, interpolated and integrated in the pursuit to create one "improved" air quality dataset for the Highveld region. This new air quality dataset for the Highveld was further interrogated against the DEA's, WHO's and EC's ambient air quality standards to map and identify potential risk to human health and ecosystems from power station emissions. The potential harm to health and ecosystems was mapped as categories of low, medium and high risk areas.

The results of the study have shown that although the concentration value for the NO_2 tropospheric column is greater than the values observed on the ground there is a good correlation between measured observations and SCIAMACHY retrievals.

The regression analysis of measured concentrations on the ground and SCIAMACHY retrievals at 9:00 revealed a poor correlation as compared to the regression analysis conducted on SCIAMACHY data retrieved at 10:00 alluding to

the fact that there may be sensitivity for acquisition times.

No SCIAMACHY retrievals where available for SO_2 comparisons.

The results from the validation of the CALPUFF model indicate with respect to SO_2 predictions that the model is only reliable for 62% of the time within the United States Environmental Protection Agency's model performance guideline of acceptance i.e. predictions within a factor of 2. Statistical analysis of SO_2 measured and modelled concentrations indicate that out of eight monitoring stations the model under predicts at five monitoring stations (Elandsfontein, Verkykkop, Leandra, Makalu and Palmer) and over predicts at the other three monitoring stations (Kendal, Majuba1 and Majuba 3). The comparison of the measured concentrations to the upper and lower limits of the model also indicated that the model does not conform at three monitoring stations (Majuba 1, Majuba 3 and Palmer).

For NO_2 the CALPUFF model predictions were reliable for only 50% of the time. The comparisons of the measured concentrations to the lower and upper limits reveal that the modelled values did not conform at two monitoring sites (Camden and Palmer).

There is also no constant value by which the model under predicts and over predicts as demonstrated in the expected excursions calculated for both SO_2 and NO_2.

The analysis of the CDF graphs indicate a break line in the quantiles for both SO_2 and NO_2 modelled data at all monitoring stations. It seems to appear that the CALPUFF model predicts the highest values from the bulk of the distribution rather that the tail of the distribution where the extremes lie. This could possibly account for the large variance between measured and modelled outputs.

The results on the analysis of potential risk from SO_2 emissions reveal that hotspots for high to very high risk to human health from SO_2 emissions occur around all power stations. Generally the category of high risk seems to be located in areas with population agglomerations between 0 1 000 and 2 001 to 5001 per km^2.

Several high risk areas for potential harm to ecosystems from SO_2 emissions can be seen on the Highveld with a large spatial extent around Kendal, Matla and Kriel power station. Approximately 871 wetlands fall within the high risk areas. The vegetation risk map indicates a high risk to several grassland and bushveld types.

There is no potential risk to human health from emissions of NO and subsequent conversion to NO_2 in the atmosphere..

In conclusion it can be established that a GIS is a powerful tool which can be utilised to statistically analyse, interrogate and integrate different air quality datasets. This study demonstrated that a GIS can be utilised to improve and quantify the evaluation of impacts from power station emissions on ecosystems and human health by identifying areas of potential risk to exposure.

7.2 RECOMMENDATIONS FOR FUTURE RESERACH

Although this study proves that it is possible to refine CALPUFF modelled outputs using measured values via a GIS, the ground monitoring stations should be strategically located to represent an adequate sample distribution which will further improve the accuracy of the model outputs.

One of the findings of this study was that the CALPUFF model seems to use an equation based on the bulk of the distribution to predict behaviour of variables in extreme scenarios. The cumulative distribution function graphs show unique behaviour at the tails of the distribution were the extremes occur and predictions by the model should be made based on equations derived at the tail of the distribution. This should be further investigated as it would increase the reliability of the predictions. It is suggested that a new algorithm for the model based on an empirical equation be formulated. This should be based on greater than 10 years of continuous data and performance should be compared against the current algorithm.

Results showed that SCIAMACHY retrievals of NO_2 concentrations were not representative of measured surface concentrations. The concentration retrieved by the satellite is given for the total amount of NO_2 per tropospheric column. This cannot be

easily translated to the concentration at the ground without complex physical science calculations and assumptions. Future research should investigate the robustness of the assumptions made for the conversion. Research should be focused on determining the amount of NO_2 at varying altitudes within the tropospheric column for comparative analysis with surface measurements and boundary layer characteristics for example mixing height variability, turbulent mixing, thermal and mechanical turbulence, albedo, etc.

The SCIAMACHY pixel resolution of 60 km x 30 km is too coarse for comparative analysis with a point which represents a concentration on the ground. The results from the analysis on satellite retrievals seem to show that there could be high sensitivity to the time of acquisition of satellite data. This should be further investigated with a different dataset as the 2003 dataset did not have sufficient intersects between SCIMACHY pixels and monitoring stations. Surface measurements are recorded hourly whereas there is a time lag due to the orbit cycle of the satellite with regards to concentrations retrieved by a satellite. Greater dispersion and dilution of pollutants occur with increasing time which could account for discrepancies between satellite retrievals and measured surface concentrations. It is recommended that other satellites with finer resolutions be investigated for example OMI and GOME. SCIAMACHY overpasses the Highveld region once every four days whereas OMI and GOME have daily orbits.

The study revealed that integration of available air quality datasets with a GIS can improve the evaluation of impacts from power station emissions on human health and ecosystems by identifying hotspots. It is recommended that these areas of concern should be verified by research in the field.

****

The following chapter lists all references utilised in this dissertation.

CHAPTER 8
REFERENCES

Aghedo , A. M., Schultz, M. G., Rast S., 2007: The influence of African air pollution on regional and global tropospheric ozone, *Atmospheric Chemistry and Physics*, 7, 1193-1212.

Agrawal, I.C., Gupta, R.D., Gupta, ER.V.K., 2003: *GIS as modelling and decision support tool for air quality management: a conceptual framework*, in Proceedings of Map India Conference.

Ames, M.R., Zemba, S.G., Yamartino, R.J., Valberg, P.A., Green, L.C., 2002: Comments on: Using Calpuff to evaluate the impacts of power plant emissions in Illinois: model sensitivity and implications, *Atmospheric Environment***,** 36, 2263-2265.

Anderson, S., 2001: *An Evaluation of Spatial Interpolation methods On Air Temperature in Phoenix,* Department of Geography, Arizona State University Tempe, AZ 85287-0104.

Andreae, M.O., and Rosenfeld, D., 2008: Aerosol – cloud precipitation interactions. Part 1. The nature and sources of cloud – active aerosols, *Earth-Science Reviews*, 89, 13-41.

Annegarn, H.J., Kneen, M.A., Piketh, S.J., Horne, A.R., Hlapolosa, H.P.S., Kirkman, G.A., 1993: *Evidence for large scale circulation of anthropogenis sulphur over Southern africa*, in Proceeding of the 24th National Association for Clean Air Conference, Clean Air Challenges in a Changing South africa, Brits, October 2003.

Annegarn, H.J., Turner, C.R., Helas, G., Tosen, G.R. and Rorich, R.P., 1996: Gaseous pollutants. In: *Air Pollution and Its Impacts on the South African Highveld* (Eds: 228 Held, G., Gore, B.J., Surridge, A.D., Tosen, G.R., Turner, C.R. and Walmsley, R.D.),

Environmental Scientific Association, Cleveland, South Africa, 25 - 33.

Anon, 1983: Report on the European Community epidemiology survey on the relationship between air pollution and respiratory health in primary school children, Brussels.

ASTM, 2000: *Standard guide for statistical evaluation of atmospheric dispersion model performance*, American Society for Testing and Materials, PA 19428-2959, West Conshohocken.

Atkinson, R., 2000: Atmospheric Chemistry of VOCs and NOx, *Atmospheric Environment*, 34, 2063 – 2101.

Bachmann, J., 2003: Intercontinental Air Pollution: Introduction to the Topic, *Air and Waste Mangement Association's Magazine for Environmental Managers*, 11 December.

Balmes, J.R., Fine, J.M., Gordon, T., Sheppard, D., 1989: Potential Bronchoconstrictor Stimuli in Acid Fog, *Environmental Health Perspectives*, 79, 163-166.

Barna, M.G., and Gimson, N.R., 2002: Dispersion modelling of a winter time particulate pollution episode in Christchurch, New Zealand, *Atmospheric Environment*, 36, 3531-3544.

Becker, S., 2004: *Analysis and Modelling of Atmospheric Boundary Layer Characteristics and the Near Ground Sulphur Dioxide Pollution Levels Over the South African Mpumalanga Highveld*, Thesis, University of Wisconsin, Oshkosh.

Beirle, S., 2004: *Estimating Source Strenghts And Lifetime Of Nitrogen Oxides From Satellite Data*, PhD Thesis, The Ruperto-Carola University Of Heidelberg, Germany.

Bell, M.L., 2006: The use of ambient air quality modeling to estimate individual and population exposure for human health research: A case study of ozone in the Northern Georgia Region of the United States, *Environment International*, 32, 586–593.

Bernhardsen, T., 1992: *Geographic Information Systems*, Arendal, Norway.

Beychok, M. R., 2005: *Fundamentals of Stack Gas Dispersion*, 88-102, Irvine, California.

Binkowski, F.S., and Roselle S.J., 2003: Models-3 community multi-scale air quality (CMAQ) model aerosol component-1. Model description, *Journal of Geophysical Research*, 6, 99-108.

Borell, P., Burrows, J.P., Platt, U., Richter, A., Wagner, T., 2003: New directions: new developments in satellite capabilities for probing the chemistry of the troposphere, *Atmospheric Environment*, 37, doi:10.1016/S1352-2310(03)00150-X.

Boersma, K.F., H.J. Eskes, E.J. Brinksma, 2004: Error analysis for tropospheric NO_2 retrieval from space, *Journal of Geophysics*, 109, 4311, doi: 10.1029/2003JD003961.

Bolstad, P., 2008: *GIS Fundamentals A first text on Geographic Information Systems*, Eider Press, White Bear Lake.

Boubel, R.W., Fox, D.L.,Turner, D.B., Stern, A.C., 1994: *Fundamentals of Air Pollution*, Academic Press, California.

Bovensmann, H., Burrows, J.P., Buchwitz, M., Frerick, J., Noel, S., Rozanov, V.V., Chance, K.V., Goede, A. P. G., 1999: SCIAMACHY: Mission objectives and measurement modes, *Journal of Atmospheric Science*, 56, 127-150.

Bradshaw, J., Davis, D., Grodzinsky, G., Smyth, S., Newell, R., Sandholm, S., Liu, S., 2000: Observed distributions of nitrogen oxides in the remote free troposphere from the NASA Global Tropospheric Experiment Program, *Reviews of Geophysics*, 38 (1), 61 – 116.

Bridhikitti, A., 2006: *Application Of Moderate-Resolution Technologies For Surface Air Pollution Monitoring In South East Asis*, Unpublished Phd disertation, Graduate School of Clemson University, South Carolina.

Brunekreef, B., and Holgate, S.T., 2002: Air pollution and health, *Lancet*, 360, 1233-1242.

Brunner, D., Staehelin, J., Jeker, D., 1998: Large-scale nitrogen oxide plumes in the tropopause region and implications for ozone, *Science*, 282, 1305–1309.

Burrough, P., and McDonnell, R.A., 1998: *Principles of Geographic Information Systems*, Oxford University Press, U.S.A.

Burrows, P.J., Buchwitz, M., Eisinger, M., Rozanov, V., Weber, M., Richter, A., Ladstaetter-Weissenmayer, A., 1999: The Global Ozone Monitoring Equipment (GOME): Mission concept and first scientific results, *Journal of Atmospheric Science*, 56, 151-175.

Carmichael, G. R. and Peters, L. K., 1984: An Eulerian Transport/Transformation/Removal Model for SO_2 and Sulfate-I. Model Development, *Atmospheric Environment*, 18, 5, 937-951.

Carruthers, D.J., Holroyd, R.J., Hunt, J.C.R., Weng, W.S., Robins, A.G., Apsley, D.D., Thomson, D.J., Smith, F.B., 1994: UK-ADMS-a new approach to modelling dispersion in the Earth's atmospheric boundary layer, *Journal of Wind Engineering and Industrial Aerodynamics*, 52, 139-153.

Carver, S., 1998: *Innovations in GIS 5*: Selected papers from the fifth National Conference on GIS Research UK Volume 5, Taylor and Francis, Oxford.

Carvalho, J.D., and Degrazia, G.A., 2002: Lagrangian stochastic dispersion modelling for the simulation of the release of contaminants from tall and low sources, *Meteorologische Zeitschrift*, 11, 89–97.

Chang, J.C., 2002: *Methodologies for evaluating performance and assessing uncertainty of atmospheric dispersion models*, PhD thesis, George Mason University, Fairfax.

Chang, J.C., and Hanna, S.R., 2004, Air quality model performance evaluation, *Meteorological Atmospheric physics*, 87, 167-196.

Chrisman, N., 1999: *Exploring Geographic Information Systems 2nd Edition*, John Wiley and Sons, New Jersey.

Coles, S., 2001: *An Introduction to Statistical Modeling of Extreme Values*, Springer, London.

Collett, K.S., Piketh, S.J., Ross, K.E., 2010: An assessment of atmospheric nitrogen budget on the South African Highveld, *South African Journal of Science*, 106, doi:10.4102/sajs.v4016i5/6.220.

Cosijn, C. and Tyson, P.T., 1996: Stable discontinuities in the atmosphere over South Africa, *South African Journal of Science*, 92, 381-386.

Cradle, R.D. and Powers, J.W., 1966: Some aspects of atmospheric chemical reactions of atomic oxygen, *Tellus*, 18, 176-185.

Coetzee, A.M., 1986: Die invloed van lugbesoedeling op gesondheid in die Sasolburg gebied, SAMT 70/6, 339-343.

Cressie, N., 1991: *Statistics for Spatial Data*, Wiley, New York.

Crutzen, P.J., 1974: Photochemical reactions by and influencing ozone in the toposphere, *Tellus*, 26, 47-57.

Cullis, C. F. and Hirschler, M. M., 1980: Atmospheric Sulphur: natural and man-made sources, *Atmosphere Environment*, 14, 11, 1263 - 1278.

Chylek, P., Ramaswamy, V., Ashkin, A., Dziedzic, J. M., 1983: Simultaneous determination of refractive index and size of spherical dielectric particles from light scattering data, *Applied Optics*, 22, 15, 2302 - 2307.

Davakis, E., Andronopoulos, I., Bartzisd, J.G., Nychasa, S.G., 2007: Data assimilation in meteorological pre-processors: Effects on atmospheric dispersion simulations, *Atmospheric Environment*, 41, 2917–2932.

Deligiorgi, D., and Philippopoulos, K., 2011: *Advanced Air Pollution*. Spatial Interpolation Methodologies in urban air pollution modelling: Application for the Greater Area of Metropolitan Athens, Greece, InTech.

DeMers, M.N., 2002: *Fundamentals of Geographic Information Systems*, John Wiley and Sons, United States.

Department of Environmental Affairs and Tourism, 2001: *Invitation for public comments on the technical background document for the development of a national ambient air quality mangement standard for sulphur dioxide*, Government Gazette Number 22134.

Department of Environmental Affairs and Tourism, 2003: *Mpumulanga State of the Environment Report*,
http://www.environment.gov.za/soer/reports/mpumalanga/website/documents/MPU_SOE_2003_CH01-03.pdf.

Department of Environmental Affairs and Tourism, 2009a: Publication Series A Book 5: *An introduction to air quality management*,
www.airqualitylekotla.co.za/downoads/2008/po.

Department of Environmental Affairs, 2009b: *Government Gazette on National Ambient Air Quality Standards*, 534, 32816.

Department of Environmental Affairs, 2011: *Draft Highveld Priority Area Air Quality Management Plan*.

Diab, R.D and Zunckel, M., 2005: *The Air Quality Act Companion*, Air quality management booklets done on behalf of the Department of Environmental Affairs.

Douglas, G.F., 1982: Uncertainty in air quality modelling, A summary of the AMS workshop on quantifying and communicating model uncertainty, *Bulletin American Meteorological Society*, 65, 28-31.

Earth Tech, 2000: *A Users Guide for Calpuff Dispersion Model*, http://www.src.com/calpuff/calpuff1.htm

Engelbrecht, E., 1987: *Effects of Sulphur Dioxide on Bean Cultivar Under Greenhouse Conditions*, Research Report Number TRR/N87/013, Eskom, Johannesburg.

Englund, E.J., 1990: a Variance of Geostastisticiansm, *Journal of Mathematical Geology*, 22, 417-455.

EPA, 2006: *Technology Transfer Network Support Centre for Regulatory Atmospheric Modeling*, http://www.epa.gov/scram001/dispersion_alt.htm.

EPA, 2007: *New categorical metrics for air quality model evaluation*, http://www.epa.gov/scram001/guidance/guide/appw_05.pdf.

Eskom, http://www.eskom.co.za.

Fenger, J., 2002: Urban air quality, in J. Austin, P. Brimblecombe and W. Surges (eds.), *Air Pollution for the 21st Century*, Elsevier Science Ltd., Oxford, 1-54.

Fourie, G.D., 2002: AERMOD & ADMS-3: *Two New Generation Dispersion Models*, Sasol Technology Research & Development Report, Sasolburg.

Fourie, G.D., 2006: *Modelling the Long-Range Transport and Transformation of Air Pollutants Over The Southern African Region*, Unpublished PhD, University of North West, Potchefstroom.

Freiman, M.T., and Piketh, S.J., 2003. Air transport into and out of the industrial Highveld region of South Africa., *Journal of Applied Meteorology*, 42, 994-1002.

Fuentes, M., and Smith, R., 2002: *A New Class of Non Stationary Spatial Models*, under review for JASA, http://132.248.182.189/cursos/geost/articulos/…%20nonstationary%20spatial%2020 models.pdf

Fugas, M. and Gentilizza, M., 1978: The relationship between sulphate and sulphur dioxide in the air, *Atmospheric Environment*, 12, 335 - 337.

Garstang, M., G.D., and Houston, S., 1985: *Mesoscale Studies and Developments*, Programme for the Atmospheric Water Supply, Annual Report 1984/85, Water Research Commission, Pretoria, 54-72.

Garstang, M., Tyson, P.D., Swap, R., Edwards, M., Kållberg, P., Lindesay, J.A., 1996: Horizontal and vertical transport of air over southern Africa, *Journal of Geophysical Research*, 101 (D19), 23 721-23 736.

Genton, M.G., and Furrer, R., 1998: Analysis of Rainfall Data by Simple Good Sense: Is Spatial Statistics Worth the Trouble?, *Journal of Geographic information and Decision Analysis*, 2, 11-17.

Gerhard, E.R. and Johnston, H.F., 1955: Photochemical oxidation of sulphur dioxide in air, *Industrial Engineering Chemistry*, 47, 972-976.

Gertler, A.W., Miller, D.F., Lamb, D., Katz, U., 1984: Studies of sulphur dioxide and nitrogen dioxide reactions in haze and cloud. In: Durham, J.L. (Ed.), Teasley, J.I. (Series, Ed.), *Chemistry of Particles, Fogs and Rain*, Acid Precipitation Series, Butterworth, Boston, 2, 131–160.

Gifford, F.A., 1976: Consequences of effluent releases, *Nuclear Safety*, 17, 68-86.

Godfrey, J.J., and Clarkson, T.S., 1998: Air Quality Modeling in a Stable Polar Environment- Ross Island Antarctica, *Atmospheric Environment*, 32, 899-2911.

Goldreich, Y., 1984: Urban topoclimatology, *Physical Geography*, 8, 336-364.

Goodchild, M., Haining, R., Wise, S., 1992: Integrating GIS and Spatial Data Analysis: Problems and Possibilities, *International Journal Geographic Information Systems*, 6,5, 407-423.

Gumel, E.J., 2004: *Statistics of Extremes*, Mineola, New York.

Guptill, S., 1995: *Elements of Spatial Data Quality*, Elsevier Science, Amsterdam.

Gurlit, W., Gerilowski, K., Krause, H., Burrows, J.P., 2003: *SCIAMACHY solar irradiance validation using radiometric calibration of balloonborne spectrometers*, in: 16th ESA Symposium on European Rocket and Balloon Programmes and Related Research, ESA SP-530, 433-437, http://adsabs,harvard.edu/abs/2003erbp.conf.433G.

Hall, D.J., and Spanton, A.M., 2002: Evaluation of new generation atmospheric dispersion models, *International Journal of Environment and Pollution*, 18, 22–32.

Hanna, S.R., 1989: Confidencelimits for air quality model evaluations as estimated by bootstrap and jackknife resampling methods, *Atmospheric Environment*, 23, 1385-1398.

Held, G., 1985: *Study of the Escarpment Breeze and its Influence on the Ventilation Potential of the Eastern Transvaal Highveld*, ATMOS/85/21, Atmospheric Sciences Division, CSIR, Pretoria.

Held, G., Snyman, G. M., Scheifinger, H., 1993: Seasonal Variations and Trends of Atmospheric Particulate on the South African Highveld, *The Clean Air Journal*, 8, 8, 4 - 11.

Held, G., Scheifinger, H. Synman, G. M., Tosen, G. R., Zunckel, M., 1996: The

Climatology and Meteorology of the Highveld. in: *Air pollution and its impacts on the South African Highveld* (Eds: Held, G., Gore, B. J., Surridge, A. D., Tosen, G. R., Turner, C. R. and Walmsley, R. D.), Environmental Scientific Association, Cleveland, South Africa, 60 - 71.

Helmas, G. and Pienaar, J.J., 1996: The influence of vegetation fires on the chemical composition of the atmosphere, *South African Journal of Science*, 99, 132-136.

Hewitt, C.N., 2001: The atmospheric chemistry of sulphur and nitrogen in power station plumes, *Atmospheric Environment*, 35, 1155–1170.

Hidy, G.M., Brook, J.R., Chow, J.C., Green, M., Husar, R.B., Lee, C., Scheffe, R.D., Swanson, A., Watson, J.G., 2009: 2009 critical review discussion: Remote sensing of particulate pollution from space: Have we reached the promised land?, *Journal of the Air and Waste Management Association*, 59, 1130-1139.

Holland, E. A., Dentener, F.J., Braswell, B.H., Sulzman, J.M., 1999: Contemporary and pre-industrial global reactive nitrogen budgets, *Biogeochemistry*, 46, 7-43.

Holloway, T., Kinney, P.L., Sauthoff, A., 2005*:* Application of air quality models to public health analysis, *Energy for Sustainable Development*, 3, 1563-1570.

Holmes, N.S., Morawska, L., 2006: A review of dispersion modelling and its application to the dispersion of particles: an overview of different dispersion models available, *Atmospheric Environment*, 40, 5902-5928.

Igbafe, A.I., 2007: *Resolving the Atmospheric Sulphur Budget Over the Elandsfontein Area of the Mpumalanga Highveld*, Phd dissertation, University of Witwatersrand, Johannesburg.

Jacobson M.Z., 1999: *Fundamentals of Atmospheric Modelling*, Cambridge University Press, USA.

Jeffery, S., Piketh, S.J., Kahn, R., Bruintjes R.T., Holben, B.N., 2005: *A Summary Of First Year Activities Of the United Arab Emirates Unified Aerosol Experiment*, Naval Research Laboratory, Report Number NRL/MR/7534-05-8899.

Jenkin, M.E., and Clemitshaw, K.C., 2000: Ozone and other secondary photochemical pollutants: chemical processes governing their formation in the planetary boundary layer, *Atmospheric Environment*, 34,16, 2499-2527.

Johnson, W.B., Sklarew, R.C., Tuner, D.B., 1976: Urban Air Quality Simulation Modeling in Stern, A.C, Air Pollution Volume 1: *Air Pollutants, their transformation and transport*, 3rd edition, 511-557, New York, Academic Press.

Joubert, A.M., 1994: *General Circulation Model Simulations of Southern African Regional Climate*, unpublised MSc dissertation , University of Witwatersrand, Johannesburg.

Josipovic, M., 2009: *Acidic Deposition Eminating from the South Aafrican Highveld:A Critical Level and Critical Loads Assessment*, Phd thesis, University of Johannesburg.

Kaynak, B., 2009: *Assimilation of trace gase retrievals obtained from satellite (SCIAMACHY), air craft and ground observationssimulations into a regional scale air quality model (CMAQ-DDM/3D)*, Phd thesis, Georgia Institute of Technology.

Kirchstetter, T.W., Novakov, T., Hobbs, P.V., Magi, B., 2003: Airborne measurements of carbonaceous aerosols in southern Africa during the dry biomass burning season, *Journal of Geophysical Research*, 198, doi: 10.1029/2002JG002171.

Kelly, B.I., 1986: *Visual Response of Pinus patula*, *Pinus elliotti* and *Eucalyptus gradis to Sulphur Dioxide Fumigations*, Research Report number TRR/N86/101, Eskom, Johannesburg.

Kellog, W.W., Cradle, R.D., Allen, E.R., Lazrus, A.L., Martell, E.A., 1972: The sulfur cycle, *Science*, 175, 587-596.

Kitagawa, T., 1984: Cause Analysis of the Yokkaichi Asthma Episode in Japan, *Journal of the Air Pollution Control Association*, 34, 7, 743-746.

Koosialee, A., 2006: Technology review of prognostic 3-d meteorogical models, Report done on behalf of Sasol Technology Research & Development, Sasolburg.

Koppmann, R., von Czapiewski, K., Reid, J.S., 2005: A review of biomass burning emissions, part 1:gaseous emissions of carbon monoxide, methane, volatile organic compounds and nitrogen containing compounds, *Atmospheric Chemistry and Physics Discussions*, 5, 10455-10516.

Kozlowski, T.T. and Constantinidou, H.A., 1986: Responses of woody plants to environmental pollution: Part 1 sources and types of pollutants and plant responses, *Forestry Abstracts*, 47, 105-132.

Lee, D.S., Köhler, I., Grobler, E., Rohrer, F., Sausen, R., Gallaardo-Klenner, L., Olivier, J.G.J., Dentener, F.J., Bouman, A.F., 1997: Estimates of global NOx emissions and their uncertainties, *Atmospheric environment*, 31, 1735-1749.

Li, C., Kai-Han Lou, A., Mao, J., Chu, D.A., 2005: Retrieval, validation and application of the 1-km aerosol optical depth from MODIS measurements over Hong Kong, *Geo Science and Remote Sensing*, 3,11, 2650-2658.

Li, J., and Heap, A.D., 2008: *A review of Spatial Interpolation Methods for Environmnetal Scientists*, Department of Resources, Energy and Tourism, Report Number 2008/23 GeoCat # 68229, Australia.

Lillesand, T.M., Kiefer, R.W., Chipman, J.W., 2008: *Remote Sensing and Image Interpretation*, John Wiley and Sons, New York.

Lipfert, F.W., 1994: *Air Pollution and Community Health: a Critical Review and Data Sourcebook* , Van Nostrand and Reinhold, New York.

Lippmann, M. and Schlesinger, R.B., 1979: *Chemical Contamination in the Human Environment*, 1st Ed., Oxford University Press, New York, 217-231.

Liptrot, G.F., 1992: *Modern Inorganic Chemistry 4th Edition*, Scotprint, Musselburgh.

Lo, C.P., and Yeng, A.K.W., 2007: *Concepts and Techniques of Geographic Information Systems*, Pearson Prentice Hall, New Jersey.

Lozano, A., Usero, J., Vanderlinden, E., Raez, J., Contreras, J., Navarrete, B., EL Bakouri, H., 2009*:* Design of air quality monitoring networks and its application to NO2 and O3 in Cordova, Spain, *Microchemical Journal*, 93, 2, 211-219.

Lydia, A.O., 2010: *Characteristics of particulate matter over the southern African industrialised Highveld, MSc thesis*, University of the Witwatersrand, Johannesburg.

Main, H. H., and Roberts, P. T., 2001: *PM 2.5 Data Analysis Workbook*, Workbook prepared for the U.S. Environmental Protection Agency, Office of Air Quality Planning and Standards, Report No. STI-900242-1988-DWB, Research Triangle Park, North Carolina.

Manahan, S. E., 1991: *Environmental Chemistry 5th Edition*, Lewis Pub. Michigan, 583.

Martin, R.V., 2008: Satellite remote sensing of surface air quality, *Atmospheric Environment*, 42, 7823-7843.

Maynard, R., 2004: Key airbourne pollutants-the impact on health, *Science of the Total Environment*, 334-335, 9-13.

McKechnie, C.J, 2010: *Monitoring biomass burning emissions using satellite imagery for southern Africa*, MSc thesis, University of the Witwatersrand, Johannesburg.

Meszaros, E., 1981: *Atmospheric Chemistry Fundamental Aspects*, Elsevier Scientific Publishing Company, New York.

Meyer, B., 1977: *Sulfur, Energy and Environment*, Elsevier Scientific, New York.

Goodchild, M.F., Steyaert, L.T., Parks, B.O., 1996: GIS and Environmental Modeling:Progress and Research Issues, John Wiley and Sons, New York.

Mijling, B., 2012: *Satellite observations of ozone and nitrogen di oxide from retrievals to emission estimates*, Phd thesis, University of Eindhoven.

Miller, H.J., 2004: Toblers first law and spatial analysis, *Annals of the Association of American Geographers*, 94, 284-289.

Ministry Of The Environment, 2004: *Good Practice Guide for Atmospheric Dispersion Modelling*, Wellington, New Zealand, ME number 522, http://www.mfe.govt.nz/publications/air/.

Mofarrah, A., and Husain, T., 2010: Aa holistic approach for optimal design of air quality monitoring network expansion in an urban area, *Atmospheric Environment*, 44, 3, 432-440.

Mookken, M., Joy, P.M., Narayanan, N., 2011: *Analysis of Spatial Variation of Ambient Air Temperature*, University of Calicut, India.

Moussiopoulos, N., 1997: State of the art of air pollution models, needs and trends, *International Journal Environment and Pollution*, 8, 250-259.

Murray, D.G., and de Beer, G.H., 2004: *Kendal Power Station Air Quality and Dust Monitoring Annual Report 2003*, Research report number TRR/T04/374, Eskom, Johannesburg.

Murray, D.G., and de Beer, G.H., 2004: *Majuba Power Station Air Quality and Dust Monitoring Annual Report 2003*, Research report number TRR/T04/376, Eskom, Johannesburg.

National Framework, 2007: The National Framework for Air Quality Management in the Republic of South Africa as Contemplated in Section 7 of the National Environmental Management: Air Quality Act, 2004 (Act No. 39 of 2004), http://www.saaqis.org.za/Downloads.aspx?type=AQ

Nilgard, B., 1985: The ammonium hypothesis-an additional explanation to the forest dieback in Europe, *Ambio*, 14, 2-8.

Nunnari, G., Dorling, S., Schlink, U., Cawley, G., Foxall, R., Chatterton, T., 2004: Modelling SO2 concentration at a point with statistical approaches,*Environmental Modelling & Software*, 19, 887–905.

Pasquill, F., 1961: The estimation of the dispersion of windborne material, *Meteorology Magazine***,** 90, 33-40.

Pasquill F., and Smith, F.B., 1983: *Atmospheric Diffusion*, 3rd edition, John Wiley and Sons, New York.

Penkett, S.A., 1972: Oxidation of SO_2 and other atmospheric gases by ozone in aqueous solution, *Nature Physical Science*, 240, 105-106.

Personal communication1, Dr Ronald van der A, Climate Observations, KNMI (Royal Netherlands Meterological Institute).

Pham, M., Muller, J.F., Brasseur, G.P., Granier, C., and Mi~Gie, G., 1995: 3D model study of the global sulphur cycle: contributions of anthropogenic and biogenic sources, *Atmospheric Environment*, 30, 1815-1822.

Piketh, S.J., 1994: *Generation and Transportation Characteristics of Suspended Particles in the Eastern Transvaal*, Unpublised MSc dissertation , University of Witwatersrand, Johannesburg.

Piketh, S.J. and Prangley, A.R., 1998: *Trajectory Climatology of Transboundary Transport for the Highveld*, Eskom Report no. TRR/T98/038, Cleveland, Johannesburg.

Piketh, S. J., 2000: *Transport of Aerosol and Trace Gases over Southern Africa*, PhD Thesis, University of the Witwatersrand, Johannesburg, 158.

Piketh, S.J., Swap, R.J., Maenhaut, W., Annergarn, H.J., Forment, P., 2002: Chemical evidence of long-range atmospheric transport over southern Africa, *Journal of Geophysical Research*, 107, doi:10.1029/2002JD002056.

Piketh, S.J., Walton, N., Snow, N.H., 2003: *Air Quality Impact Research Facility (AQIRF) at Elandsfontein*, Research Report number RES/RR/03/021490, Eskom, Johannesburg.

Piketh, S.J., and Walton, N.M., 2004: Characteristics of atmospheric transport of air pollution for africa, *The Handbook of Environmental Chemistry*, 4, 173-195.

Platt, U., and Perner, D., 1983: *Measurements Of Atmospheric Trace GasesBy Long Path Differential UV/Visible Absorption Spectroscopy*, *Optical And Laser Remote Sensing*, Springer Verlag, New York.

Platt, U., 1994: Differential optical absorption spectroscopy (DOAS), *Chemical Analysis Series*, 127, 27-83.

Pompella, M., 1998: *Basic Air Pollution Meteorology*, Report conducted on behalf of United States Environmental Protection Agency, North Carolina.

Priest, P., Navarre, J. L., Ronneau, C., 1981: Elemental background concentration in the atmosphere of an industrialized country**,** *Atmospheric Environment*, 15, 1325 - 1330.

Preston-Whyte, R.A., Diab, R.D., Tyson, P.D., 1977: Towards an inversion climatology of Southern Africa: Part II non-surface inversions in the lower atmosphere, *South African Geographic Journal*, 59, 45-59.

Preston-Whyte R.A., Tyson P.D., 1988: *The Atmosphere and Weather of Southern Africa*, Oxford University Press, Cape Town.

Pretorius, R.W., Auret, I., Held, G., Brassel, K.M., Danford, I.R., Waldie, D.D., 1986: *The climatology of the boundary layer over the Eastern Transvaal and its impact on sulphur dioxide concentrations at ground level*, Report to the Foundation for Research Development, CSIR, ATMOS/86/16, Atmospheric Sciences Division, NPRL, CSIR,Pretoria.

Puxbaum, H.J, Rendl, R., Allabashi, L.O., Scholes, M.C., 2000: Mass balance of the atmospheric aerosols in a subtropical South African savanna, *Journal of Geophysics*, 105, 20697- 20706.

Raghunandan, A., Matooane, M., Oosthuizen, R., 2006: Impacts of air pollution, Report done on behalf of CSIR Natural Resources and the Environment, Congella.

Ramandh, A., 2011: *An Air Qualiy Assessment of the Vaal Triangle Airshed Using Dispersion Modeling*, Unpublished Master of Science, University of Kwa-Zulu Natal, Durban.

Richter, A., Burrows, J.P., NÜß, H., Granier, C., Niemier, U., 2005: Increase in tropospheric nirtogen dioxide in China observed from Space, *Nature 04092*, 437, doi:10.1038.

Roberts, G., Wooster, M.M., Lagoudakis, E., 2008: Annual and diurnal Aafrican biomass burning temporal dynamics, *Biogesciences Discussions*, 5, 3623-3663.

Rodhe, H., 1978: Budgets and Turn-Over Times of Atmospheric Sulphur Compounds, *Atmospheric Environment*, 12, 671-680.

Rorich, R.P., and Galpin, J.S., 1998: Air quality in the Mpumalanga Highveld region, South Africa, *South African Journal of Science*, 94, 109-113.

Rorich, R., 2005: *Annual Ambient Air Quality Data Report for 2003*, Research Report number RES/RR/04/24620, Eskom, Johannesburg.

Raghunandan, A., Matooane, M., Oosthuizen, R., 2006: *Impacts of Air Pollution*, Report done on behalf CSIR Natural Resources and the Environment, Durban.

Scheifinger, H., and Held, G., 1997: Aerosol Behaviour on the South African Highveld, *Atmospheric Environment*, 31, 21, 3497-3509.

Schnelle, K.B., and Partha, R.D.,1999: *Atmospheric Dispersion Modeling Compliance Guide*, McGraw-Hill Professional, New York.

Schulze, B.R., 1965: *Climate of South Africa part 8: General Survey*, Government Printer and Weather Bureau, Pretoria.

Schulze R.H., and Turner D.B., 1996: *Practical Guide to Atmospheric Dispersion Modelling*, Trinity Consultants, Dallas.

Schuurman, N., 2004: *GIS: A Short Introduction*, Blackwell, Malden.

Scire, J.S., Strimaitis, D.G., Yamartino, R.J., 2000a: *A User's Guide for the CALPUFF Dispersion Model (Version 5.0)*, Earth Tech, Concord.

Scire, J.S., Robe, F.R., Fernau, M.E., Yamartino, R.J., 2000b: *A User's Guide for the CALMET Metrological Model (Version 5)*, Earth Tech, Concord.

Scorgie, Y., Annegarn, H.J., Randell, L., 2003: *Air Quality Management Plan for the City Of Johannesburg*, Report No. MTX/03/JHB-01b done on behalf of the City of Johannesburg.

Scorgie, Y. and Venter, C., 2005: *Air Pollution Compliance Assessment of Cumulative Operations of Current and Proposed Eskom Power Stations*, Research Report number AAP/05/ESKOM-05, Eskom, Johannesburg.

Scott, G.M., and Diab, R.D., 2000: Forecasting Air Pollution Potential: A synoptic climatological approach, *Journal of Air and Waste Management Association*, 50, 1831-1842.

Sharma, P., Chandra, A., Kaushik, S.C., Sharma, P., 2012: Predicting violations of national ambient air quality standards using extreme value theory for Delhi City, *Atmospheric Pollution Research*, 3, 170-179.

Sierk, B., Richter, A., Rozanov Von Savigny, C.H., Schmoltner, A.M., Buchwitz, M., Bovensmann, H., Burrows, J.P., 2006: Retrieval and monitoring of atmospheric trace gas concentrations in nadir and limb geometry using the space-borne SCIAMACHY instrument, *Environmental Monitoring and Assessment*, 120, doi: 10.1007/s10661-005-9049-9.

Sinha, P., Hobbs, P.V., Yolkelson, R.J., Bertschi, I.T., Blake, D.R., Simpson, I.J., Gao, S., Kirchstetter, T.W., Novakov, T., 2003: Emissions of trace gas and particles from savanna fires in Southern Africa, *Journal of Geophysical Research*, 108, doi:10.1029/2002JD002325.

Skidmore, A.K., 2003: *Environmental Modelling with GIS and Remote Sensing*, Taylor and Francis, New York.

Snow, N., 2004: *Annual Eskom Air Quality Data Report For 2004*, Research Report number RES/RR/05/26565, Eskom, Johannesburg.

Snyman, G. M., Held, G., Brassel, K. M., 1990: Vertical Profiles of Particulates on the South Africa Highveld, *1st IUAPPA Regional Conference on Air Pollution Towards the 21st Century Implications, Challenges, Options and Solutions*, 1, 52, 1 - 17.

SRC., 2005: *Calpuff Modelling Course Notes*, University of Johannesburg, Johannesburg May 16-20 2008, Instructors: Joseph Scire and Christelle Escoffier-Czaja, TRC, 196 Baker Avenue, Concord, Massachusetts, 01742.

Statistics South Africa, 2001: Census 2001, http://www.statssa.gov.za/census01/html/default.asp[2011].

Statistics South Africa, 2007: Community Survey 2007, http://www.statssa.gov.za/publications/p03011/p030112007.pdf.

Statistic South Africa, 2012: Census 2011 Municipal fact sheet, http://www.statssa.gov.za.

Stutz, J., and Platt, U., 1996: Numerical analysis and estimation of the statistical error of differential optical absorption spectroscopy measurements with least-squares methods, *Journal of Applied Optics*, 35, 6041-6053.

TEMIS, 2011: *Tropospheric Emission Monitoring Internet Service website*, http://www.temis.nl/airpollution/no2.html.

Terblanche, D.E., Mittermaier, M.P., Piketh, S.J., Bruintjes, R.T., Burger, R.P., 2000: The Aerosol Recirculation and Rainfall Experiment: an initial study on aerosol-cloud interactions over South Africa, *South African Journal of Science*, 96, 15-21.

Thunis, P., Pederzoli, A., Pernigotti, D., 2012: Performance criteria to evaluate air quality modeling application, *Atmospheric Environment*, 59, 476-482.

Tuncel, S. G., Olmez, I., Parrington, J. R., Gordon, G. E., Stevens, R. K., 1985: Composition of Fine Particle Regional Sulphate Component in Shenandoah Valley, *Environmental Science and Technology*, 19, 529-537.

Turner, D.B 1970 : *Workbook of Atmospheric Dispersion Estimates*, CRC Press, New York.

Turner, D.B., 1994: *World Book of Atmospheric Dispersion Estimates: An Introduction to Dispersion Modelling*, 2nd edition. CRC Press, Boca Ratoon, New York.

Tyson, P.D., Garstang, M., Emmitt, G.D., 1973: *The Structure of Heat Islands*, Environmental Studies Occassional Paper No 12, Department of Geography and Environmental Studies, University of the Witwatersrand, Johannesburg.

Tyson, P.D., Preston-Whyte, R.A., Diab, R.D., 1976: Towards an inversion climatology of Southern Africa:Part 1 surface inversions, *South Africa Geographical Journal*, 58, 151-163.

Tyson, P.D., Garstang, M., Swap, R.J., Edwards, M., Kallberg, P., 1996a: An air transport climatology for subtropical southern Africa, *International Journal of Climatology*, 16, 265-91.

Tyson, P.D., Garstang, M., Swap, R., 1996b: Large-Scale Recirculation of Air over Southern Africa, *Journal of Applied Meteorology*, 35, 2218 – 2235.

Tyson, P.D., Kruger, F. J., Louw, C.W., 1998: *Atmospheric Pollution and Its Implications in the Eastern Transvaal Highveld*, Graphic Arts Division of the CSIR, Pretoria.

Tyson, P.D., and Preston-Whyte, R.A., 2000: *The Weather and Climate of Southern Africa*, Oxford University Press Southern Africa , Cape Town.

UNESCO., 1995: Series of Learning Material in Engineering Sciences, *Module on Air Pollution Control*, Ch 5, Department of Geography and Environmental Sciences, University of Kwa-Zulu Natal, Durban.

United States Environmental Protection Agency, Research Management Committee, 1981: *The National Crop Loss Assessment Network 1980 Annual Report*, Corvallis Environmental Research Laboratory, Oregon.

United States Environmental Protection Agency, Research Management Committee, 1982: *The National Crop Loss Assessment Network 1981 Annual Report,* Corvallis Environmental Research Laboratory, Oregon.

United States Environmental Protection Agency., 2002: *The Air Pollution Training Institute (APTI),* Updated 22 August 2002, htttp://www.epa.gov/air/oaqps/eog/apti.html.

United States Environmental Protection Agency, 2003: *Guideline on Air Quality Models,* Federal Register 40 CFR Part 51 Appendix W, http://www.epa.gov/scram001/tt25.htm#guidance.

United States Environmental Protection Agency, 2004: *Developing Interpolated Surfaces and Estimating Uncertainties,* EPA-454/R-04-004.

United States Environmental Protection Agency, 2005: *40 CFR Part 51 Revision to the Guideline on Air Quality Models: Adoption of a Preferred General Purpose (Flat and Complex Terrain) Dispersion Model and Other Revisions*; Final Rule Appendix W (PDF), Extract from the Guideline on Air Quality Models, Federal Register, 68256-8

Unworths, M.H., 1984: Evaporation from forest in cloud enhances the effects of acid deposition, *Nature*, 312, 262.

Unsworth, M.H., and Crossley, A., 1985: Consequences of cloud water deposition on vegetation at high elevation, in: *Proceedings of the NATO advanced research workshop on effects of acidic deposition on forests, wetlands and agricultural ecosystems,* 1-24.

Update and revision of the Air Quality Guidelines for Europe Meeting of the Working Group "Classical Air Pollutants", Bilthoven, Netherlands, 11-14 October 1994, EUR/HFA target 21.

Van der Werf, G.R., Randerson J.T., Collatz, G.J., Giglio, L., 2003, Carbon emission from fires in tropical and sub-tropical ecosystems, *Global Change Biology*, 9, 547-562.

Van der Werf, G.R., Randerson J.T., Giglio, L., Arellano Jr, A.F., Collatz, G.J., Kasibhatla, P.S., 2006: Interannual variability in global biomass burning emissions from 1997 to 2004, *Atmospheric Chemistry and Physics*, 6, 3423-3441.

Van Tienhoven A.M., Zunckel, M., Emberson, L., Koosailee, A., Otter, L., 2006: Preliminary Assessment of Risk of Ozone Impacts To Maize (Zea Mays) in South Africa, *Environmental Pollution*, 140, 220-230.

Venkatram, A., 1983: On dispersion in the convective boundary layer, *Atmospheric Environment*, 17, 529-533.

Venkatram, A., Isakov, V., Thoma, E., Baldauf, R., 2007: Analysis of air quality data near roadways using a dispersion model, *Atmospheric Environment***,** 1-17.

Vijayarhavan, K., Snell, H.E., Seigneur, C., 2008: Practical aspects of using satellite data in air quality modelling, *Environmental Science Technology*, 42, 11, 8187-8192.

Von Gogh, R.G., 1978: *Elements of the winter time temperature and wind structure over Pretoria*, Environmental Studies Occasional paper no 12, Department of Geography and Environmental Studies, University of the Witwatersrand, Johannesburg.

Wade , T., Sommer, S., 2006: *A to Z GIS*, ESRI Press, California.

Warneck, P., 1988: *Chemistry of the Natural Atmosphere Volume 41*, Academic Press, United States of America.

Watt Committee on energy, 1984: *Acid Rain*, Report 14, Savory Hill, London.

Webb, A.H. and Hunter, G.C., 1998: Power-station contributions to local concentrations of NO_2 at ground level, *Environmental Pollution*, 102 (S1), 283–288.

Weiner, D. and Harris, T.M., 2003: Community-integrated GIS for land reform in South Africa, *URISA Journal*, 15, 61-73.

Wells, R.B., Lolyd, S.M., Turner, C.R., 1996, National air pollution source inventory, in Held, G., Gore, B.J., Surrigde, A.D., Tosen, G.R., Turner, C.R., and Walmsly, R.D., (eds), *Air pollution and Its Impacts on the South African Highveld*, Environmental Science Association, Cleveland, Johannesburg, 3-9.

Wenig, M., Spichtinger, N., Stohl, A., Held, G., Beirle, S., Wagner, T., Jahne, B., Platt, U., 2003: Intercontinental transport of nitrogen oxide pollution plumes, *Atmospheric Chemistry and Physics Discussions*, 3, 387-393.

Winner, W.E., Mooney, H.A. and Goldstein, R.A., 1985: *Sulfur Dioxide and Vegetation: Physiology, Ecology and Policy Issues*, Stanford University Press, Stanford.

World Health Organisation (WHO)., 2000a: *Air Quality Guidelines for Europe*, second edition. WHO Regional Publications, European Series, No. 91, http:www.euro.who.int/eprise/main/who/informationsources/publications/catalogue/200100910_6.

World Health Organisation., 2000b: *Air Quality Guidelines for Europe*, second edition. WHO Regional Publications, European Series, No. 91, WHO Regional Office for Europe, Copenhagen (chapter 7.4).

World Health Organisation., 2001: *Health Impact Assessment of Air Pollution in the WHO European Region*, WHO/Euro product no:876.03.01(50263446).

World Health Organisation., 2003: *WHO air quality guidelines global update 2003*, http://www.who.int/whr/previous/en/

World Health Organisation., 2005: *Air Quality Guidelines Global Update 2005*, EUR/05/5046029, WHO Regional Office for Europe, Scherfigsvej 8, DK-2100 Copenhagen, Denmark.

Zannetti, P., 1990: *Air Pollution Modelling: Theories, Computational Methods and Available Software*, Computational Mechanics Publication, Southampton.

Zannetti, P., 1993: *Numerical Simulation Modelling of Air Pollution: An overview, in air pollution*, Computational mechanics publication, Southampton.

Zawar-Reza, P., and Sturman, A., 2008: Application of airshed modelling to the implementation of the New Zealand National Environmental Standards for air quality, *Atmospheric Environment*, 42, 8785–8794.

Zhoua, Y., Levy, J.I., and Evans, J.S., 2006: The influence of geographic location on population exposure to emissions from power plants throughout China, *Environment International*, 32, 365 –373.

Zib, P., 1977: Urban air pollution dispersion models: a critical survey, Department of Geography and Environmental Studies Occasional Paper No. 16: Department of Geography and Environmental Studies, University of Witwatersrand, Johannesburg.

Zunkel, M., John, J., Naidoo, M., 2004: The national air quality management programme output air quality information review, Centre for Science and Industrial Research, Environmentek, Pretoria.

Zunckel, M., Koosialee, A., Yarwood, G., Maure, G., Venjonoka, K., van Tienhoven, A. M., Otter, L., 2006: Modelled surface ozone over Southern Africa during the Cross Border Air Pollution Impact Assessment Project, *Journal of Environmental Modelling and Software*, 21, 911-924.

Zunckel, M., 2007: *Air Quality Modelling Activities In Southern Africa and The Feasibility of a Regional Modelling Centre*, Report done on behalf of APINA.

Zwi, S., Davies, J.C.A., Becklake, M.R., 1987: *Impact On Human Health of Atmospheric Pollution in the Eastern Transvaal Highveld*, Report to the Foundation for Research Development, CSIR, Department of Medicine, University of the Witwatersrand.